IMPERIAL COLLEGE LONDON

MSc IN QUANTUM FIELDS AND FUNDAMENTAL FORCES

MSc Dissertation : Pulsed Geometric Quantum Gates with Dissipation

---

Author : Manuel PACE - 01935626
Supervisor : Professor Myungshik KIM

Imperial College London

24th September 2021

Academic year 2020-2021

Acknowledgements

This dissertation concludes my master's degree in Quantum Fields and Fundamental Forces at *Imperial College London*, and a year at Imperial, as well as my training to become a physicist. I was very passionate about the material covered in this degree. While one has to overcome some mathematical complexity to get there, I think it is impossible not to marvel at how closely nature's behaviour matches the elegance of some of the great work that has so far been done in theoretical Physics.

This dissertation could not have been completed without the continuous help of two people from one of the *Quantum Information and Control* research groups from the *Department of Physics* of the *Faculty of Natural Sciences* at Imperial.

I would like to thank my supervisor, Professor Myungshik Kim, Chair in Theoretical Quantum Information Sciences. Despite his busy schedule and personal matters, he accepted to supervise my MSc dissertation. I am very grateful for his help throughout this work, and would like to thank him for being very supportive and encouraging in all of our contacts.

I would also like to thank Yue Ma for her amazing help. She is one of Professor Kim's PhD students, and followed my progress closely throughout the last few months. She helped in setting objectives for the dissertation and in identifying some of the mistakes I made along the way. She was always available when I had technical questions and was overall of great help for the full project.

This has been one of the most difficult years of my life. The impact of the COVID-19 pandemic led me to work on this degree mostly alone and isolated from my peers, and generated many other problems. The death of my father in early September 2020, after a battle with late stage cancer, is still difficult to process and overcome, and I miss him dearly. Amidst the large amounts of administrative worries I encountered, and the prospect of leaving to the US to start my PhD in late 2021, this year was truly full of questions and uncertainties. But I also received a lot of support from my family and some of my friends to overcome these difficulties, and I would like to thank them here.

I would like to thank my mother and "my Christophe", as I called him being little. While this year was difficult, I cannot imagine how much worse things would have been without you. I would like to thank my little sister, for being one of the beautiful things in my life, and for motivating me to always better myself. I would then like to thank my whole family, with an additional note for my amazing grandparents and their unwavering support.

For some of the times where I was able to forget everything else to just enjoy the present, I would like to thank everyone in the "Amways" group, and everyone in "Mercataule". In these groups, I would like to thank those who are closest to me and with whom I had more profound conversations. I will directly thank Martin Vanbrabant here, you have no idea how much some of our late night talks helped me.

Finally, I would like to thank my girlfriend, Eléonore. I wish to be able to make you laugh and smile for as long as possible.

It is by overcoming difficulties and suffering that one has the opportunity to improve oneself. And while happiness and good times cannot last forever, the same is true for sadness and difficult times. While mildly depressing in a general setting, I think these two facts can be of comfort for anyone traversing a difficult period.

Manuel C. C. Pace

Prerequisites, Notations, and Conventions

While this document aims at being self-sufficient, some prerequisites are nonetheless required to understand the following. And even if new symbols, conventions, or constants, are generally introduced when they are first used, some are just so ubiquitous in Physics that it makes a lot more sense to just remind them here in a quick summary.

Prerequisites

In the writing of this dissertation, the rule was to write while supposing the level of the reader to be similar to the level of any Imperial College London student who has recently followed the compulsory courses from the *Quantum Fields and Fundamental Forces* master's degree. In other words, all peers from the same master's degree should be able to understand the core of the developments made in this work, only referring to the cited resources for further details if necessary.

In case anyone from another background wishes to read this document, a short list of the prerequisites that are necessary is included here.

For understanding the purely mathematical aspects

- Elementary trigonometric identities

- Graduate level linear algebra (infinite dimensional spaces, operators, etc)

For understanding the Physics

- Advanced quantum mechanics (bra/kets, interaction picture, density matrices, etc)

- Some quantum field theory (second quantization Hamiltonians)

Symbols

As mentioned above, the following table lists the symbols that are so common that they will not be reminded throughout the text.

Symbol	Description	Unit
x	Position	$[m]$
p	Momentum	$[kg\,m\,s^{-1}]$
t	Absolute time	$[s]$
Δt and τ	Time intervals	$[s]$
m	Mass	$[kg]$
ω	Angular frequency	$[s^{-1}]$

k	Wavenumber (spatial angular frequency)	$[m^{-1}]$
$\hat{H}$	Hamiltonian	$[J]$
$\hat{U}$	Time evolution operator / Gate operator	$[/]$
$\hat{a}^\dagger$ and $\hat{a}$	Creation and annihilation operators	$[/]$
i	Imaginary unit	$[/]$

Table 1: List of the common symbols used in this document, and their corresponding SI derived unit.

Constants

The only constant used in the following is the reduced Plank constant, $\hbar = 1.0546 \cdot 10^{-34} \ [Js]$.

Abbreviations

While most abbreviations are cited with their definition at their first use in this document, the following table summarises the main abbreviations used throughout this work.

Abbreviation	Definition
BCH	Baker-Campbell-Hausdorff
RWA	Rotating Wave Approximation
HOC	Higher Order Commutators
HOT	Higher Order Terms
h.c.	Hermitian conjugate (of the previous term)

Table 2: List of the abbreviations used in this document (both in text or equation).

Conventions

As seen in Table 1, the most commonly used convention for constant quantities and operators was chosen here (*i.e.*: constants are represented by regular symbols and operators are represented by an additional "hat" symbol. *e.g.* $\hat{x}$ is the operator for the position, x is one of its eigenvalues). Some additional notes can also be made here in order to further avoid any confusion

- Any physical constant specific to a given subsystem will be written with a unique index in order to make its identification clear (*e.g.* $\boldsymbol{\omega}_m$ could be the angular frequency of some mechanical subsystem).

- The precise definition of HOC terms (see Table 2) is intentionally left relatively loose. The reason for this is that these commutators can appear in both the BCH formula and the Magnus expansion, but in slightly different forms. The point being that "higher order commutators" have one or more additional nested commutators, and result in a sum of terms that are of overall higher order than the previous terms. In order to avoid any confusion, the following example can be used : $[A, [A, B]]$, $[B, [A, B]]$ and $[A, [B, C]]$ are all considered to be HOC terms when compared to $[A, B]$.

Figures in this Work

All figures in this work were created by the author.

Contents

Chapter 1

Introduction

1.1 Preamble

The following preamble gives a general overview of the context around current quantum computing research. After a brief summary of the early days of the field, it also lists the motivations and some notable achievements that are of interest to contextualise this work.

It can be useful to note that the following overview is not exhaustive. It was written to introduce this work in particular, and not the field in its entirety.

1.1.1 Modern Classical Computers and Quantum Systems

While modern computers and the electronic devices they are based on are constantly improving, setting new goals and breaking new records in terms of performance [1; 2], it has long been known that this rapid progress will come to an end. Despite the use of new materials and new structures to reach smaller scales and higher switching speeds, the ever-increasing computing power density of systems based on classical field effect transistors will one day hit the insurmountable obstacle that is the miniaturisation limit of classical electronic systems [3].

It has long been hypothesised that what is next for information technologies will be quantum computing devices. As of today, some quantum systems have already been designed to be the logical next step to overcome the miniaturisation obstacle and improve performances. These take advantage of some quantum phenomena, such as the tunnelling effect or spin interactions [4; 5; 6]. They could therefore be called "quantum" devices, however, research in quantum information led to the discovery of actual quantum algorithms. These constitute an entirely new approach to computing. An approach that is not based on single two-valued bits anymore, but on more complex objects called quantum bits (often shortened as "qubits"). Qubits are, fundamentally, quantum states. They can be realised from many different systems, but the central point is that these quantum states themselves can be manipulated. If coherence is maintained, quantum states can stay in a given superposition and exhibit quantum interference. If they have no interaction with their environment, quantum states can also be entangled. These two fundamental phenomena make it possible to use these states for more complex operations than the boolean logic that is applied on classical binary values.

This led to the definition of actual *quantum computers* : devices which are able to directly take advantage of the properties of quantum states (*i.e.* quantum coherence and quantum entanglement) in order to perform computations, by using the quantum states themselves.

1.1.2 Quantum Computing, Algorithms, and Performances

The challenges the new field of quantum computing faced to create devices which would be able to maintain the very fragile properties of quantum coherence and quantum entanglement were numerous. But in spite of the difficulties, enthusiasm for quantum computers has not decreased over time, on the

contrary. The reason for this lies in the possibilities that arise when some quantum algorithms are applied to particular problems.

Thanks to their fundamentally different behaviour when compared to classical algorithms, quantum algorithms have been shown to achieve impressive performances in some particular areas. Solving search and optimisation problems, as well as solving large systems of differential equations are two key areas where quantum algorithms exhibit particularly impressive performances. Apart from calculations, the fundamentally different behaviour of quantum states when compared to classical bits led to more general considerations. Notably, in addition to using quantum states for local computations, the question of whether quantum states could also be used as a direct mean of communications between quantum computers arose. This in turn led to the design of theoretically unbreakable cryptosystems, further increasing global research interest to develop quantum computers [7; 8].

Apart from the practical applications listed above, there are also important theoretical questions which motivate research in quantum computing. One famous example is "Feynman's question". First formulated in 1981, the question underlined the possibility that quantum computers may be inherently more adapted to accurately simulate physical phenomena (and quantum Physics) than classical computers [9; 10]. And even if this idea was presented as a theoretical point, it quickly leads to very practical considerations concerning modern chemistry. Due to its potential in accurate simulation of small scale system, quantum computing is expected to have important applications in chemistry [11].

In spite of all these exciting facts, it is important to still take note of the current reality. Quantum computing is an exciting field, and both researchers and journalists have written about it. Despite what is sometimes implied, quantum computers are currently not expected to replace classical computers. Using a simplistic analogy, just like the first nuclear reactors, quantum computers are expected to open the door to many exciting possibilities. However, just like nuclear reactors did not end up replacing internal combustion engines in cars, quantum computers are not expected to replace standard laptop computers, at least not any time soon.

1.1.3 Practical Devices and Challenges

The design of the first physical systems which were able to experimentally realise quantum algorithms was the final proof of concept necessary to be able to start seriously considering the birth of actual quantum computers. While the first devices focused on ensembles of molecules ("bulk" NMR quantum computers, [12]), these were quickly shown to have strong limitations regarding the large noise which would be generated in future scaled systems [13]. The global interest then shifted to systems which were able to manipulate single quantum states (as opposed to ensembles of molecules "averaged" as one state, as in bulk RMN technology). One such system is the trapped ions device, which uses a single trapped ion for each quantum state [14]. Since then, many different physical systems that have the potential to be used as a basis for qubits have been proposed. A couple of examples include; atomic spin [12; 15], trapped ion excitation level [10; 14], photon number or photon polarisation [16; 17], etc.

Unfortunately, the problem of maintaining quantum coherence and low enough noise levels to exploit quantum interference and quantum entanglement phenomena in these systems remains. The main source of noise is by far the thermal excitation of the surroundings of the system. Because of this, the only solution has been to go down to extremely low temperatures (up to $[mK]$), and to use systems that are very well isolated from their environment. More recently, experiments have demonstrated possible operation of silicon qubits at temperatures as high as 5 to 10 $[K]$ [15], but even if this is already a large improvement[1], this is far from solving the problem (and it has only been shown on this particular type of qubit).

Despite these difficulties, important progress has been made towards working quantum computers. Remote access to use some of the first working systems has been proposed by some as a commercial application. Notably, Ionq is one company capitalising on this model with a quantum computer based on trapped ions (≈ 32 qubits) [18].

---

[1]Since liquid helium 4 has a boiling point of $\approx 4.2\,[K]$, reaching $\approx 5\,[K]$ enables the use of simpler cryogenic techniques.

In the future, larger systems that include many qubits are likely to be interfaced with classical integrated circuits in a single structure. Integrating the two in a single chip will then be a new challenge from a heat transfer point of view [19; 20]. While efforts have been made in order to design ways to correct and reduce the impact of some unavoidable noise and errors (notably, quantum error correction schemes, decoherence-free subspaces, dynamical methods, and others [8; 21; 22]), it appears clear that the main weakness and challenge for quantum computing is to design devices with higher fidelity and lower noise sensitivity. This has led to a lot of research efforts, both in the design of the qubits themselves, and in the design of the operations done on the qubits; the *quantum gates*.

1.2 Context of this Work

Following the summary given above treating the state of research in quantum computing in general, it is now possible to move on and contextualise this work in its field.

Quantum gates are the building blocks of quantum algorithms at the lowest level of abstraction, they are to quantum computing what logic gates are to classical computing.

As seen from its title, this work studies a given type of geometric quantum gate. Before moving on to the structure and objectives of this work, geometric gates are therefore presented. Their advantages and drawbacks are given, as well as some general context.

1.2.1 General Quantum Gates

Similarly to the classical case in boolean logic, there are universal quantum gates which can be used to build all other possible operations. Despite their conceptual similarity, the two ensembles are not mathematically equivalent. The universal gates of boolean logic can be obtained from universal quantum gates, but the converse is not true (which is to be expected, given the fundamental difference between classical and quantum computing). Similarly to how logic gates can be used to build simple logic circuits (such as the full adder, and many others), quantum gates are used to build quantum circuits.

In practice, quantum gates being operations done on quantum states, they are unitary time evolution operators corresponding to a given manipulation of the qubit. Approaches to interact with and manipulate the different physical realisations of qubits mentioned above have been studied, and many different physical realisations of different fundamental quantum gates have been proposed. An overview of some of the quantum gates that are fundamental to quantum computing, and how they operate can be found in [8], their uses with ancillas[2] and additional examples of quantum circuits can also be found in [23].

1.2.2 Quantum Geometric Gates

The object of this document are quantum geometric gates. Sometimes called "geometric phase gates", and often referred to as simply "geometric gates", these are a particular type of quantum gates that exhibit several surprising advantages. This gate type has been used extensively, both via theoretical research and practical experiments. Companies and research groups that have been and still are investigating the subject include Ionq, Oxford University, ETH Zurich, Universtät Innsbruck, University of Sussex, and many others. The physical realisation of these gates on trapped ion systems via the use of laser interactions is the most commonly used. As is seen in the present document, pulsed optomechanical interactions is another way to implement this type of gates.

---

[2]Ancillas are constant qubits (or constant bits) that are used as inputs in quantum (or logic) circuits. As a simple boolean example, one could use a NAND gate and a "1" ancilla to create a simple NOT gate (first input being the "1" ancilla, the output will always be NOT the second input). While this example can seem of little interest, the use of ancillas in quantum circuits has largely more interesting consequences, such as generating an interaction between previously non interacting subsystems (as seen in this work), and even produce entanglement between states (using the Milburn gate presented in this work, see [23]).

1.2.2.1 A Brief History

The first step towards geometric gates was taken by Berry in 1984. In [24], he showed a mathematical behaviour leading a state to show an additional phase factor after travelling along a closed loop in its phase space. While this seemed interesting for more theoretical reasons at first[3], his discovery was studied further and some of his assumptions modified. It was then noted that a generalisation of this behaviour enabled quantum computing, because these loops could generate a set of universal quantum gates [25; 26]. From then onward, the "geometrical approach" to quantum computing was born [27]. It was then extensively studied and refined, and is now one of the most promising approaches to quantum computing, used on many different physical realisations of quantum bits [21; 22; 28; 29].

1.2.2.2 High Level Description

In order to understand the nature of these gates, the following presents the typical case corresponding to the action of some general geometric gate. A simplified schematic can be found in Figure 1.1, and can be of help to understand the operation of an ideal geometric gate on some pure state.

Firstly, it is important to note that geometric gates are not single qubit gates, they are designed to act on several states at once. Geometric gates can take as input a complex quantum state which is the result of the states of several subsystems (*i.e.* a tensor product of the pure states of the elements composing the system). In these states, one is taken as an ancilla (generally, it is the mechanical vibrational state of the system, $|\alpha\rangle$ in Figure 1.1). This ancilla state is displaced along a closed loop in its phase space (therefore coming back to its original value), however, by doing that, the area of this loop in turn results in some operator applied on the full state.

When representing the travelled loop in the phase space as a set of shorter displacements, a geometrical shape is then drawn in the phase space of the ancilla state (hence the "geometric" in the name). The resulting operation of the whole gate is an operator function of the area enclosed by the loop (the reason for the "geometric phase" term being that this operator is in the form of a "phase" operator ; $e^{iA\hat{B}}$ with some operator $\hat{B}$, and the area of the loop A).

This will of course all be shown mathematically and more precisely in the coming technical chapters, but is a sufficient description to introduce the subject.
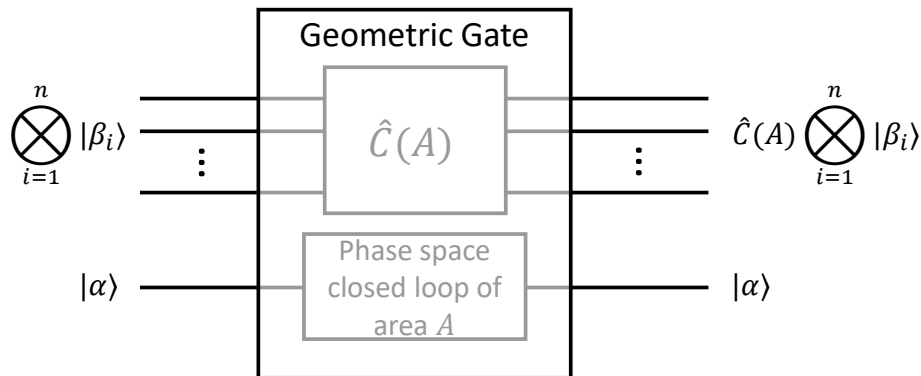
Figure 1.1: Schematic of an ideal geometric gate, showing its "inner workings" in transparency. The ancilla state (typically, a mechanical vibrational state $|\alpha\rangle$) is made to go through a phase space loop, but since the loop is closed, it is ultimately left unchanged. A is the area of the said loop, and $\hat{C}$ is some operator depending on this area. One can write $\hat{C}(0) = \mathbb{1}$.

1.2.2.3 Advantages and Drawbacks

There are several advantages to this type of gate, the main one being their robustness. Since the gate output only depends on the area of the loop and not on its detailed features, it was suspected that these

---

[3]This meant that, in some way, quantum states "remembered" the path taken, independently from the starting and ending points, which indeed is an interesting theoretical fact.

new gates would be less susceptible to noise than their counterparts when they were first discovered [21]. While this was just a reasonable assumption at first, it was later shown rigorously, accurately quantified, and it is now a well acknowledged result [21; 22; 27; 28].

Apart from the robustness of the result, the fact that the mechanical vibrational state ($|\alpha\rangle$ in Figure 1.1) is left unchanged whatever its initial value has important implications. First, it confirms that the application of the gate does not heat the system further. And second, it also shows that geometric gates do not necessarily require the initial system to be cooled down to its vibrational ground state.

In addition to having a very convenient behaviour with respect to both noise and vibrational states, these gates also have the advantage of being able to couple previously uncoupled subsystems. This phenomenon was widely used to simulate quantum gates in different systems, as well as to simulate nonlinear interactions (as it will appear later, the resulting action of the geometric gate is nonlinear) [10; 23; 30]. This particularity has especially interesting implications for trapped ions system. Due to the Coulomb force that makes the ions repel each other, they are separated by distances which are too long to easily create entangled states. However, since the ions can be mechanically coupled, geometric gates are able to use this mechanical state as an ancilla to entangle different ions [23; 31]

Despite all this, geometric gates also have disadvantages.

Geometric gates are in general slower[4] than their counterparts. This was at first due to the adiabatic condition that was set [24; 28], and newer systems have partly overcome this problem [22; 27; 29]. However, the choice of nonadiabatic or adiabatic gates remains contested in some physical systems [32].

Another drawback that is difficult to overcome is that the phase space loops the gate uses must be exactly closed. This, in turn, requires very precise control of the time during which some internal operations of the gate are done. This is challenging, and is the main reason why the gate presented in Figure 1.1 was qualified to be "ideal". In practice, the outgoing $|\alpha\rangle$ state is not exactly equal to the input. Some ideas to reduce the impact of this problem and study it were proposed in [27; 30].

1.3   Objectives of this Work and Overall Structure

The main objective of the present work is to examine a particular type of geometric gate on an optomechanical system subject to pulsed interactions. Once this gate has been demonstrated and understood in an ideal system, the aim is to introduce mechanical dissipation and examine its impact. Before this, in order to develop the necessary understanding of geometric phase gates (both conceptually and mathematically), the original trapped ion realisation of the Milburn gate (*i.e.* the simplest geometric gate) is to be presented.

To achieve this, this document is structured around three main chapters. Before these central chapters, the present introduction contextualised the subject of geometric gates from a quantum computing point of view. And after these, a final conclusion will summarise the main results of the dissertation, as well as possibilities for future work.

The goal of the first chapter is to examine the simplest geometric gate, the Milburn gate on trapped ions, as it was first presented in [10]. By doing this, this chapter should achieve two key objectives. Firstly, it should build an understanding of the trapped ion realisation of geometric gates, and in particular of the Milburn gate. This will then allow for a comparison with other gates, such as the Sørensen-Mølmer gate and the Cirac-Zoller gate, which will give a global understanding of how geometric gates work and of their advantages. Secondly, in order to present and demonstrate this first geometric gate, this chapter will have to rigorously develop the necessary set of mathematical tools and explains the associated conceptual points. Many of these theoretical results are general and not limited to trapped ion systems. These results (mainly the ones concerning coherent states, coherent state basis, displacement operators, and phase space loops) will be needed in the next chapters.

---

[4]This has not been clearly stated yet, but since quantum coherence is difficult to maintain, the time a gate takes to output its result is of importance. In a system that can maintain coherence for a set amount of time, a "slow" gate will be costly in terms of how much of the total available coherence time it spends to operate once.

The second chapter will move on to consider the main subject of this work, which is the gate obtained from pulsed interactions in an optomechanical system. The physical system will first be presented, as well as some additional mathematical tools that are needed. The objective will then be to derive the time evolution operator of the system, starting with time independent interactions as a preliminary study. After the time dependent case of pulsed interactions, the final result will be shown to act like a geometrical gate, with a more general type of phase space loop than the Milburn gate. In particular, the goal of this chapter will be to derive two different forms for this time evolution operator. The first form is a fully explicit result that should be confirmed by comparison with the literature. And the second form will be an expression split according to the different pulses, which should help in both the interpretation of the approximations made and in the coming introduction of dissipation in the next chapter.

The goal of the third chapter will then be to discuss the effect of dissipation. Since dissipation generates mixed states, density matrix formalism will have to be presented and explained, as well as the dissipation master equation. Once the tools are available, the objective will be to obtain a general expression for the impact of a given number of interaction pulses on a starting state, which will then be interpreted.

Throughout the different chapters, the longer mathematical developments that are not central to understanding the main points are to be moved in appendix, at the end of this document.

Chapter 2

Milburn Gate with Trapped Ions

This chapter is divided into four parts, a physical description of the system of trapped ions, some mathematical developments showing how the ions can be manipulated and controlled, theoretical developments concerning coherent state basis and displacement operators, and finally, the derivation of the expression of the Milburn gate (first presented in [10]), a discussion of its advantages and comparison with some other gates.

It can be useful to note that the theoretical developments concerning coherent states and displacement operators done in this chapter are general, and not limited to trapped ion systems. They will be used extensively in later chapters.

2.1   Trapped Ion Systems

Physically, one way to realise a trapped ion system is by using a quadrupole ion trap. A general schematic is found in Figure 2.1.
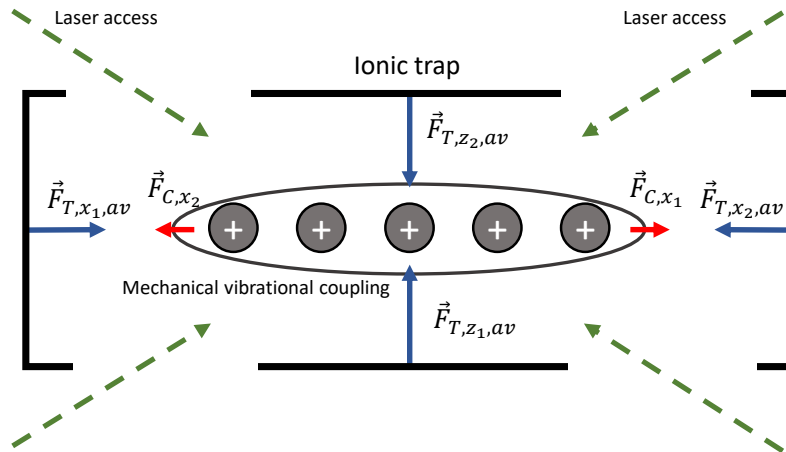
Figure 2.1: Schematic of a quadrupole ion trap. The different resulting forces relevant to the system are drawn and named. Index T is used for forces coming from the trap oscillations, index C for the coulomb forces between the ions. Index av is used to remind the reader that to obtain all the T forces, one needs to average over one full trap oscillation. The number of ions represented here is arbitrary.

Quadrupole ion traps are realised by using electric fields arranged to form a saddle-shaped potential (to obtain this, one can imagine each black side in Figure 2.1 to be charged with a sign different from its two closest neighbours and qualitatively draw the resulting potential). This saddle potential will generate a force confining the ions in one of the two main directions. Next, the signs are alternated

at radiofrequency, which gives a time dependent saddle-shaped potential alternating its direction. The constant oscillation between forces confining the ions vertically and horizontally average out to produce a trap that confines them in the two directions.

By tuning the relative strength of the fields for the different directions, it is then possible to align the ions in one of the directions. Since the ions are of the same sign, they repel themselves and align on a given axis. From the coulomb force trying to separate them and the trap forces trying to bring them together, these ions are mechanically coupled (as a whole, the set of ions forms a quantum mechanical oscillator). Generally, the ions in the trap are then cooled via different processes[1].

In addition to this mechanical vibrational quantum state, each ion can be considered as a two level quantum system, with level transition that can be excited by laser interactions. As seen in Figure 2.1, accesses are kept to shine lasers on the set of ions (from a global point of view, these lasers are the only means used to interact with the trapped ions). Thanks to their good spectral flexibility, Raman lasers are usually chosen for this role. Once the lasers are tuned to precise frequencies close to the resonant frequency of the internal state of the ions, a set of operations can be done on the quantum states.

2.2 Hamiltonian and Ion Manipulation

This section proves the Hamiltonian used in [10], and aims at giving an overview of the mathematical aspects of the main manipulations that can be done on the ions.

2.2.1 Approximate Hamiltonian

As a first step, let us prove the expression of the interaction picture (indicated by the I index) Hamiltonian used for the interaction of the laser with the ions of the ion trap. As mentioned in [10], the expression is

$$H_I = -\frac{i}{2}\hbar \sum_{i=1}^{N}(\Omega_i \hat{\sigma}_+^{(i)} - \Omega_i^* \hat{\sigma}_-^{(i)}) \tag{2.1}$$

The variables and notations used in the above expression will be explained throughout the proof. This Hamiltonian is very similar to the one mentioned in the quantum information course [8], with the additional subtlety that it includes the interaction Hamiltonians for each trapped ion in a single one (sum on the i index, which corresponds to the different ions). As a starting point, the case of a single trapped ion is examined.

2.2.2 Single Trapped Ion Interaction Picture Hamiltonian

For a single trapped ion exposed to a Raman laser, the full Hamiltonian is written

$$\hat{H} = \hat{H}_{0,el} + \hat{H}_{0,m} + H_{int} = \frac{\hbar\omega_0}{2}\hat{\sigma}_z + \hbar\omega_m \hat{a}^\dagger \hat{a} + A\hat{\sigma}_x cos(\omega t - k\hat{x} + \phi) \tag{2.2}$$

Where one can recognise the different Hamiltonian terms :

$\hat{H}_{0,el}$ The free two-level system[2] Hamiltonian, $\hbar\omega_0$ being defined as the energy difference between the two energy levels of the system.

$\hat{H}_{0,m}$ The free mechanical oscillator Hamiltonian, with its characteristic frequency ω_m.

---

[1]Some powerful cooling methods being Doppler cooling and resolved sideband cooling [33; 34]

[2]The index *el* stands for "electronic", because the two-level system corresponds to two (non degenerate) electronic configurations of the ion.

$\hat{H}_{int}$ The interaction Hamiltonian[3] that couples the two systems, induced by the presence of the laser. With t the time, ω the Raman laser frequency, k its wavenumber, and ϕ its phase. One notes that the factor A has units of $[J]$.

One also recognises several well known operators, such as the Pauli operators, which act on the two-level system. In matrix form, these can be written

$$\sigma_x = \begin{pmatrix} 0 & 1 \\ 1 & 0 \end{pmatrix} \qquad \sigma_y = \begin{pmatrix} 0 & -i \\ i & 0 \end{pmatrix} \qquad \sigma_z = \begin{pmatrix} 1 & 0 \\ 0 & -1 \end{pmatrix}. \tag{2.3}$$

The creation / annihilation operators $\hat{a}^\dagger$ / $\hat{a}$, for adding or removing one quantum of energy to the mechanical oscillator. And finally, the position operator $\hat{x}$ (as expected, it acts on the position of the ion, and is therefore related to the mechanical oscillating system, not to the two electronic energy levels of the ion).

It is interesting to note that in this approach to atom-field interactions, the laser is not a quantised system, and it is therefore absent from the quantum state (it is not modelled as an ensemble of photons, as in second quantisation using the Fock space). Instead, the laser acts as an external influence that can exchange energy with the system and, by its presence, the laser generates a coupling between the mechanical and the electronic states (*i.e.* $\hat{H}_{int}$ includes both $\hat{\sigma}_x$ and $\hat{x}$).

Knowing the relations

$$\hat{x} = \sqrt{\frac{\hbar}{2m\omega_m}}(\hat{a}^\dagger + \hat{a}) \qquad \text{and} \qquad \hat{p} = i\sqrt{\frac{\hbar m\omega_m}{2}}(\hat{a}^\dagger - \hat{a}), \tag{2.4}$$

the interaction picture Hamiltonian[4] can be computed

$$\hat{H}_I = \hat{U}_0^{-1}(t) H_{int}(t) \hat{U}_0(t) \tag{2.5}$$

$$= \hat{U}_0^{-1}(t) A\hat{\sigma}_x \cos(\omega t - k\hat{x} + \phi) \hat{U}_0(t) \tag{2.6}$$

$$= \hat{U}_0^{-1}(t) A\hat{\sigma}_x \cos\left(\omega t - k\sqrt{\hbar/2m\omega_m}(\hat{a} + \hat{a}^\dagger) + \phi\right) \hat{U}_0(t) \tag{2.7}$$

$$= \hat{U}_0^{-1}(t) A\hat{\sigma}_x \left(\frac{e^{i\left(\omega t - k\sqrt{\hbar/2m\omega_m}(\hat{a}+\hat{a}^\dagger)+\phi\right)} + e^{-i\left(\omega t - k\sqrt{\hbar/2m\omega_m}(\hat{a}+\hat{a}^\dagger)+\phi\right)}}{2} \right) \hat{U}_0(t) \tag{2.8}$$

$$= \hat{U}_0^{-1}(t) \hbar\hat{\sigma}_x \left(\frac{\Omega e^{i\left(\omega t - k\alpha(\hat{a}+\hat{a}^\dagger)\right)} + \Omega^* e^{-i\left(\omega t - k\alpha(\hat{a}+\hat{a}^\dagger)\right)}}{2} \right) \hat{U}_0(t) \tag{2.9}$$

To improve readability, the notations $\alpha = \sqrt{\hbar/2m\omega_m}$ and $\hbar\Omega = Ae^{i\phi}$ are used (Ω being the Rabi frequency). In addition, some of the hat notations to indicate which symbols are operators will be omitted (one just needs to keep in mind that σ's and a's are all operators, and therefore do not necessarily commute). Since

$$\hat{U}_0(t) = e^{-i\frac{\hat{H}_0}{\hbar}t} = e^{-i\left(\frac{\omega_0}{2}\hat{\sigma}_z + \omega_m \hat{a}^\dagger \hat{a}\right)t} \tag{2.10}$$

$\hat{H}_I$ can therefore be written as

$$\hat{H}_I = \hbar e^{i\left(\frac{\omega_0}{2}\sigma_z + \omega_m a^\dagger a\right)t} \sigma_x \left(\frac{\Omega e^{i\left(\omega t - k\alpha(a+a^\dagger)\right)} + \Omega^* e^{-i\left(\omega t - k\alpha(a+a^\dagger)\right)}}{2} \right) e^{-i\left(\frac{\omega_0}{2}\sigma_z + \omega_m a^\dagger a\right)t} \tag{2.11}$$

---

[3]While this is a common result of intermediate to advanced quantum mechanics courses, it may not seem entirely familiar. This Hamiltonian is obtained via the dipole approximation applied on atom-field interactions in the semi-classical approach (only the atom is quantised). Following this, since the atom is considered to be moving in this case, the additional $-k\hat{x}$ factor is introduced. One can consult [35; 36] for additional details.

[4]The coming calculation is a straightforward use of interaction picture formalism. All operators are time independent, and the evolution of the interaction picture state is simply given according to the transformed interaction Hamiltonian. Since some future applications of interaction picture will require more care, a theoretical reminder about it is available in Section 3.2.1. If the following does not seem logical, one can first refer to Section 3.2.1 before coming back here.

Using h.c. to denote the hermitian conjugate of the previous term, and remembering that σ_x / σ_z operators commute with a / $a^\dagger$ operators (σ operators are related to electronic excitations and a to vibrational excitations[5]), the expression further simplifies

$$\hat{H}_I = \frac{\hbar}{2}e^{i\frac{\omega_0}{2}\sigma_z t}\sigma_x e^{-i\frac{\omega_0}{2}\sigma_z t}e^{i\omega_m a^\dagger a t}\left(\Omega e^{i\omega t - ik\alpha(a+a^\dagger)} + \text{h.c.}\right)e^{-i\omega_m a^\dagger a t} \tag{2.12}$$

The easiest is now to split this and examined the two different parts. Starting with the first three factors (omitting the constant $\hbar/2$)

$$e^{i\frac{\omega_0}{2}\sigma_z t}\sigma_x e^{-i\frac{\omega_0}{2}\sigma_z t} = \sigma_x e^{-i\frac{\omega_0}{2}\sigma_z t}e^{-i\frac{\omega_0}{2}\sigma_z t} \tag{2.13}$$

$$= \sigma_x e^{-i\omega_0\sigma_z t} \tag{2.14}$$

$$= \sigma_- e^{-i\omega_0 t} + \sigma_+ e^{i\omega_0 t} \tag{2.15}$$

While the first step is a direct consequence of $[\sigma_z, \sigma_x] = -1$, the last step might seem non trivial. The result becomes clear when expressing all the σ operators as matrices and taking the Taylor expansion of the exponential. As some of other developments, this short proof is included in Appendix A.1. The two new σ operators that were introduced are defined as

$$\sigma_+ = \begin{pmatrix} 0 & 1 \\ 0 & 0 \end{pmatrix} \qquad \sigma_- = \begin{pmatrix} 0 & 0 \\ 1 & 0 \end{pmatrix} \tag{2.16}$$

Now examining the second part of the factors of Equation 2.12, the easiest is to consider the first term before moving on to its Hermitian conjugate.

$$e^{i\omega_m a^\dagger a t}e^{i\omega t - ik\alpha(a+a^\dagger)}e^{-i\omega_m a^\dagger a t} = \exp\left(i\omega t - ik\alpha e^{i\omega_m a^\dagger a t}(a+a^\dagger)e^{-i\omega_m a^\dagger a t}\right) \tag{2.17}$$

where the mathematical trick $X^{-1}e^Y X = e^{X^{-1}YX}$ on the exponential was used (easily provable via Taylor expansion). To proceed, the best way is to make use of a lemma associated with the Baker-Campbell-Hausdorff formula (shortened as "BCH formula" in the following). With general operators, it can be stated as

$$e^{\hat{X}}\hat{Y}e^{-\hat{X}} = \sum_{n=0}^{\infty}\frac{[(\hat{X})^n, \hat{Y}]}{n!} \quad \text{with} \quad [(\hat{X})^n, Y] = \underbrace{[\hat{X}, ...[\hat{X}, [\hat{X}, \hat{Y}]]...]}_{\text{n times}} \quad \text{and} \quad [(\hat{X})^0, \hat{Y}] = \hat{Y} \tag{2.18}$$

Since this lemma will be used extensively in the following work, it is proved in Appendix A.2. In addition to the lemma, the commutation relation $[a, a^\dagger] = 1$ is used to derive the simple commutators

$$[a^\dagger a, a] = a^\dagger aa - aa^\dagger a = (aa^\dagger - 1)a - aa^\dagger a = -a \tag{2.19}$$

$$[a^\dagger a, a^\dagger] = a^\dagger aa^\dagger - a^\dagger a^\dagger a = a^\dagger \tag{2.20}$$

With these and the lemma, the two operators in Equation 2.17 are easily simplified[6]

$$e^{i\omega_m a^\dagger a t}ae^{-i\omega_m a^\dagger a t} = \sum_{n=0}^{\infty}\frac{[(i\omega_m a^\dagger a t)^n, a]}{n!} = \sum_{n=0}^{\infty}\frac{(-i\omega_m t)^n}{n!}a = e^{-i\omega_m t}a \tag{2.21}$$

---

[5]Fundamentally, the first notations were already simplified. With everything written in a fully explicit manner, the full state $|\psi\rangle \otimes |\phi\rangle$ would for instance have electronic state $|\psi\rangle$ and vibrational state $|\phi\rangle$. Then, the σ_x operator would be written as $\hat{\sigma}_x \otimes \mathbb{1}$, and the raising operator as $\mathbb{1} \otimes \hat{a}^\dagger$. The fundamental reason why these operators commute then becomes fully explicit.

[6]Apart from using this method, the same results can also be obtained by inserting aa^{-1}, using the $X^{-1}e^a X = e^{X^{-1}aX}$ trick, and using the commutation relation $[a, a^\dagger] = 1$

$$e^{i\omega_m a^\dagger a t} a^\dagger e^{-i\omega_m a^\dagger a t} = \sum_{n=0}^{\infty} \frac{[(i\omega_m a^\dagger a t)^n, a^\dagger]}{n!} = \sum_{n=0}^{\infty} \frac{(i\omega_m t)^n}{n!} a^\dagger = e^{i\omega_m t} a^\dagger \tag{2.22}$$

Equation 2.17 is therefore rewritten

$$\exp\left(i\omega t - ik\alpha e^{i\omega_m a^\dagger a t}(a + a^\dagger)e^{-i\omega_m a^\dagger a t}\right) = \exp\left(i\omega t - ik\alpha(ae^{-i\omega_m t} + a^\dagger e^{i\omega_m t})\right) \tag{2.23}$$

With a bit of thought and the results in Equation 2.12, 2.15, and 2.23 the final expression for the interaction picture Hamiltonian can be written (reinstating the hat notation and the value of α)

$$\hat{H}_I = \frac{\hbar}{2}\left(\hat{\sigma}_- e^{-i\omega_0 t} + \hat{\sigma}_+ e^{i\omega_0 t}\right)\left(\Omega \exp\left(i\omega t - ik\sqrt{\frac{\hbar}{2m\omega_m}}\left(\hat{a}e^{-i\omega_m t} + \hat{a}^\dagger e^{i\omega_m t}\right)\right) + \text{h.c.}\right) \tag{2.24}$$

This expression[7] can then be expanded for small Lamb-Dicke parameters (*i.e.* $\eta = k\sqrt{\hbar/2m\omega_m} << 1$. It is useful to note that this requires low temperatures. Even if the coming geometrical gates do not require the vibrational ground state, they still need low temperatures for some approximations to be valid.). Thanks to the small Lamb-Dicke parameter, the HOT of the expansion in η are neglected.

$$\hat{H}_I = \frac{\hbar}{2}\left(\hat{\sigma}_- e^{-i\omega_0 t} + \hat{\sigma}_+ e^{i\omega_0 t}\right)\left(\Omega e^{i\omega t}\left(1 - i\eta\left(\hat{a}e^{-i\omega_m t} + \hat{a}^\dagger e^{i\omega_m t}\right)\right) + \text{h.c.}\right) \tag{2.25}$$

Once this is done, the last approximation used is the rotating wave approximation (often shortened RWA in the literature, it corresponds to setting to zero all rapidly oscillating terms). This approximation is made after choosing a frequency ω for the applied laser, the different choices leading to different results.

Choosing the Raman laser at the charge carrier transition ω_0 (stimulating the electronic energy level transition of the ion), the result is

$$\hat{H}_I = \frac{\hbar}{2}(\Omega^*\sigma_+ + \Omega\sigma_-) \tag{2.26}$$

Which is the expression to prove, up to a redefinition of Ω. To get the exact expression used in the paper, one needs to redefine $\Omega \to i\Omega^*$. This indeed gives the interaction picture Hamiltonian from [10]

$$\hat{H}_I = -i\frac{\hbar}{2}(\Omega\sigma_+ - \Omega^*\sigma_-) \tag{2.27}$$

It is important to understand that while the norm of the Rabi frequency Ω is of importance (it impacts the interaction strength between the two systems), the choice of its phase for this demonstration is purely arbitrary[8]. For a single laser on a single ion, the overall phase holds no physical meaning. However, when several lasers are used, the relative phases become very important, and this is why the demonstration was done with a given unknown phase ϕ.

2.2.3 Multiple Trapped Ions Interaction Picture Hamiltonian

In the case of multiple ions (let us suppose N ions), there are different Pauli operators for each ionic two-level system. In order to differentiate them, these are written with the ion number in brackets. For instance, the Pauli z operator on ion number i is denoted as $\hat{\sigma}_z^{(i)}$. Staying general, the different ions could also be exposed to different laser fields, this leads to the definition of different effective Rabi frequencies Ω_i (the i denoting the ion on which this laser is used). In this case, the full Hamiltonian in Equation 2.2 will be modified accordingly, summing on i for the electronic and interaction parts. The final result is then obtained very similarly to the single ion case, only working with sums of Pauli operators instead of a single Pauli operator. The interaction picture Hamiltonian then gives

---

[7]mentioned in [8]

[8]In this particular case, it can be understood that the difference between the two results simply boils down to some starting choices. If this demonstration was started by using a sine with negative phase instead of a cosine with positive phase (see Equation 2.2), the result would have been exactly Equation 2.27, as in [10]. In this case there would be no need to redefine Ω.

$$\hat{H}_I = -i\frac{\hbar}{2}\sum_{i=1}^{N}\left(\Omega_i\hat{\sigma}_+^{(i)} - \Omega_i^*\hat{\sigma}_-^{(i)}\right) \tag{2.28}$$

Considering that the same laser field is applied to the different ions (*i.e.* there is no relative phase or intensity change in the field seen by the different ions[9]), the expression then simplifies as (since all Ω_i have the same phase, the overall phase can also be chosen to be zero)

$$\hat{H}_I = -i\frac{\hbar}{2}\Omega\sum_{i=1}^{N}i\hat{\sigma}_y^{(i)} = \frac{\hbar}{2}\Omega\hat{J}_y \tag{2.29}$$

In the above, the collective spin operator $\hat{J}_y$ was defined as the sum of the N $\hat{\sigma}_y^{(i)}$ operators, additional details concerning it can be found below.

If this type of laser interaction (*i.e.* the laser is seen as identical by all ions) is the only possible interaction the outside world can have with the system, there are a number of implications. These are discussed in the next section.

2.2.4   Ion Access, Hilbert Space, and Operations

The end of the previous section skipped slightly ahead by using some of the general operators before properly defining the Hilbert space and the rigorous forms of the main operators. Starting back from the general system, and taking the previous interaction Hamiltonian as a known result, the following sections discuss the system in general, and what can be done with the different operators.

As in the previous case, let us consider a trap that contains N ions that are all mechanically coupled together. These ions are arranged in a line by the trap forces, and repel each other due to Coulomb forces, the overall picture can be considered to be similar to Figure 2.1[10].

2.2.4.1   Full Hilbert Space and Basic Operators

Firstly, let us consider the mechanical states. Thanks to the cooling of the whole system to low temperatures, it is considered that all complex vibrational modes of the ions are unoccupied (*i.e.* no longitudinal and transverse modes between the ions). Rather, the only mode that is not considered unoccupied is the simplest vibrational mode of the whole system (*i.e.* the "centre of mass" vibrational mode, in which the whole line behaves like a single object moving in the global potential of the trap, in a manner similar to how a single ion would). The mechanical states can therefore be considered to be identical to the ones of the quantum harmonic oscillator. In the energy eigenstate basis

$$|n\rangle \qquad \text{with } n \in \mathbb{N}, \text{ such that} \qquad \hat{H}_{0,m,S}|n\rangle = \hbar\omega_m n|n\rangle \tag{2.30}$$

Next, each ion is also a two-level system. In the energy eigenstate basis, each system is therefore either in its excited or ground state, indicated by the letters e or g

$$|e\rangle \text{ or } |g\rangle \qquad \text{such that} \qquad \hat{H}_{0,el}|g\rangle = -\frac{\hbar\omega_0}{2}|g\rangle \qquad \text{and} \qquad \hat{H}_{0,el}|e\rangle = \frac{\hbar\omega_0}{2}|e\rangle \tag{2.31}$$

Physically, these excited and ground states for each two-level system are the consequence of different electronic configurations. Since these are then associated with a difference in total angular momentum, which is a physical quantity associated with a direction, several bases can be chosen for the two-level system. In the above, the z basis was used ($\hat{\sigma}_z$ being the operator in $\hat{H}_{0,el}$, see Equation 2.2), but the other Pauli operators can also be used. By changing laser polarisation, one can easily switch from one eigenbasis to another. Table 2.1 (included below) summarises the different eigenbases. While its theoretical description will not be reminded here, one may also use the Bloch sphere for visual representation.

---

[9]According to the actual physical realisation, the orientation of the laser with respect to the line of trapped ions, the spatial frequency of the laser, and the distance separating the ions, this can be a very good approximation of reality.

[10]With the possible exception of the direction of the interaction lasers with respect to the direction of the ion line, as mentioned, some directions are more adapted to ensure that the same field approximation is correct (see previous footnote).

basis	up state	down state
z	$\lvert e\rangle_z = \lvert e\rangle$	$\lvert g\rangle_z = \lvert g\rangle$
y	$\lvert e\rangle_y = \dfrac{\lvert g\rangle - i\,\lvert e\rangle}{\sqrt{2}}$	$\lvert g\rangle_y = \dfrac{\lvert g\rangle + i\,\lvert e\rangle}{\sqrt{2}}$
x	$\lvert e\rangle_x = \dfrac{\lvert g\rangle + \lvert e\rangle}{\sqrt{2}}$	$\lvert g\rangle_x = \dfrac{\lvert g\rangle - \lvert e\rangle}{\sqrt{2}}$

Table 2.1: Summary of the eigenstates of the different bases in terms of the z eigenstates.

Selecting the z basis for each of the two-level subsystems, a given state of the whole system could then be written as

$$\lvert\psi\rangle = \underbrace{\lvert g\rangle \otimes \lvert e\rangle \otimes \lvert e\rangle \otimes \lvert g\rangle \otimes \lvert e\rangle \otimes \lvert g\rangle \otimes ... \otimes \lvert e\rangle}_{N \text{ ionic states}} \quad \otimes \quad \underbrace{\lvert n\rangle}_{mechanical\ state} = \lvert geegeg...e\rangle \otimes \lvert n\rangle \tag{2.32}$$

The basic operators that act on these states are then

$$\hat{\sigma}_z^{(i)} = \underbrace{\underbrace{\mathbb{1} \otimes ... \otimes \mathbb{1}}_{i-1 \text{ times}} \otimes \hat{\sigma}_z \otimes \mathbb{1} \otimes ... \otimes \mathbb{1}}_{N+1 \text{ operators}} \tag{2.33}$$

$$\hat{a} = \underbrace{\mathbb{1} \otimes ... \otimes \mathbb{1}}_{N \text{ times}} \otimes \hat{a} \tag{2.34}$$

with the other Pauli operators (x and y) for ion i and the creation operator $\hat{a}^\dagger$ for the mechanical oscillator defined similarly.

Of course, these fully explicit notations are not used throughout the calculations in this work, as they would make most development long and hard to read. However, it is useful to keep them in mind in order to precisely understand the space that is used, and the actual reason behind some commutation relations.

The goal of this short discussion was to make sure that the bases were covered, and this should all seem pretty familiar to the reader. However, there is already an interesting remark that can be made here, concerning the actual Hilbert space that is accessible when one uses laser fields on all ions at once.

2.2.4.2 Collective Spin Operator and Reduced Hilbert Space

If the only way to interact with the N trapped ions is with lasers similar to the one used in Equation 2.29 (*i.e.* lasers in a setting which makes them shine on all ions at once without variation in phase or intensity), it is known that the only observables that are really accessible are the collective spin operators $\hat{J}_\alpha$ (with α being x, y or z).

Writing some general state

$$\lvert\Psi\rangle = \lvert egeeg...eg\rangle \otimes \lvert\phi\rangle \tag{2.35}$$

with $\lvert\phi\rangle$ specifying a general vibrational state of the system, and e or g giving the states of each ion (numbering the ions with their position in the ket). The impact of applying the collective spin operator (in the z direction[11]) is

---

[11] The following calculation leads to exactly the same result in the other bases, z was only chosen to shorten notations.

$$\hat{J}_z \ket{\Psi} = \sum_{i=1}^{N} \hat{\sigma}_z^{(i)} \ket{egeeg...eg} \otimes \ket{\phi} \tag{2.36}$$

$$= \frac{1}{2} \ket{egeeg...eg} \otimes \ket{\phi} + \sum_{i=2}^{N} \hat{\sigma}_z^{(i)} \ket{egeeg...eg} \otimes \ket{\phi} \tag{2.37}$$

$$= \frac{1}{2} \ket{egeeg...eg} \otimes \ket{\phi} - \frac{1}{2} \ket{egeeg...eg} \otimes \ket{\phi} + \sum_{i=3}^{N} \hat{\sigma}_z^{(i)} \ket{egeeg...eg} \otimes \ket{\phi} \tag{2.38}$$

$$= \frac{N_e - N_g}{2} \ket{\Psi} \tag{2.39}$$

with N_e the total number of excited ions and N_g the total number of ground state ions (of course these two variables are related by $N = N_e + N_g$).

This result has an interesting implication concerning the actual Hilbert space that corresponds to the system and the observable used. One sees from it that the only observable with the collective spin operators is the value $N_e - N_g$. This means that the only possible measurements range from $-N/2$ to $N/2$ by steps of 1. In addition, it also means that without additional lasers that can address a single ion at a time, there is no need to use the full Hilbert space described in Equation 2.32. The position of the ions in the excited or ground state in the sequence is impossible to measure with the available observable (there is permutation symmetry between the ions). This means that, when measured with these observables, the system is fully characterised when written in the basis of the eigenstates

$$\ket{\psi_{jn}} = \ket{j} \otimes \ket{n} \tag{2.40}$$

Where $\ket{j}$ is an eigenstate of the collective spin operator with eigenvalue j ($j \in \{-N/2, -N/2 + 1, ..., N/2 - 1, N/2\}$), and represents the difference between the total number of excited ions and the total number of ground state ions, and $\ket{n}$ is the energy eigenstate of the mechanical harmonic oscillator corresponding the the vibrational state of the system (a general state of the system will then be written as a given superposition of these eigenstates). This Hilbert space is called the "reduced" Hilbert space, because it has smaller dimension (instead of 2^N, the ionic subsystem only has dimension $N + 1$). Once again, physically, nothing changed, the "full" Hilbert space is still the fundamentally correct description. But since the observables that are available cannot distinguish some of its states, it is also unnecessary to distinguish them in the notations.

2.2.4.3 Simple Gates, $\hat{\sigma}_\alpha$ and collective pulses

Now that the definition of the quantum system is made and that the Hilbert space and the basic laser interactions are well understood, it is possible to showcase some simple quantum gates. As the first quantum gates presented in this work, these are not geometric gates yet, and they will only impact the two-level ionic systems (each ionic state corresponding to one computational qubit). The Milburn gate (a geometric gate) that will be presented later will require additional lasers to generate a slightly more complex interaction (and it will use the mechanical state as an ancilla qubit).

Remembering the interaction picture Hamiltonian derived in Equation 2.29, let us start with an even simpler expression, the single ion version of this operator

$$\hat{H}_I = \frac{\hbar\Omega}{2}\hat{\sigma}_\alpha \tag{2.41}$$

Where α stands for x, y, or z. Noting that $\hat{\sigma}_\alpha^2 = \mathbb{1}$, the impact of turning the laser on during a time τ (*i.e.* the impact of a "$\hat{\sigma}_\alpha$" pulse of time τ) can be written (in the interaction picture) as applying the time evolution operator

$$\hat{U}(\tau) = e^{-i\hat{H}_I t/\hbar} = e^{-i\Omega\hat{\sigma}_\alpha\tau/2} \tag{2.42}$$

$$= \sum_{n=0}^{\infty} \frac{(-i\Omega\hat{\sigma}_\alpha\tau/2)^n}{n!} \tag{2.43}$$

$$= \sum_{n=0}^{\infty} \frac{(-i\Omega\tau/2)^{2n}}{(2n)!} \mathbb{1} + \sum_{n=0}^{\infty} \frac{(-i\Omega\tau/2)^{2n+1}}{(2n+1)!} \hat{\sigma}_\alpha \tag{2.44}$$

$$= \sum_{n=0}^{\infty} \frac{(-1)^n}{(2n)!} (\Omega\tau/2)^{2n} \mathbb{1} - i \sum_{n=0}^{\infty} \frac{(-1)^n}{(2n+1)!} (\Omega\tau/2)^{2n+1} \hat{\sigma}_\alpha \tag{2.45}$$

$$= \cos(\Omega\tau/2)\mathbb{1} - i\sin(\Omega\tau/2)\hat{\sigma}_\alpha \tag{2.46}$$

A simple example of an application of this result can be given here. Considering a $\hat{\sigma}_x$ pulse where τ is chosen such that $\Omega\tau/2 = -\pi/4$ $(+2k\pi, k \in \mathbb{Z})$, one finds that it is the rotation[12] needed to go from the $\hat{\sigma}_z$ eigenbasis to the $\hat{\sigma}_y$ eigenbasis. It gives

$$\hat{U}\left(\tau = \frac{7\pi}{2\Omega}\right) = \frac{1}{\sqrt{2}} \begin{pmatrix} 1 & i \\ i & 1 \end{pmatrix} \quad \text{and} \quad \begin{cases} \hat{U}(\tau = \frac{7\pi}{2\Omega})\left|g\right\rangle = \frac{\left|g\right\rangle + i\left|e\right\rangle}{\sqrt{2}} = \left|g\right\rangle_y \\ \hat{U}(\tau = \frac{7\pi}{2\Omega})\left|e\right\rangle = i\frac{\left|g\right\rangle - i\left|e\right\rangle}{\sqrt{2}} = e^{i\pi/2}\left|e\right\rangle_y \end{cases} \tag{2.47}$$

One could note that this operator does also adds an overall $\pi/2$ phase to the positive eigenvalue state (this overall phase is not relevant when the only interest is to obtain the correct eigenstate, but it is good practice to stay rigorous).

Generally, if this kind of operation is applied for some unspecified time on some state, it will result in the precession of this state around the axis of interest in the Bloch sphere. One can write the general result

$$\hat{U}_\alpha(t)\left|\psi\right\rangle = e^{-i\Omega\hat{\sigma}_\alpha t/2} \left(a\left|e\right\rangle_\alpha + b\left|g\right\rangle_\alpha\right)$$
$$= ae^{-i\Omega t/2}\left|e\right\rangle_\alpha + be^{i\Omega t/2}\left|g\right\rangle_\alpha$$

Up to a redefinition of overall phase, this is just

$$\hat{U}_\alpha(t)\left|\psi\right\rangle = a\left|e\right\rangle_\alpha + be^{i\Omega t}\left|g\right\rangle_\alpha \tag{2.48}$$

With the above, one confirms that the probability to measure $\left|e\right\rangle_\alpha$ or $\left|g\right\rangle_\alpha$ does not change, but the probability to obtain e or g in another basis exhibits Rabi oscillations (with frequency Ω, the Rabi frequency). Using the Bloch sphere, one understands that this corresponds to the precession of the direction of angular momentum around axis α.

Now that the spin pulse on a single ion is well understood, one can easily generalise this to the collective spin pulse. Since the spin operators for the different ions commute and the same laser shines on all ions with the same phase and intensity, this boils down to simply apply the gate defined in Equation 2.46 on all ions. Once again, the permutation symmetry can be used to simplify the notations and only write that there are N_g ground and N_e excited states in some basis α. In the following, another example is given, a $\pi/2$ $\hat{J}_y$ pulse on the starting state $\left|-N/2\right\rangle$ (which corresponds to $\left|ggg...gg\right\rangle$). Using Equation 2.46, the result for a single ion is

$$\hat{U}_y\left(\tau = \frac{\pi}{2\Omega}\right)\left|g\right\rangle_z = (\cos(\pi/4)\mathbb{1} - i\sin(\pi/4)\hat{\sigma}_y)\left|g\right\rangle \tag{2.49}$$

$$= \left(\frac{1}{\sqrt{2}}\begin{pmatrix} 1 & 0 \\ 0 & 1 \end{pmatrix} - i\frac{1}{\sqrt{2}}\begin{pmatrix} 0 & -i \\ i & 0 \end{pmatrix}\right)\begin{pmatrix} 0 \\ 1 \end{pmatrix} \tag{2.50}$$

---

[12]It is encouraging to note here that rotations are already one of the requirements for universal quantum gates [37]

$$= \frac{1}{\sqrt{2}} \begin{pmatrix} 1 & -1 \\ 1 & 1 \end{pmatrix} \begin{pmatrix} 0 \\ 1 \end{pmatrix} \tag{2.51}$$

$$= \frac{1}{\sqrt{2}} \begin{pmatrix} -1 \\ 1 \end{pmatrix} = \frac{|g\rangle - |e\rangle}{\sqrt{2}} = |g\rangle_x \tag{2.52}$$

Since the same thing happens on all ions at once, the result for the collective spin pulse is

$$\hat{U}_{\hat{J}_y} \left(\tau = \frac{\pi}{2\Omega} \right) |-N/2\rangle_z = |-N/2\rangle_x \tag{2.53}$$

While this is easily understood using a single spin pulse and considering the same is applied on each ion, one may wonder how to show this with the more general notations that are adapted for more complex cases. This is detailed in Appendix A.3.

This last result closes what is covered here concerning the fundamentals of the trapped ion system. With a good understanding of the Hilbert space and of some of the basic operations, everything is in place to move on to more complex calculations. The objective here being to develop the equations for the Milburn geomtric gate, the crucial subject of coherent state bases and displacement operators must be first presented.

2.3 Coherent States and (Conditional) Displacement Operator

The subject of coherent states and its associated basis, as well as the displacement operator and its associated conditional version, are fundamental mathematical tools that have to be first presented before talking about any geometric gate. While the Milburn gate could be derived without some of the coming developments (thanks in part to its simplicity), these results both simplify the derivation and are fundamentals that are of crucial importance to really understand the concepts behind the gate. Apart from the physical realisation of the operator (which, of course, has to be particularised to a given system), all the results below are general, they are not limited to trapped ion systems. Many of these results will often be used in the calculations done later (notably in the chapter discussing dissipation in the optomechanical system).

The approach used in this work is to start with the expression of the *conditional* displacement operator and how to obtain it physically. Then, the general displacement operator is examined in a fully general way. Coherent states and the associated basis are presented, as well as their links with the displacement operator. Finally, some time is dedicated to the study of phase space loops and displacement operator composition.

2.3.1 Conditional Displacement Operator Physical Realisation

As given in [10], the conditional displacement operator on the ith ion is defined as

$$\hat{H} = -i\hbar(\alpha_i \hat{a}^\dagger - \alpha_i^* \hat{a}) \hat{\sigma}_z^{(i)} \tag{2.54}$$

Using equation 2.25 with the rotating wave approximation (considering $\phi = 0$), and choosing the Raman laser frequency at $\omega = \omega_0 \pm \omega_m$, one obtains the blue and red sideband interaction Hamiltonians

$$\hat{H}_{I,blue} \approx -i\eta\frac{\hbar}{2}(\Omega\hat{\sigma}_- \hat{a} - \Omega^*\hat{\sigma}_+ \hat{a}^\dagger)$$
$$\hat{H}_{I,red} \approx -i\eta\frac{\hbar}{2}(\Omega\hat{\sigma}_- \hat{a}^\dagger - \Omega^*\hat{\sigma}_+ \hat{a}) \tag{2.55}$$

Knowing this, it is possible to consider a case where these two lasers (one at $\omega_0 + \omega_m$, one at $\omega_0 - \omega_m$) are used simultaneously. Then, the resulting interaction Hamiltonian is the sum of one red sideband Hamiltonian and one blue sideband Hamiltonian. If, in addition, the two lasers are chosen to have identical intensity but opposite phase ($\Omega = \Omega_{red} = \Omega_{blue}^*$), the result is

$$\hat{H}_{I,blue}^{(int)} + \hat{H}_{I,red}^{(int)} = -i\hbar\frac{\eta}{2}\left(\Omega(\hat{\sigma}_- - \hat{\sigma}_+)\hat{a}^\dagger + \Omega^*(\hat{\sigma}_- - \hat{\sigma}_+)\hat{a}\right) \tag{2.56}$$

$$= -i\hbar\frac{\eta}{2}\left(-i\Omega\hat{\sigma}_y\hat{a}^\dagger - i\Omega^*\hat{\sigma}_y\hat{a}\right) \tag{2.57}$$

$$= -i\hbar\left(\left(-i\frac{\eta\Omega}{2}\right)\hat{a}^\dagger - \left(-i\frac{\eta\Omega}{2}\right)^*\hat{a}\right)\hat{\sigma}_y \tag{2.58}$$

$$= -i\hbar(\alpha\hat{a}^\dagger - \alpha^*\hat{a})\hat{\sigma}_y \tag{2.59}$$

Where the Hamiltonian in 2.54 was obtained, up to a collective rotation[13] (ie : $\hat{\sigma}_y$ instead of $\hat{\sigma}_z$). Since Ω is a general complex number, α can indeed be any complex number (according to the choice of laser phase and intensity).

From this, one finds that this type of Hamiltonian can be obtained from two Raman lasers used simultaneously, at different frequencies, opposite phases, and identical intensity. Later, it will also be shown that the same type of hamiltonian can be obtained from a short optomechanical interaction pulse followed by free time evolution.

2.3.2 Displacement Operator and Coherent States

In order to understand how the conditional displacement operator works, it is useful to first take a look at the displacement operator itself. The few following subsections examine the displacement operator from a purely theoretical point of view, and derive a few important results.

The general expression for the displacement operator is

$$\hat{D}(\alpha) = e^{\alpha\hat{a}^\dagger - \alpha^*\hat{a}} \tag{2.60}$$

with some complex number α. One easily confirms that this operator can for instance be obtained from the following Hamiltonian and an interaction time of $\tau = 1$.

$$\hat{D}(\alpha) = \hat{U}(\tau = 1) = e^{-i\hat{H}\tau/\hbar} \qquad \text{with} \qquad \hat{H} = i\hbar(\alpha\hat{a}^\dagger - \alpha^*\hat{a}) \tag{2.61}$$

The effect of this operator is best understood when examined in the (overcomplete[14]) basis of coherent states, which are defined as the eigenstates of the annihilation operator

$$\hat{a}\left|\alpha\right\rangle = \alpha\left|\alpha\right\rangle \tag{2.62}$$

As can directly be seen, these states are quite interesting conceptually, they do not change by subtracting an excitation from the system (a behaviour that is completely opposite to the Fock states basis, being energy eigenstates). It can be noted that these coherent states are states of minimum uncertainty between momentum and position[15] (represented by discs in the x-p phase space). In addition, $\hat{a}$ is not Hermitian, so $\left\langle\alpha\right|\hat{a} \neq \alpha^*\left\langle\alpha\right|$, in fact, from $\hat{a}\left|\alpha\right\rangle = \alpha\left|\alpha\right\rangle$, one can see that $\left\langle\alpha\right|\hat{a}^\dagger = \alpha^*\left\langle\alpha\right|$.

Understanding the nature of coherent states is closely linked to understanding the effect of the displacement operator, let us consider the operator

$$\hat{F} = \hat{D}^\dagger(\alpha)\hat{a}\hat{D}(\alpha) \tag{2.64}$$

Calculating this operator product is a bit harder than what one could expect (one could for instance try to introduce $\hat{a}\hat{a}^{-1}$ and use $Xe^AX^{-1} = e^{XAX^{-1}}$ to simplify, but unfortunately this does not help). One

---

[13]This collective rotation can for instance be obtained from results derived in the previous section, see Equation 2.46.

[14]The basis states used are therefore not necessarily orthogonal.

[15]This fact helps in understanding the nature of coherent states, but has no direct implications in this work, so it is not proven here. In order to prove it, a straightforward approach checks whether coherent states verify the minimum uncertainty relation $\sigma_x\sigma_p = \hbar/2$. Using the definition of the uncertainty of operator $\hat{A}$ (written σ_A) as

$$\sigma_A = \sqrt{\langle A^2\rangle - \langle A\rangle^2} \tag{2.63}$$

A full discussion including all intermediate proofs can be found in [38].

way to approach it, however, is to take the derivative of the expression with respect to a real parameter s that is introduced.

$$\frac{d}{ds}\hat{F}(s) = \frac{d}{ds}\left(\hat{D}^\dagger(s\alpha)\hat{a}\hat{D}(s\alpha)\right) = -(\alpha\hat{a}^\dagger - \alpha^*\hat{a})\hat{D}^\dagger(s\alpha)\hat{a}\hat{D}(s\alpha) + \hat{D}^\dagger(s\alpha)\hat{a}(\alpha\hat{a}^\dagger - \alpha^*\hat{a}))\hat{D}(s\alpha)$$
$$= \hat{D}^\dagger(s\alpha)\left[\hat{a},(\alpha\hat{a}^\dagger - \alpha^*\hat{a}))\right]\hat{D}(s\alpha) \qquad (2.65)$$
$$= \alpha$$

This simple result can then be used as a differential equation to solve for $\hat{F}(s)$.

$$\frac{d}{ds}\hat{F}(s) = \alpha \quad\implies\quad \hat{F}(s) = s\alpha + F(0) = s\alpha + \hat{a} \quad\implies\quad \hat{F}(1) = \hat{D}^\dagger(\alpha)\hat{a}\hat{D}(\alpha) = \hat{a} + \alpha \qquad (2.66)$$

With this result, the main impact of the displacement operator on any coherent state can be calculated. Using $\hat{F}(1)$ on some coherent state $|\beta\rangle$ and multiplying each side by the displacement operator ($\hat{D}$ is unitary), one writes

$$\hat{a}\hat{D}(\alpha)|\beta\rangle = \hat{D}(\alpha)(\hat{a} + \alpha)|\beta\rangle = (\beta + \alpha)\hat{D}(\alpha)|\beta\rangle \qquad (2.67)$$

Which shows that $\hat{D}(\alpha)|\beta\rangle$ is an eigenstate of $\hat{a}$, with eigenvalue $\alpha + \beta$. From this, it can be said that

$$\hat{D}(\beta)|\alpha\rangle = C|\alpha + \beta\rangle \qquad \text{with} \qquad C \in \mathbb{C} \qquad (2.68)$$

Thanks to this important result, one understands both the name "displacement operator" (it acts in a manner similar to a translation operator in the basis of coherent states) and how to build these coherent states. It is however important to note that only the proportionality was proved yet, the value of C for different cases will be discussed later. However, one can note from Equation 2.67 (where β is taken to be the vibrational ground state) that[16]

$$\hat{D}(\alpha)|0\rangle = |\alpha\rangle \qquad (2.69)$$

Thanks to this expression, each pure coherent state is precisely defined with respect to the ground state via a given displacement operator. It is important to note that the vacuum is the same state in both the energy eigenstate basis and the coherent state basis (both are the unique state annihilated by $\hat{a}$). Thanks to the above, the relation between these coherent states and the usual energy eigenstates can also be shown. Starting with

$$\hat{D}(\alpha)|0\rangle = e^{\alpha\hat{a}^\dagger - \alpha^*\hat{a}}|0\rangle \qquad (2.70)$$

the BCH formula for the factorisation of an exponential of non commuting operators is used

$$e^X e^Y = e^Z \qquad \text{with} \qquad Z = X + Y + \frac{1}{2}[X,Y] + HOC \qquad (2.71)$$

Where the notation "HOC" is used for terms including higher order commutators. Here, since X and Y are terms in $\hat{a}$ and $\hat{a}^\dagger$, their commutator will give the identity (up to a sign), and since any operator commutes with the identity, it can be said that these HOC are all zero in this case. The result then gives

$$e^{\alpha\hat{a}^\dagger}e^{-\alpha^*\hat{a}} = e^{\alpha\hat{a}^\dagger - \alpha^*\hat{a} + \frac{1}{2}[\alpha\hat{a}^\dagger, -\alpha^*\hat{a}]} = e^{\alpha\hat{a}^\dagger - \alpha^*\hat{a} + \frac{1}{2}|\alpha|^2\mathbb{1}} = \hat{D}(\alpha)e^{\frac{1}{2}|\alpha|^2} \qquad (2.72)$$

This then easily leads to an expression for a coherent state $|\alpha\rangle$ in the energy eigenbasis

$$|\alpha\rangle = \hat{D}(\alpha)|0\rangle = e^{\alpha\hat{a}^\dagger}e^{-\alpha^*\hat{a}}e^{-\frac{1}{2}|\alpha|^2}|0\rangle \qquad (2.73)$$

---

[16]One could argue that the following equation, too, should include some unknown phase C. However, defining the basis such that $|\alpha\rangle$ is the eigenstate of $\hat{a}$ with eigenvalue α is not a full definition of $|\alpha\rangle$, since it does not fix any phase, this remaining freedom can be used by defining $|\alpha\rangle = \hat{D}(\alpha)|0\rangle$.

$$= e^{-\frac{1}{2}|\alpha|^2} \sum_{n=0}^{\infty} \frac{(\alpha \hat{a}^{\dagger})^n}{n!} |0\rangle \tag{2.74}$$

$$= e^{-\frac{1}{2}|\alpha|^2} \sum_{n=0}^{\infty} \frac{\alpha^n}{\sqrt{n!}} |n\rangle \tag{2.75}$$

Where the fact that the annihilation operator annihilates the vacuum was used (only the 1 in the Taylor expansion of its exponential remains), as well as the definition of the creation operator $\hat{a}^{\dagger} |n\rangle = \sqrt{n+1} |n+1\rangle$. With this expression, the overlap between coherent states is easily calculated (see Appendix A.4)

$$\langle \beta | \alpha \rangle = e^{\beta^* \alpha - \frac{1}{2}(|\beta|^2 + |\alpha|^2)} \tag{2.76}$$

This proves that the coherent state basis is overcomplete (non-orthogonal states), but it also proves that the basis states have unit norm.

The coherent states used in the above (and in the rest of this document) are sometimes called *canonical coherent states*, because they minimise the uncertainty of both $\hat{x}$ and $\hat{p}$ (other types of coherent states do exist, such as *squeezed coherent states*). However, this distinction has no real impact in the work done in this document. The next section moves on to consider the phase space and the impact of the displacement operator.

2.3.3 X-P Phase Space

To understand the impact of the displacement operator, it is useful to introduce the phase space using the coherent states previously mentioned. In this quantum harmonic oscillator context, the quadrature will be defined using modified (dimensionless) position and momentum operators

$$\hat{P} = \sqrt{\frac{1}{\hbar m \omega}} \hat{p} \qquad \hat{X} = \sqrt{\frac{m\omega}{\hbar}} \hat{x} \tag{2.77}$$

Since creation/annihilation operators are built on the $\hat{x}$ and $\hat{p}$ operators, they can then easily be expressed using these quadrature operators

$$\hat{a} = \sqrt{\frac{m\omega}{2\hbar}} \left(\hat{x} + \frac{i}{m\omega} \hat{p} \right) = \frac{\hat{X} + i\hat{P}}{\sqrt{2}} \tag{2.78}$$

$$\hat{a}^{\dagger} = \sqrt{\frac{m\omega}{2\hbar}} \left(\hat{x} - \frac{i}{m\omega} \hat{p} \right) = \frac{\hat{X} - i\hat{P}}{\sqrt{2}} \tag{2.79}$$

Now solving the above for $\hat{X}$ and $\hat{P}$, the quadrature can be written

$$\hat{P} = i\frac{\hat{a}^{\dagger} - \hat{a}}{\sqrt{2}} \qquad \hat{X} = \frac{\hat{a}^{\dagger} + \hat{a}}{\sqrt{2}} \tag{2.80}$$

Which results in the commutation relation $[\hat{X}, \hat{P}] = i$ (from Equation 2.77, this result is simply the dimensionless version of the usual $[\hat{x}, \hat{p}] = i\hbar$). While other conventions do exist (regarding the constant factor, $\sqrt{2}$ or 2), the above is the convention that will be preferred throughout this work.

Next, it is useful to see how the expectation values of these quadratures behave with respect to coherent states.

$$\langle \alpha | \hat{X} | \alpha \rangle = \frac{1}{\sqrt{2}} (\langle \alpha | \hat{a}^{\dagger} | \alpha \rangle + \langle \alpha | \hat{a} | \alpha \rangle) = \frac{1}{\sqrt{2}} (\alpha^* + \alpha) = \sqrt{2}\mathcal{R}(\alpha) \tag{2.81}$$

Where one remembers that $\langle \alpha | \hat{a}^{\dagger} = \alpha^* \langle \alpha |$, and that coherent states have unit norm ($\langle \alpha | \alpha \rangle = 1$). Similarly,

$$\langle \alpha | \hat{P} | \alpha \rangle = \frac{i}{\sqrt{2}} (\langle \alpha | \hat{a}^{\dagger} | \alpha \rangle - \langle \alpha | \hat{a} | \alpha \rangle) = \frac{i}{\sqrt{2}} (\alpha^* - \alpha) = \sqrt{2}\mathcal{I}(\alpha) \tag{2.82}$$

From this and what was said earlier, it becomes clear that the real and complex parts of the complex parameter α which defines the coherent state are (up to a factor $\sqrt{2}$) the expectation value of the quadratures, which are known to be the dimensionless position and momentum. To this, the fact that coherent states are minimum uncertainty states in the X-P phase space must be added.

Their representation in the phase space then appears as a disc (of radius $\sqrt{\hbar/2}$ representing the minimised uncertainty) that is centred around $X = \sqrt{2}\mathcal{R}(\alpha)$ and $P = \sqrt{2}\mathcal{I}(\alpha)$.

Physically, coherent states are therefore the quantum states that are the closest to classical states in terms of how they can be interpreted. And the displacement operator corresponds to an actual displacement in the X-P phase space[17].

Some additional details concerning the interpretation of the displacement operator are found in Appendix B (where the interpretation of the operator as a displacement in the X-P phase space is shown on a fully general state). An additional approach to the operator and its links to classical mechanics can also be found in [39].

2.3.4 Composition and Phase Space Loops

This section examines the composition of several displacement operators and its impact. This will answer the previous questions concerning the nature of the phase C (first mentioned in Equation 2.68), and then enable the introduction of phase space loops. Contrary to what one may think following the previous developments, consecutive displacement operators do not exactly behave like simple translations, they generate an additional phase.

$$\hat{D}(\beta)\hat{D}(\alpha) = e^{\beta\hat{a}^\dagger - \beta^*\hat{a}}e^{\alpha\hat{a}^\dagger - \alpha^*\hat{a}} \tag{2.83}$$

$$= e^{\beta\hat{a}^\dagger - \beta^*\hat{a} + \alpha\hat{a}^\dagger - \alpha^*\hat{a} + (\beta\alpha^* - \beta^*\alpha)/2} \tag{2.84}$$

$$= e^{(\beta\alpha^* - \beta^*\alpha)/2}e^{(\beta+\alpha)\hat{a}^\dagger - (\beta+\alpha)^*\hat{a}} \tag{2.85}$$

$$= e^{(\beta\alpha^* - \beta^*\alpha)/2}\hat{D}(\beta + \alpha) \tag{2.86}$$

Where the BCH formula was used once again. Interestingly, this confirms that despite the similarity, the quantum displacement operators do not compose in the same way as translations do in classical mechanics. There is an additional phase factor[18] that is generated, and it can be computed in terms of α and β as

$$\frac{\beta\alpha^* - \beta^*\alpha}{2} = (|\beta|e^{i\arg\beta}|\alpha|e^{-i\arg\alpha} - |\beta|e^{-i\arg\beta}|\alpha|e^{i\arg\alpha})/2 \tag{2.87}$$

$$= \frac{|\beta||\alpha|}{2}(e^{i(\arg\beta - \arg\alpha)} - e^{-i(\arg\beta - \arg\alpha)}) \tag{2.88}$$

$$= i|\beta||\alpha|\sin(\arg\beta - \arg\alpha) \tag{2.89}$$

From this, it is shown that a set of consecutive displacements which are parallel in the phase space does not lead to an additional phase factor. However, in general, two nonparallel displacements will generate this additional phase. An illustration of the situation in the phase space can be found in Figure 2.2.

---

[17]It is important to note that due to the yet undiscussed additional phase C (see Equation 2.68), displacement operators are however not equivalent to classical translations, this is discussed in more detail in the next section.

[18]Seeing Equation 2.86, one can easily see that $\beta\alpha^* - \beta^*\alpha$ is a pure imaginary number. In addition, even before doing the calculation, since $\hat{D}$ is unitary ($\hat{D}^\dagger(\alpha) = \hat{D}(-\alpha) = \hat{D}^{-1}(\alpha)$), the factors C could only be phase factors (any number of unitary operators applied on a normalised state will still result in a normalised state).
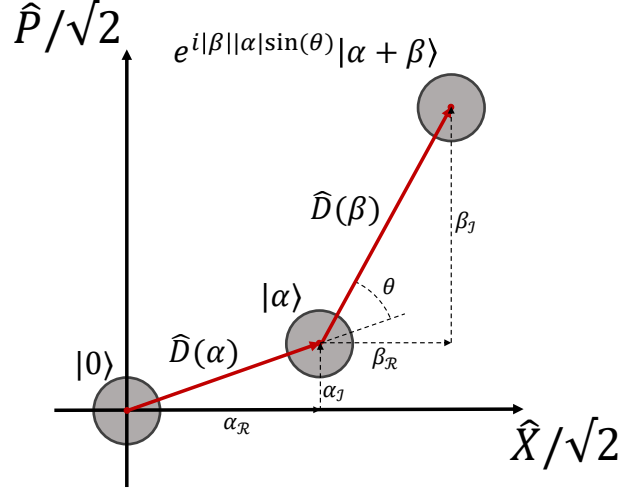
Figure 2.2: Schematic of the X-P phase space and of the impact of two displacement operators applied on $|0\rangle$. The grey disks represent the resulting coherent states after applying each operator. The origin is the state $|0\rangle$. It is important to remember that axes are slightly modified (see the $\sqrt{2}$ factor on each axis), this was done in order to simplify the expression of the distances added on the dashed lines (see Equation 2.81 and 2.82). Indices $\mathcal{R}$ and $\mathcal{I}$ are used to denote real and imaginary parts of complex numbers.

The last point examined in this section is the impact of sets of displacement operations which create loops in the phase space. These loops are crucial to how geometrical gates work. As a starting point, a simple parallelogram shape in the phase space is examined. The total operator associated with it is called $\hat{U}$, and some notations are shortened by using $\hat{D}(\beta) = e^{\hat{X}}$ and $\hat{D}(\alpha) = e^{\hat{Y}}$.

$$\hat{U} = \hat{D}(-\beta)\hat{D}(-\alpha)\hat{D}(\beta)\hat{D}(\alpha) = e^{-\hat{X}}e^{-\hat{Y}}e^{\hat{X}}e^{\hat{Y}} \tag{2.90}$$

$$= e^{-\hat{X}}e^{-\hat{Y}}e^{\hat{X}+\hat{Y}}e^{(\beta\alpha^*-\beta^*\alpha)/2} \tag{2.91}$$

$$= e^{-\hat{X}}e^{-\hat{Y}+\hat{X}+\hat{Y}}e^{\beta\alpha^*-\beta^*\alpha} \tag{2.92}$$

$$= e^{-\hat{X}}e^{\hat{X}}e^{\beta\alpha^*-\beta^*\alpha} \tag{2.93}$$

$$= e^{i2|\alpha||\beta|\sin(\arg\beta-\arg\alpha)} = e^{iA} \tag{2.94}$$

Where A is the area of the parallelogram in the phase space[19]. This result can be generalised relatively easily by carefully examining Equation 2.90 to 2.93.

Firstly, the last displacement operator which closes the loop (Equation 2.93) has no effect on the global phase, its only role is to cancel the remaining operator ($e^{\hat{X}}$ in Equation 2.93). To see that this result is general, one can refer to Figure 2.2 and think in terms of translations. To close a loop with translations, the last step necessarily has to be the opposite of the resulting translation of all other steps. In terms of displacement operators, these two are (anti)parallel, and there is therefore no additional phase generated.

Secondly, one can see from Equation 2.90 and 2.91, by using Equation 2.89 that the combination of two displacement operators leads to the displacement operator of the sum with an additional phase factor of the (triangular) area included (in X-P phase space). This phase factor is positive if the triangle is drawn in an anti-clockwise manner, and negative if it is drawn in a clockwise manner[20].

---

[19]It would then be twice the area measured in the "$X/\sqrt{2}$-$P/\sqrt{2}$" phase space used in Figure 2.2.

[20]Taking Figure 2.2 as an example, the triangle (defined by its two sides as the two displacement vectors, or by its vertices as the three states the displacements link) is drawn in an anti-clockwise manner (ie : θ is positive). In this case, if $\beta_{\mathcal{I}}$ was negative, then θ would be negative too, and the triangle drawn would be drawn in a clockwise fashion, which would lead to a negative phase contribution.

By the same arguments used on infinitesimal triangles, one can then see that (in the X-P phase space) any anti-clockwise closed loop will lead to a phase factor of iA ($-iA$ if clockwise). An example is available in Figure 2.3 in the case of only positive (anti-clockwise) contributions. The example represents the following mathematical progression

$$\hat{D}(\lambda)\hat{D}(\epsilon)\hat{D}(\delta)\hat{D}(\gamma)\hat{D}(\beta) = \hat{D}(\lambda)\hat{D}(\epsilon)\hat{D}(\delta)e^{iA_1}\hat{D}(\gamma + \beta) \tag{2.95}$$

$$= \hat{D}(\lambda)\hat{D}(\epsilon)e^{i(A_1+A_2)}\hat{D}(\delta + \gamma + \beta) \tag{2.96}$$

$$= \hat{D}(\lambda)e^{i(A_1+A_2+A_3)}\hat{D}(\epsilon + \delta + \gamma + \beta) \tag{2.97}$$

$$= \hat{D}(\lambda)e^{iA}\hat{D}(-\gamma) \tag{2.98}$$

$$= e^{iA} \tag{2.99}$$
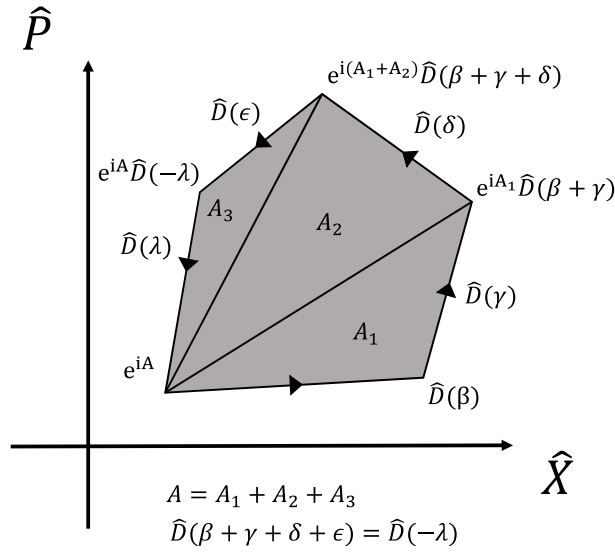
Figure 2.3: Schematic underlining how a succession of displacement operators forming a loop in the X-P phase space is equivalent to an overall phase factor equal to the area enclosed by the loop. This result is just an example using 5 displacement operators, but can be generalised to any number of them. The sign of the phase factor depends on whether the surface is defined in an anti-clockwise ($+$) or clockwise ($-$) manner.

Moving on to a sum of infinitesimal displacements, this generalises to any complex shape in the phase space. One can for instance imagine tracing a closed curve that intersects itself, as shown in Figure 2.4. As mentioned in the caption, this will result in the phase factor $e^{i(A_1-A_2)}$, with A_2 the area of the clockwise "sub-loop", and A_1 the area of the anti-clockwise "sub-loop".
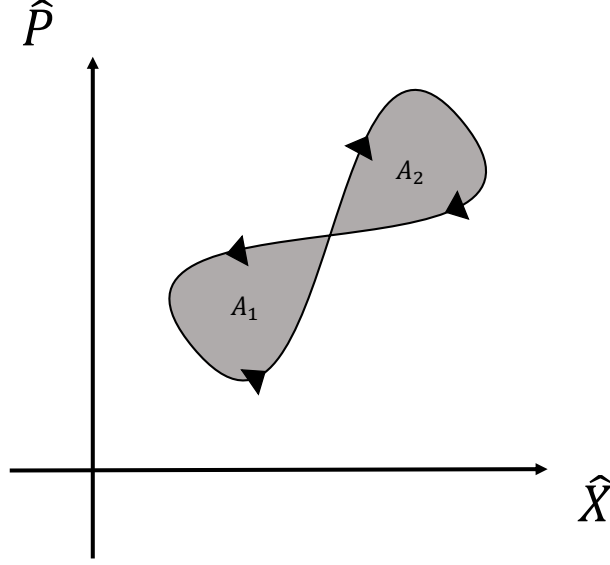
Figure 2.4: Schematic of a more complex loop in the phase space. By generalising the above result on each closed section of the complex loop, the phase factor will be of $e^{i(A_1 - A_2)}$.

2.3.5 Conditional Displacement Operators

In addition, this result can also be generalised to the *conditional displacement operator* mentioned earlier and other similar operators. If one uses an operator that is similar to the displacement operator but has the form

$$\hat{D}_{\hat{Y}}(\alpha) = e^{(\alpha \hat{a}^\dagger - \alpha^* \hat{a})\hat{Y}} \tag{2.100}$$

where $\hat{Y}$ is an operator that commutes with both $\hat{a}$ and $\hat{a}^\dagger$ (and therefore $\hat{Y}$ commutes with $\hat{D}_{\hat{Y}}$). Then, the use of this on the ket $|\alpha\rangle \otimes |y\rangle$ where $|y\rangle$ is an eigenstate of $\hat{Y}$ will just lead to a "conditional" displacement operator (*i.e.* the amplitude of the displacement α will just become $y\alpha$, and change according to witch $\hat{Y}$ eigenstate it is applied to). In this case, all the calculations made above can easily be adapted, just adding this new $\hat{Y}$ operator. Looking back at the previous developments, one can easily confirm that a set of these $\hat{D}_{\hat{Y}}$ operators forming a closed loop in the X-P phase space will give

$$\hat{U}_{\text{closed}} = e^{iA\hat{Y}^2} \tag{2.101}$$

with A the area discussed above (either positive or negative according to orientation). This is of crucial importance for geometric gates. The use of a seemingly trivial operation on a first ancilla state (the coherent state is left unchanged by the closed loop, apart from the new overall phase) generates a nonlinear action on the second state.

2.4 Milburn Gate

With all that was done in the previous sections of this chapter, deriving the expression for Milburn gate becomes a very easy task. By using the very last result for loops in the X-P phase space, it could even be considered trivial. In the following, the expression for the gate is derived and a comparison is made with other similar gates

2.4.1 Derivation

The set of operations proposed by G.J. Milburn in [10] for his new "Non Linear" (NL) gate is

$$U_{NL} = e^{i\kappa_x \hat{X} \hat{J}_z} e^{i\kappa_p \hat{P} \hat{J}_z} e^{-i\kappa_x \hat{X} \hat{J}_z} e^{-i\kappa_p \hat{P} \hat{J}_z} \tag{2.102}$$

This can easily be rewritten as a set of conditional displacement operators forming a phase space loop (using Equation 2.80), for which the result of Section 2.3.5 can be used

$$\hat{U}_{NL} = \hat{D}_{\hat{j}_z}(i\kappa_x/\sqrt{2})\hat{D}_{\hat{j}_z}(-\kappa_p/\sqrt{2})\hat{D}_{\hat{j}_z}(-i\kappa_x/\sqrt{2})\hat{D}_{\hat{j}_z}(\kappa_p/\sqrt{2}) = e^{i\kappa_x\kappa_p\hat{J}_z^2} \tag{2.103}$$

Apart from a bit of care for the factors of $\sqrt{2}$ that must be applied on the displacement lengths (see Equations 2.81 and 2.82), obtaining this result is made extremely easy by the above discussions on the displacement operator and the X-P phase space.

If the only interest here was to obtain the final answer, this section could already be closed here. However, the general displacement operator results that were used here are not used in [10]. As was mentioned, the main objective of this chapter is to present the Milburn gate and the mathematical tools that can be of use. In order to present a larger set of mathematical tools to solve the problem, the following also presents an approach that does not require the displacement operator developments of the previous section.

Starting from Equation 2.102 without using displacement operators, simplifying the expression requires the use of the intermediate result

$$e^{i\kappa_p\hat{P}\hat{J}_z}\hat{X}e^{-i\kappa_p\hat{P}\hat{J}_z} = \hat{X} + \kappa_p\hat{J}_z \tag{2.104}$$

which is proven in Appendix A.5.
Using this result, one can write (using the usual trick $X^{-1}e^a X = e^{X^{-1}aX}$)

$$U_{NL} = e^{i\kappa_x\hat{X}\hat{J}_z}e^{i\kappa_p\hat{P}\hat{J}_z}e^{-i\kappa_x\hat{X}\hat{J}_z}e^{-i\kappa_p\hat{P}\hat{J}_z} \tag{2.105}$$

$$= e^{i\kappa_x\hat{X}\hat{J}_z}e^{-i\kappa_x e^{i\kappa_p\hat{P}\hat{J}_z}\hat{X}e^{-i\kappa_p\hat{P}\hat{J}_z}\hat{J}_z} \tag{2.106}$$

$$= e^{i\kappa_x\hat{X}\hat{J}_z}e^{-i\kappa_x\left(\hat{X}+\kappa_p\hat{J}_z\right)\hat{J}_z} \tag{2.107}$$

$$= e^{-i\theta\hat{J}_z^2} \tag{2.108}$$

Where $\hat{J}_z$ commutes with all other operators. This is exactly the result that was required.

Depending on the number of ions in the trap, this result is a phase gate with the resulting phase depending on the amplitude of the collective spin. Taking an example with two ions, this gives the two qubit gate described by Table 2.2. By using this gate with other single qubit gates, it is possible to transform it into one of the universal quantum gates, such as the CNOT gate.

Input state	Output state
$|gg\rangle$	$e^{-i\theta}|gg\rangle$
$|ge\rangle$	$|ge\rangle$
$|eg\rangle$	$|eg\rangle$
$|ee\rangle$	$e^{-i\theta}|ee\rangle$

Table 2.2: Milburn gate result on a two ion system (since it is left invariant, the mechanical state is omitted from the notations).

2.4.2 Other Similar Gates

The Milburn gate presented in this chapter is not the only gate that was proposed which exhibits the same type of interesting behaviour[21]. While some context for geometric gates in general was given in the

---

[21] As mentioned previously, this behaviour includes its ability to couple previously uncoupled subsystems (which has several implications, such as generating entangled states between trapped ions.), and its robustness.

introduction of this work, the Milburn gate was not compared to other gates. Now that the theoretical aspects are understood, it is possible to do so.

Since these other gates are not the object of this work, the following discussion will not directly prove the cited results, but will always provide the relevant references when citing mathematical results.

2.4.2.1   Sørensen-Mølmer Gate

One geometric gate that is very similar to the Milburn gate is the Sørensen-Mølmer gate [30; 40]. This section presents it and relates it to the Milburn gate.

This new geometric gate can be seen as the generalisation of the Milburn gate to a continuous case. While the Milburn gate relies on a rectangular loop in the phase space, the Sørensen-Mølmer gate uses a circular loop. From a limit point of view, this gate can be seen as the limit of a regular polygon shaped loop as its number of sides grows (the limit of this being a circle). The expression that will be derived in the coming chapter for a pulsed optomechanical system could be used to derive the Sørensen-Mølmer, in the limit of a high number of pulses forming a closed loop (this is actually directly discussed in [30]).

From a physical realisation point of view, this gate still relies on a bichromatic laser interaction (two lasers at different frequencies), but these lasers use different frequences from the Milburn gate case. The Milburn gate is realised with two lasers of identical intensity (and no relative phase) with frequencies equal to the lower and upper sidebands[22] of the system . The Sørensen-Mølmer gate however, uses slightly detuned lasers ($\omega_0 \pm \delta$ instead of $\omega_0 \pm \omega_m$). When these lasers are used to obtain a global interaction Hamiltonian (in a similar way to what was done in Section 2.3.1), the expression obtained is

$$\hat{H}_I = 2\Omega \hat{J}_x \cos(\delta t) - \sqrt{2}\Omega \hat{J}_y \bigg(\hat{x}\Big(\cos((\omega_m - \delta)t) + \cos((\omega_m + \delta)t) \Big)$$
$$+ \hat{p}\Big(\sin((\omega_m - \delta)t) + \sin((\omega_m + \delta)t) \Big) \bigg) \quad (2.109)$$

where notations were adapted from [40] to match the ones used here, δ being the detuning (it is close to ω_m). After some approximations and calculations, the evolution operator for the Sørensen-Mølmer gate gives (see [40] for details)

$$\hat{U}(t) = e^{-iA(t)\hat{J}_y^2} e^{-iF(t)\hat{J}_y \hat{x}} e^{-iG(t)\hat{J}_y \hat{p}} \quad (2.110)$$

which can be linked to an overall phase and a displacement operator (which is logical, since the gate is a continuous operator, the phase space loop will only be closed for a particular choice of t, when $G(t) = F(t) = 0$). This result directly gives a single operator amounting to a continuous circular loop in the phase space (an explicit calculation of $A(t)$, $F(t)$ and $G(t)$ can be used to show that the loop is indeed a circle of particular radius). This loop is either closed or open depending on the choice of the parameters. A comparison of the phase space loops between the two gates can be found in Figure 2.5

---

[22] The main energy transition being ω_0 ($\hbar\omega_0 >> \hbar\omega_m$), the two sidebands are $\omega_0 + \omega_m$ and $\omega_0 - \omega_m$.
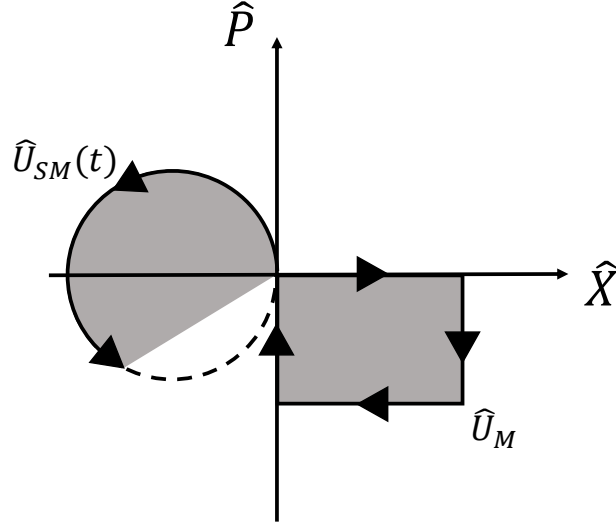
Figure 2.5: Schematic of a simple representation of the phase space loops of the Milburn gate ($\hat{U}_M$) and an application of the Sørensen-Mølmer for time t ($\hat{U}_{SM}(t)$). In this example t was chosen such that the circular loop is not closed yet.

The implication from the nature of the Sørensen-Mølmer gate seems to be that this new gate can be faster and more reliable than Milburn's gate. Since it is the result of a single bichromatic laser interaction, there is no need to have a set of four different pulses (which all need accurate control in time, relative phase, and frequency). Given its relative simplicity in terms of laser control, a potential improvement in rapidity could be argued. In addition, since the interaction time only needs to be accurately controlled once (a single continuous operation) instead of four times, it also seems to indicate a lower susceptibility to control errors[23].

While these points may have an impact, the full picture is more complex than that, and different schemes can be imagined to improve the performance of both gates (see [30]). One example of a scheme that was proposed in [30] to improve Sørensen-Mølmer gate performance was to use the gate on a very small circular path that is followed many times. In this case, the full area would be summed for each time the system goes through the loop, but since the loop is small, any control error would not bring the (mechanical) system far from its starting state.

In practice the Sørensen-Mølmer gate has first been experimentally realised by the research groups Boulder, Ann Arbor, and Oxford [31].

2.4.2.2 Cirac-Zoller Gate

There are several features of the Cirac-Zoller gate ([41]) that set it apart from the two previous gates. The most important being that this new gate is not a geometrical phase gate. It does not take advantage of a loop in the phase space of the mechanical system. However, the similarities lay in the fact that the Cirac-Zoller gate can be used in similar applications (in the trapped ion setting, it also uses the mechanical state as an ancilla to couple the states of different ions). Another feature that sets the Cirac-Zoller gate apart from the two previous geometric gates is that it uses individual ion access, while the others where described here with collective spin operators.

The fundamental idea behind this gate is to have as set of three consecutive operations on two separate ions. The set of operations is described below, and a representation is available in Figure 2.6

1. A laser shining on the first ion, at frequency $\omega_0 - \omega_m$, this couples $|e\alpha 0\rangle$ and $|g\alpha 1\rangle$ (where α is a placeholder representing the state of the second ion, which can be anything). The duration of the pulse is chosen in order for the transition to be complete (π pulse).

---

[23]One may come to this conclusion by imagining the system to be susceptible to a maximum error on t of ϵ, for each pulse.

2. Next, a specially tuned laser on the second ion excites an auxiliary state "a", the pulse duration is set such that the state stays unchanged, but an additional -1 phase is added (2π pulse).

3. Finally, another laser on the first ion, identical to the first one, for the same time (π pulse).
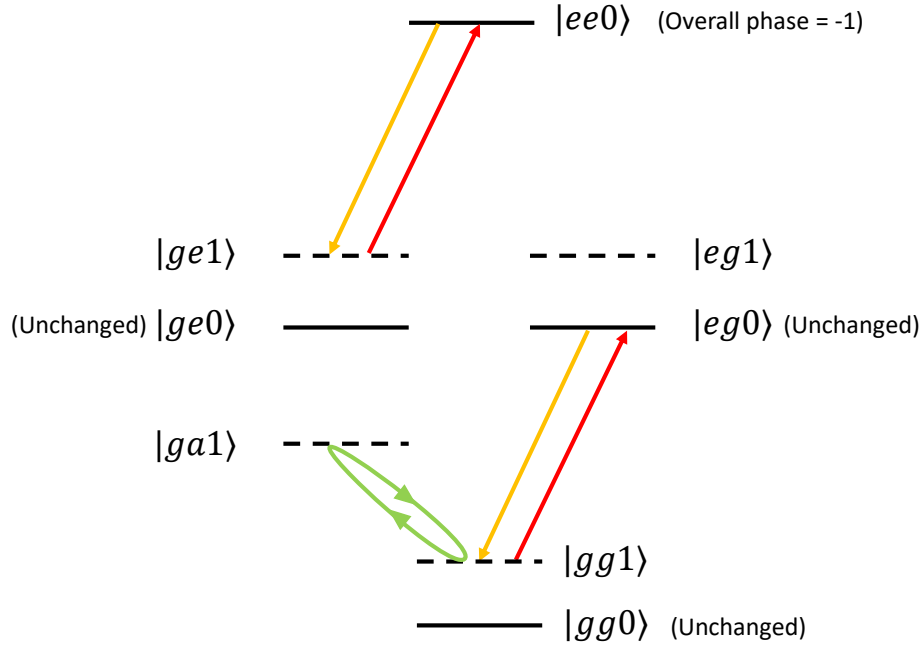
Figure 2.6: Schematic of the application of the Cirac-Zoller gate. The yellow giving the effect of the first, green of the second, and red of the last laser pulse. Dashed lines represent energy levels that are temporarily used by the gate but that are not used as qubit states. Yellow and red pulses generate a $-i$ additional phase, and green a -1 additional phase.

This action on any starting state (that is still in the mechanical ground state) is summarised in Table 2.3.

Starting state	After pulse 1	After pulse 2	After pulse 3
$|gg0\rangle$	$|gg0\rangle$	$|gg0\rangle$	$|gg0\rangle$
$|ge0\rangle$	$|ge0\rangle$	$|ge0\rangle$	$|ge0\rangle$
$|eg0\rangle$	$-i\,|gg1\rangle$	$i\,|gg1\rangle$	$|eg0\rangle$
$|ee0\rangle$	$-i\,|ge1\rangle$	$-i\,|ge1\rangle$	$-\,|ee0\rangle$

Table 2.3: Representation of the evolution of the internal states throughout the different steps implementing the Cirac-Zoller gate.

As can be seen from this Table 2.3, the Cirac-Zoller gate is an implementation of the controlled phase gate (which can be seen as equivalent to the CNOT gate [41]).

While this gate does not use an overall trivial displacement of the mechanical state in its phase space, it uses a trivial displacement of the mechanical state in the space of its energy eigenstates. As can be seen from Figure 2.6, the first vibrational mode was used, but overall, no mechanical excitation was added to the output state.

The disadvantages of this approach when compared to the geometric gates presented above can actually be relatively strongly linked to the discussion in Section 1.2.2.3. The main disadvantage of the

Cirac-Zoller gate being that it is not well adapted to systems that are not cooled to the ground state. For instance, let us consider the starting state $|gg1\rangle$ instead of $|gg0\rangle$, this state will be affected by the first and last pulses, and end up with a -1 phase, while the gate was supposed to leave it invariant.

One could also consider heating rate as a factor, which, if large enough, will generate mechanical state changes during the gate's operation. Heating rate could actually be seen as a bigger problem for geometric gates, since they are slower (adiabatic condition). However, the Cirac-Zoller gate is impacted by any mechanical state change anyway. This means that this difference will only favour the Cirac-Zoller gate if its action is so much faster that the heating rate can be neglected for it, but not for the geometric gates.

In practice, the Cirac-Zoller gate has been experimentally realised by the Innsbruck research group [31].

Chapter 3

Pulsed Geometric Gate in Optomechanics

So far in this document, the first chapter introduced the field of quantum gates and geometric phase quantum gates via a general discussion about quantum computing. Next, the second chapter presented the Milburn gate on trapped ions, and with it most of the mathematical tools necessary to understand geometric gates in general. This chapter can now examine the implementation of a pulsed geometric gate in an optomechanical system.

It should be noted here that optomechanical systems are a bit different in their applications than the previously presented trapped ion devices. Optomechanical systems are more often studied with the application of advanced sensors than quantum computers in mind. The reason for this being that they have not been shown to constitute very promising qubits. However, apart from the qubit themselves, the phonon-light interaction phenomena that can happen in quantum computers also leads to research on optomechanical systems [42]. In addition, quantum gates in optomechanical systems are also an important research subject, as they constitute a precise way to manipulate the quantum states of light and matter [17; 43]. As a tool to manipulate the quantum states of light, optomechanical systems similar to the one studied in this work could be used in both advanced sensing and quantum computing applications.

The optomechanical gate relies on periodic short interactions between the optical state and the mechanical oscillator. Even with the mathematical tools developed in the previous chapter, there are still a few mathematical hurdles to overcome in order to rigorously derive the corresponding operator. After an introduction to the physical realisation of this system, the following therefore presents some mathematical prerequisites. Once this is done, a preliminary study for the case of constant interaction is made, followed by the core discussion on time dependent interactions. This chapter ends with the derivation of a final closed form expression for the geometric gate operator in this system.

3.1 Physical realisation

While it is rather the mathematical behaviour of the optomechanical system than its actual physical realisation that is of interest here, it is still important to examine how the actual physical system should operate. This is done in order to have a global understanding of what is actually happening in such a system, and to avoid completely losing our grip on the physical reality while doing longer mathematical developments. In addition, taking the time to consider the physical reality behind the equations can help in having some intuition of what should or should not happen in the coming mathematical developments.

An optomechanical system is created by the physical coupling of an optical cavity and a mechanical oscillator. Both systems are quantised[1] and have their own set of creation-annihilation operators, named $\hat{a}/\hat{a}^\dagger$ and $\hat{b}/\hat{b}^\dagger$. A schematic of the situation can be found in Figure 3.1, which shows the simplest

---

[1]Contrarily to the previous chapter, the optical field is therefore quantised as a part of the full quantum state. Its creation/annihilation operators act on the corresponding Fock space to create/annihilate photons.

optomechanical system : an optical cavity with one of its sides affixed to a mechanical spring. This side of the optical cavity can then move according to the strength exerted by both the mechanical spring and the optical cavity, coupling the two systems. While this physical realisation of an optomechanical system is not the only possibility (other possibilities include for instance the membrane approach discussed in [17; 43], or the more complex system in [42]), it is a lot simpler (both mathematically and from a fabrication point of view).
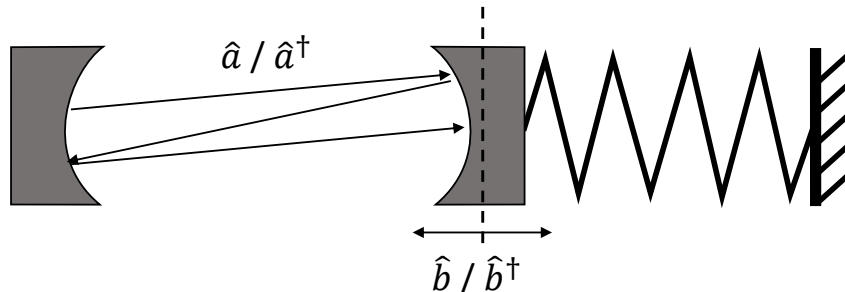

Figure 3.1: General schematic of an optomechanical system. The $\hat{a}$ and $\hat{b}$ sets of ladder operators correspond to the optical and mechanical subsystems respectively.

The main idea behind this optomechanical realisation of geometric gates is to use the optical states as the system of interest (*i.e.* the quantum element on which the gate is applied). Conceptually, the mechanical system is the tool used to apply the transformation on the system of interest (*i.e.* the optical system), via the coupling that exists between the two (this is similar to the previous case, where the mechanical states were used as a tool to influence the ionic states). This type of approach has seen some interest in different papers, such as in [16; 44].

In practice, the gate is realised by a set of very short periodic interactions separated by free evolution of both systems. For the system to behave in this way (ie : to have free mechanical evolution between the interactions), the optical states must be stored outside of the cavity represented in Figure 3.1 for some time intervals. Some physical apparatus must therefore be able to store the optical states without changing them (for the free mechanical evolution intervals), and send them back in the cavity to interact with the mechanical system (for the short interactions). This is accomplished via a delay line in which the optical states evolve freely. The type of experimental setup that this creates is similar to the one used in [16].

3.2 Fundamental Mathematical Tools

This section includes two topics, namely a reminder on the interaction picture, and an introduction about the Magnus expansion. While the interaction picture is the main approach used for solving the dynamics of interacting quantum systems, the Magnus expansion is required for solving differential equations including non commuting operators.

3.2.1 Reminder on Interaction Picture

In theory, the formalism of interaction picture could be considered to be known by the reader in this work. However, the following use of interaction picture transformations is slightly more advanced than what is usually done in postgraduate courses (as well as than what was done in the previous chapter). It was therefore considered desirable to include a quick reminder here.

The "interaction picture" approach to quantum systems is based on a transformation of the said "Schrödinger picture", which is the usual approach used to present and teach quantum mechanics. Since this work mainly uses the interaction picture, the convention chosen in the following is to add an index S to specify when an operator is in the Schrödinger picture, and no index if it is in the interaction

picture (*i.e.* the default in the present document is the interaction picture). Let a Schrödinger picture Hamiltonian be split into its free and interacting part

$$\hat{H}_S = \hat{H}_{0,S} + \hat{H}_{I,S} \tag{3.1}$$

This split via a simple sum can always be done because the corresponding non interacting system (*i.e.* the sum of the Hamiltonians of the subsystems without the coupling terms) will always have a given energy that can be expressed as an eigenvalue of $\hat{H}_{0,S}$. The impact of the interactions will then be added through a second contribution (ie : the sum of the coupling terms).

However, while this split is always possible, it is somewhat arbitrary. There is, indeed, nothing which stops one from making different choices for what is considered to be included in the "interaction" part of the Hamiltonian. For more complex Hamiltonians, different choices are possible, and it is even possible to do successive splits and transformations. It is important to be careful with this type of calculation since successive transformations may not necessarily give identical results to a single "larger" transformation. It is therefore crucial to remember which choices were made in order to avoid the inevitable confusion that would arise if one compares operators or vectors that were actually obtained in different pictures.

Before moving on to the theoretical description of the interaction picture, a quick note particular to the system of interest in this document is made. As mentioned in Section 3.1, the system of interest here is the set of optical states. In addition, the frequency of the optical system is generally far superior to the frequency of the mechanical one. It is therefore conventional to work in the interaction picture defined with respect to the free optical Hamiltonian. However, calculations can still be simplified by doing an additional interaction picture transformation with respect to the free mechanical Hamiltonian. As will be seen later, the optomechanical system defined in Section 3.1 is indeed one of the cases where it is useful to define successive interaction pictures. In this particular case the S index will be used to denote the starting Schrödinger picture, no index will be used for the conventional interaction picture (with respect to the optical free Hamiltonian), and the I index will be used to denote objects after the second transformation (with respect to the mechanical free Hamiltonian).

The idea behind the interaction picture is to modify the point of view taken by subtracting from kets their free time evolution.

$$|\psi(t)\rangle = \hat{U}_{0,S}^{-1}(t)\,|\psi_S(t)\rangle \qquad \text{with} \qquad \hat{U}_{0,S}(t) = e^{-i\hat{H}_{0,S}t/\hbar} \tag{3.2}$$

It is useful to remember (as indicated by the notation above) that the actual time evolution operator when interactions are present is not only the free part, so kets in interaction picture are not time independent[2]. Considering some operator acting on a given Schrödinger picture ket as $|\psi_S'(t)\rangle = \hat{X}_S(t)\,|\psi_S(t)\rangle$, the corresponding operation can then be expressed as

$$|\psi'\rangle = e^{i\hat{H}_{0,S}t/\hbar}\,|\psi_S'\rangle = e^{i\hat{H}_{0,S}t/\hbar}\hat{X}_S(t)\,|\psi_S\rangle = e^{i\hat{H}_{0,S}t/\hbar}\hat{X}_S(t)e^{-i\hat{H}_{0,S}t/\hbar}\,|\psi\rangle = \hat{X}(t)\,|\psi\rangle \tag{3.3}$$

And so the interaction picture operator $X(t)$ which corresponds to the Schrödinger picture operator $\hat{X}_S(t)$ is obtained

$$\hat{X}(t) = \hat{U}_{0,S}^{-1}(t)\hat{X}_S(t)\hat{U}_{0,S}(t) \tag{3.4}$$

Now that the basics of interaction picture are covered, it is possible to examine the time evolution of kets. One has to be slightly more careful here, because one cannot use the expression of the structure of the time evolution operator in Schrödinger picture and simply transform it according to Equation 3.3[3]. Instead, the correct approach is to make use of the Schrödinger equation to obtain a differential equation for the interaction picture ket $|\psi\rangle$. One writes

$$i\hbar\frac{\partial}{\partial t}\,|\psi\rangle = i\hbar\frac{\partial}{\partial t}\left(\hat{U}_{0,S}^{-1}(t)\,|\psi_S\rangle\right) = i\hbar\frac{\partial}{\partial t}\left(e^{i\hat{H}_{0,S}t/\hbar}\,|\psi_S\rangle\right) \tag{3.5}$$

$$= -\hat{H}_{0,S}e^{i\hat{H}_{0,S}t/\hbar}\,|\psi_S\rangle + i\hbar e^{i\hat{H}_{0,S}t/\hbar}\frac{\partial}{\partial t}\,|\psi_S\rangle \tag{3.6}$$

---

[2]In the case of weak interactions however, a well known approximation that is sometimes used consists in taking interaction picture kets to be close to time independent.

$$= -\hat{H}_{0,S}e^{i\hat{H}_{0,S}t/\hbar} |\psi_S\rangle + e^{i\hat{H}_{0,S}t/\hbar}\hat{H}_S(t) |\psi_S\rangle \tag{3.7}$$

$$= e^{i\hat{H}_{0,S}t/\hbar}(\hat{H}_S(t) - \hat{H}_{0,S})e^{-i\hat{H}_{0,S}t/\hbar} |\psi\rangle \tag{3.8}$$

$$= \hat{H}_I(t) |\psi\rangle \tag{3.9}$$

This shows that the time evolution of states in interaction picture is only related to $\hat{H}_I(t)$, which is the transformed interacting part of the Hamiltonian (ie : $\hat{H}_I = \hat{U}_{0,S}^{-1}\hat{H}_{I,S}\hat{U}_{0,S}$). It can be useful to note that, in the above demonstration, the free part of the (Schrödinger picture) Hamiltonian was supposed to be time independent, while no such hypothesis was made on the interacting part.

3.2.2 Magnus Expansion

Given how the previous subsection ends on the differential equation for the interaction picture time evolution operator, one could wonder why it was not directly solved. The reason for this is that the solution to this differential equation is not always as simple as often implied in calculus courses. The main problem being the commutation of the operator in it, and the question of whether $[\hat{H}_I(t_1), \hat{H}_I(t_2)]$ is zero or not.

This problem is addressed by the Magnus expansion and its corresponding Magnus series.

3.2.2.1 Magnus Series

The Magnus series give, when exponentiated, the exact solution for any first order homogeneous linear differential equation that includes a linear operator with non necessarily trivial commutation relations. The problem can be stated as follows

$$\frac{\partial f}{\partial t} = A(t)f(t) \tag{3.10}$$

with $A(t)$ a known linear operator[4], and $f(t)$ the unknown vector one wishes to compute. According to the behaviour of the linear operator, and in particular according to its commutation relations at different times, the solution to this problem could be written as

$$f(t) = \begin{cases} f(t_0)\exp\left(\int_{t_0}^t dt A(t)\right) & \text{if } [A(t_1), A(t_2)] = 0 \ \forall \ t_1, \ t_2, \\ f(t_0)\exp\left(\sum_{k=1}^{\infty} \Omega_k(t, t_0)\right) & \text{otherwise.} \end{cases} \tag{3.11}$$

Where $\Omega_k(t)$ are the terms of the Magnus series (needed if the commutation relation is not zero). The following discusses the details of the Magnus series directly, but the series itself will not be proven here (a detailed proof and discussion can be found in [45]). However, Appendix D does give some indication concerning how the usual solution fails in the case of a non commuting time dependent operator.

Using the same notations as above, the definition of the first three terms of the Magnus series ([45]) can be given as follows

---

[3]Since one knows that the time evolution operator in Schrödinger picture is simply (where a time independent Hamiltonian is supposed for this example)

$$\hat{U}_S(t) = \exp\left(-i\hat{H}_S t/\hbar\right)$$

One could be tempted to just transform it as if it was any operator (according to 3.4) and think to have obtained the time evolution operator in the interaction picture. Unfortunately, this is incorrect. One way to detect that something is not right would be to carefully take a look at the transformation law itself (Equation 3.4) and at Equation 3.3. One then notes that the transformation law only includes a single time variable t. If $\hat{X}$ in Equation 3.3 was the time evolution from t_1 to t, then $|\psi_S\rangle$ is at t_1, but the result should be $|\psi'\rangle$ at t. One would therefore obtain a contradiction in the transformation law (in this case, it should include both t and t_1 following Equation 3.3, but was defined with only t in Equation 3.4).

[4]Of course $A(t)$ does not have to be linear in t, what is meant here is that $A(t)$ is an operator linear in its action on the mathematical object $f(t)$. For instance, $A(t)$ can be a matrix and $f(t)$ a vector. In a more general setting, the vector spaces V to which $f(t)$ belongs can be infinite dimensional (like many eigenbases in quantum mechanics).

$$\Omega_1(t, t_0) = \int_{t_0}^{t} dt_1 A(t_1)$$

$$\Omega_2(t, t_0) = \frac{1}{2} \int_{t_0}^{t} dt_1 \int_{t_0}^{t_1} dt_2 \, [A(t_1), A(t_2)] \tag{3.12}$$

$$\Omega_3(t, t_0) = \frac{1}{6} \int_{t_0}^{t} dt_1 \int_{t_0}^{t_1} dt_2 \int_{t_0}^{t_2} dt_3 \left(\Big[\big[A(t_1), A(t_2) \big], A(t_3) \Big] + \Big[A(t_1), \big[A(t_2), A(t_3) \big] \Big] \right)$$

Using the Magnus series boils down to the usual solution[5] if $[A(t_1), A(t_2)] = 0$ for all t_1, t_2. While the apparent symmetry of the above formulae could lead one to suspect the existence of a simpler global expression for the nth term of the Magnus series (eg : the above n integral structure applied on the sum of possible nested commutators, divided by a global $n!$ factor), this is unfortunately not the case. The simplicity of these first three terms is deceptive, and the following terms are more complex. $\Omega_4(t)$ makes the $n!$ factor assumption break down, and $\Omega_5(t)$ includes a very lengthy sum of nested commutators where the different terms have different signs and amplitudes [46].

Fortunately, despite the difficulty in writing a global formula for any term in the series, the nth term of the Magnus series always includes integrals of commutators of order n (in the linear operator A)[6]. Thanks to this fact, as long as some commutator of order m vanishes for some operator A, then all the following terms after m vanish too. This will be used extensively in the following calculations.

The time evolution operator can now be written as

$$\hat{U}(t, t_0) = \exp\left(\sum_{k=1}^{\infty} \Omega_k(t, t_0) \right) \qquad \text{with } \Omega \text{ computed using} \qquad A(t) = \frac{-i}{\hbar} \hat{H}_I(t) \tag{3.13}$$

3.2.2.2 Composition of Magnus Expansion Solutions

Given the particular form of the first terms of the Magnus series (see Equation 3.12), one could wonder about the impact of this on the composition of several time evolution operator. By definition, the time evolution operator should obey the property of translation operators, namely

$$\hat{U}(t_2, t_1)\hat{U}(t_1, t_0) = \hat{U}(t_2, t_0) \tag{3.14}$$

While this property is still verified, it is non trivial to prove explicitly. A proof for the case of interest in this work is given in Appendix C.1

3.3 Time-independent Interaction

Now that the most important mathematical tools have been presented, it is possible to come back to the optomechanical system and its behaviour. This section presents a first preliminary study in the case of time independent Hamiltonian. In this case, the total system is evolving with its subsystems continuously interacting. Starting with the full Hamiltonian in the Schrödinger picture

$$\hat{H}_S = \hat{H}_{0,S,m} + \hat{H}_{0,S,f} + \hat{H}_{int,S} = \hbar\omega_m \hat{b}^\dagger \hat{b} + \hbar\omega_f \hat{a}^\dagger \hat{a} - \hbar g \hat{a}^\dagger \hat{a} \frac{\hat{b}^\dagger + \hat{b}}{\sqrt{2}} \tag{3.15}$$

Where one can recognize the free mechanical oscillator Hamiltonian ($\hat{H}_{0,S,m}$), the free field Hamiltonian ($\hat{H}_{0,S,f}$), and finally, the coupling term giving the interaction Hamiltonian between the two systems (all in Schrödinger picture). If this interaction Hamiltonian does not seem intuitive, a very short discussion on how it can be understood is available in Appendix C.2.

---

[5] Hence, one could consider Equation 3.11 to be a slight abuse of notation, because the Magnus expansion solution is also the correct solution for the first case.

[6] Even if they are at different times, the term "nth order commutator" will be used to denote any set of $(n-1)$ nested commutators of n elements. For instance $[A(t_1), [A(t_2), A(t_3)]]$ will be referred to as a "third order commutator".

Defining the interaction picture with respect to the system of interest (*i.e.* the optical free propagation), the Hamiltonian is split as

$$\hat{H}_S = \hat{H}_{0,S,f} + \hat{H}_{I,S} = \hat{H}_{0,S,f} + \left(\hat{H}_{0,S,m} + \hat{H}_{int,S} \right) \tag{3.16}$$

Since $\hat{H}_{0,S,f}$ is time independent, there is no need for Magnus expansion, and the free optical Schrödinger time evolution operator is built as

$$\hat{U}_{0,S,f}(t) = e^{-i\hat{H}_{0,S,f}t/\hbar} = e^{-i\omega_f \hat{a}^\dagger \hat{a} t} \tag{3.17}$$

Since this commutes with everything in the remaining "interaction Hamiltonian", the transformation amounts to only keeping the remaining Hamiltonian

$$\hat{H}(t) = \hat{U}_{0,S,m}^{-1}(t) \left(\hat{H}_{0,S,m} + \hat{H}_{I,S} \right) \hat{U}_{0,S,m}(t) \tag{3.18}$$

$$= \hat{H}_{0,S,m} + \hat{H}_{I,S} = \hat{H} \tag{3.19}$$

This is the default picture that is used (therefore written without index), and it is defined with respect to the free evolution of the optical system only. Now, a second interaction picture can be defined in this first one, to further simplify the calculations by subtracting the free mechanical evolution.

$$\hat{H} = \hat{H}_{0,S,m} + \hat{H}_{I,S} = \hat{H}_{0,S,m} + \hat{H}_{int,S} \tag{3.20}$$

In this second interaction picture (denoted by an additional I index), the interaction Hamiltonian is computed as (once again, there is no need for Magnus expansion to derive $\hat{U}_{0,S,m}$ because $\hat{H}_{0,S,m}$ is time independent)

$$\hat{H}_I(t) = \hat{U}_{0,S,m}^{-1}(t)\hat{H}_{int,S}\hat{U}_{0,S,m}(t) \tag{3.21}$$

$$= e^{i\hat{H}_{0,S,m}t/\hbar} \left(-\hbar g \hat{a}^\dagger \hat{a} \frac{\hat{b}^\dagger + \hat{b}}{\sqrt{2}} \right) e^{-i\hat{H}_{0,S,m}t/\hbar} \tag{3.22}$$

$$= -\frac{\hbar g \hat{a}^\dagger \hat{a}}{\sqrt{2}} e^{i\omega_m \hat{b}^\dagger \hat{b} t} \left(\hat{b}^\dagger + \hat{b} \right) e^{-i\omega_m \hat{b}^\dagger \hat{b} t} \tag{3.23}$$

Once again, the way to proceed is to use the lemma of the BCH formula (see Equation 2.18).

$$\hat{H}_I(t) = -\frac{\hbar g \hat{a}^\dagger \hat{a}}{\sqrt{2}} \sum_{n=0}^{\infty} \frac{\left[\left(i\omega_m \hat{b}^\dagger \hat{b} t \right)^n, \hat{b}^\dagger + \hat{b} \right]}{n!} \tag{3.24}$$

$$= -\frac{\hbar g \hat{a}^\dagger \hat{a}}{\sqrt{2}} \sum_{n=0}^{\infty} (i\omega_m t)^n \frac{\left[\left(\hat{b}^\dagger \hat{b} \right)^n, \hat{b}^\dagger + \hat{b} \right]}{n!} \tag{3.25}$$

Considering that it can be easily shown that

$$\left[\hat{b}^\dagger \hat{b}, \hat{b}^\dagger \right] = \hat{b}^\dagger \left[\hat{b}, \hat{b}^\dagger \right] = \hat{b}^\dagger \qquad \text{and} \qquad \left[\hat{b}^\dagger \hat{b}, \hat{b} \right] = \left[\hat{b}^\dagger, \hat{b} \right] \hat{b} = -\hat{b}, \tag{3.26}$$

the above then gives

$$\hat{H}_I(t) = -\frac{\hbar g \hat{a}^\dagger \hat{a}}{\sqrt{2}} \sum_{n=0}^{\infty} (i\omega_m t)^n \frac{\left[\left(\hat{b}^\dagger \hat{b} \right)^n, \hat{b}^\dagger + \hat{b} \right]}{n!} \tag{3.27}$$

$$= -\frac{\hbar g \hat{a}^\dagger \hat{a}}{\sqrt{2}} \sum_{n=0}^{\infty} (i\omega_m t)^n \frac{\hat{b}^\dagger + (-1)^n \hat{b}}{n!} \tag{3.28}$$

37

$$= -\hbar g \hat{a}^\dagger \hat{a} \frac{e^{i\omega_m t}\hat{b}^\dagger + e^{-i\omega_m t}\hat{b}}{\sqrt{2}} \tag{3.29}$$

This time, this result has non trivial commutation relations at different times. In order to compute the interaction picture time evolution operator, it is therefore necessary to use Magnus expansion. Looking back at the details in Section 3.2.2, Equation 3.12 is used to compute the first terms of the Magnus series. Using the previous notations, $A(t)$ is written as

$$A(t) = \frac{-i}{\hbar}\hat{H}_I(t) = i g \hat{a}^\dagger \hat{a} \frac{e^{i\omega_m t}\hat{b}^\dagger + e^{-i\omega_m t}\hat{b}}{\sqrt{2}} \tag{3.30}$$

The terms of the Magnus series are then computed as

$$\Omega_1(t, t_0) = \int_{t_0}^{t} dt_1 A(t_1) = \frac{g}{\omega_m}\hat{a}^\dagger \hat{a} \frac{(e^{i\omega_m t} - e^{i\omega_m t_0})\hat{b}^\dagger - (e^{-i\omega_m t} - e^{-i\omega_m t_0})\hat{b}}{\sqrt{2}} \tag{3.31}$$

$$\Omega_2(t, t_0) = \frac{1}{2}\int_{t_0}^{t} dt_1 \int_{t_0}^{t_1} dt_2 \, [A(t_1), A(t_2)] = i\frac{g^2(\hat{a}^\dagger\hat{a})^2}{2\omega_m}\left(t - t_0 - \frac{\sin\left(\omega_m(t - t_0)\right)}{\omega_m}\right) \tag{3.32}$$

Details for the calculation of Ω_2 are available in Appendix C.3.

Seeing the result for $\Omega_2(t, t_0)$, the only remaining operator is $(\hat{a}^\dagger\hat{a})^2$ which commutes with all other operators. Thus, all terms that follow in the Magnus series are null (any power of $\hat{a}^\dagger\hat{a}$ commutes with $\hat{H}_I(t)$, whatever the value of t). This is why this type of behaviour (vanishing third order commutator) was already suggested in some of the developments made in Section 3.2.2.

The time evolution operator of the interacting system is

$$\hat{U}_I(t, t_0) = \exp\left(\frac{g}{\omega_m}\hat{a}^\dagger\hat{a}\frac{(e^{i\omega_m t} - e^{i\omega_m t_0})\hat{b}^\dagger - (e^{-i\omega_m t} - e^{-i\omega_m t_0})\hat{b}}{\sqrt{2}}\right.$$
$$\left. + i\frac{g^2(\hat{a}^\dagger\hat{a})^2}{2\omega_m}\left(t - t_0 - \frac{\sin\left(\omega_m(t - t_0)\right)}{\omega_m}\right)\right) \tag{3.33}$$

While this general result is an important point to make concerning the dynamics of the interacting system, it does not yet represent the interaction of interest here. As mentioned before, this section presents a preliminary study done on the time independent case, which will be adapted when moving on to the time dependent case.

Slightly anticipating what will come next, it is interesting to consider a very short time and the choice of $t_0 = 0$ (both the length of the interaction and t are then denoted by τ). The time evolution operator for this short time τ becomes

$$\hat{U}_I(\tau) = \hat{U}_I(\tau, 0) = \exp\left(\frac{g}{\omega_m}\hat{a}^\dagger\hat{a}\frac{(e^{i\omega_m \tau} - 1)\hat{b}^\dagger - (e^{-i\omega_m \tau} - 1)\hat{b}}{\sqrt{2}} + i\frac{g^2(\hat{a}^\dagger\hat{a})^2}{2\omega_m}\left(\tau - \frac{\sin\left(\omega_m\tau\right)}{\omega_m}\right)\right) \tag{3.34}$$

Now considering that the time τ during which the interacting system is left to evolve is very short, one only keeps the highest order in τ for each operator.

$$\hat{U}_I(\tau) \approx \exp\left(i g\tau\hat{a}^\dagger\hat{a}\frac{\hat{b}^\dagger + \hat{b}}{\sqrt{2}} + i\frac{g^2(\hat{a}^\dagger\hat{a})^2}{2\omega_m^2}(\omega_m\tau)^3\right) \tag{3.35}$$

If one considers that $\omega_m\tau$ is sufficiently small, it is finally possible to neglect the impact of the $(\hat{a}^\dagger\hat{a})^2$ operator (since it is multiplied by $(\omega_m\tau)^3$), and obtain

$$\hat{U}_I(\tau) \approx \exp\left(ig\tau\hat{a}^\dagger\hat{a}\frac{\hat{b}^\dagger + \hat{b}}{\sqrt{2}}\right) \tag{3.36}$$

This can be compared to the pulsed interaction of the time varying case obtained below, and, as expected, this expression corresponds to the gate operation for a single pulse. It is now important to remember that this time evolution operator is still in the second interaction picture (as indicated by the I index). To come back to the original interaction picture, defined with respect to the optical free evolution only, one can write

$$\hat{U}_I(t)\,|\psi_I(0)\rangle = |\psi_I(t)\rangle = \hat{U}_{0,S,m}^{-1}(t)\,|\psi(t)\rangle = \hat{U}_{0,S,m}^{-1}(t)\hat{U}(t)\,|\psi(0)\rangle \tag{3.37}$$

Since $|\psi_I(0)\rangle = |\psi(0)\rangle$, the first interaction picture time evolution operator is calculated from the second interaction picture time evolution operator as

$$\hat{U}(\tau) = \hat{U}_{0,S,m}\hat{U}_I(\tau) \tag{3.38}$$

$$\approx \exp\left(-i\omega_m\hat{b}^\dagger\hat{b}\tau\right)\exp\left(ig\tau\hat{a}^\dagger\hat{a}\frac{\hat{b}^\dagger + \hat{b}}{\sqrt{2}}\right) \tag{3.39}$$

As a reminder, if one wanted to obtain the Schrödinger picture, one should just multiply by the factor $\exp\left(-i\omega_f\hat{a}^\dagger\hat{a}\tau\right)$ (following a similar reasoning to the above).

3.4 Time-varying Interaction

As mentioned before this section is the core discussion, it demonstrates how a gate similar to the Milburn gate can be obtained from an optomechanical system operating with a set of short interactions.

As a reminder, the state of interest is the optical state, which is exposed to periodic and very short interactions with the mechanical system. In between interactions, the optical states are sent into a delay line. This enables both the mechanical states and optical states to evolve freely, until the next interaction.

3.4.1 Statement of the Problem

In Shcrödinger picture, this behaviour would give the following time evolution operator for the total system

$$\hat{U}_{p,S}\,|\psi(0)\rangle = \prod_{n=0}^{p-1}\hat{U}_{1,S}\big((n+1)\Delta t, n\Delta t\big)\,|\psi(0)\rangle = |\psi(p\Delta t)\rangle \tag{3.40}$$

Where $\hat{U}_{p,S}$ is the Schrödinger picture time evolution operator for p interactions started at $t = 0$. Consequently, the notation $\hat{U}_{1,S}(t_0 + \Delta t, t_0)$ is used for a single time period (ie : a short interaction of duration τ followed by free mechanical propagation of duration $\Delta t - \tau$). The following objective is to find the interaction picture time evolution operator formulated as a product of n pulses, in a form similar to Equation 3.40.

At this point, it is important to stay rigorous with the notations. One cannot, for instance, write $\hat{U}(\Delta t)$, as the time evolution without approximation does depend on the absolute time, not only on time intervals (see Equation 3.33). In terms of notations, the single interaction time evolution operator can be defined as

$$\hat{U}_{1,S}\big((n+1)\Delta t, n\Delta t\big) = \hat{U}_{0,S}\big((n+1)\Delta t, n\Delta t + \tau\big)\hat{U}_S(n\Delta t + \tau, n\Delta t)) \tag{3.41}$$

where Δt is the periodicity of the pattern formed by turning the interaction on and off, and τ is the duration of the short interaction. In the above definition, one directly sees the short interaction with the full time evolution operator in Shcrödinger picture $\hat{U}_S$ during time τ, followed by the free propagation $\hat{U}_{0,S}$ during time $\Delta t - \tau$.

From a Hamiltonian perspective, this behaviour boils down to making the coupling depend on time

$$\hat{H}_S \to \hat{H}_S(t) \qquad \text{with} \qquad \hat{H}_S(t) = \hat{H}_{0,S,m} + \hat{H}_{0,S,f} + \hat{H}_{I,S} f(t) \tag{3.42}$$

Where $f(t)$ is a pulse wave as illustrated in Figure 3.2. As previously stated, the interaction here is very short in time, so the duty cycle $\tau/\Delta t$ is very small (this is not the case in Figure 3.2).
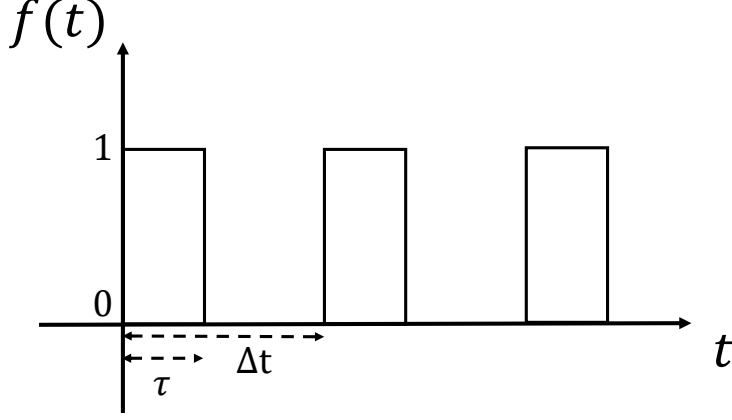

Figure 3.2: Simple plot of a general pulse wave with on time τ, periodicity Δt, and duty cycle $\tau/\Delta t$.

Looking back at Equations 3.16 to 3.23, the successive transformations in the two interaction pictures are done in the exact same manner as in the time independent case. One can for instance simply replace g by $g(t) = gf(t)$ in the final result. Following this, the (second) interaction picture interaction Hamiltonian is very similar to the previous case, only including an additional $f(t)$ factor[7]. Despite this high similarity, the following calculation of the Magnus series terms will be strongly impacted. Similarly to what was done in the time independent case, the next objective is to obtain a simple form for the (second) interaction picture time evolution operator. In this case, the object of interest is the time evolution operator for p interactions; $\hat{U}_p$.

3.4.2 Calculating the Magnus Series

Moving on to calculating Ω_1, one writes

$$\Omega_1(p\Delta t) = \Omega_1(p\Delta t, 0) = \int_0^{p\Delta t} dt \; A(t) f(t) \tag{3.43}$$

$$= ig\hat{a}^\dagger \hat{a} \int_0^{p\Delta t} dt \; \frac{e^{i\omega_m t}\hat{b}^\dagger + e^{-i\omega_m t}\hat{b}}{\sqrt{2}} f(t) \tag{3.44}$$

$$= \frac{ig\hat{a}^\dagger \hat{a}}{\sqrt{2}} \sum_{n=0}^{p-1} \int_{n\Delta t}^{n\Delta t + \tau} dt \; \left(e^{i\omega_m t}\hat{b}^\dagger + e^{-i\omega_m t}\hat{b} \right) \tag{3.45}$$

$$= \frac{g\hat{a}^\dagger \hat{a}}{\sqrt{2}\omega_m} \sum_{n=0}^{p-1} \left(\left(e^{i\omega_m(n\Delta t + \tau)} - e^{i\omega_m n\Delta t} \right)\hat{b}^\dagger - \left(e^{-i\omega_m(n\Delta t + \tau)} - e^{-i\omega_m n\Delta t} \right)\hat{b} \right) \tag{3.46}$$

$$= \frac{g\hat{a}^\dagger \hat{a}}{\sqrt{2}\omega_m} \sum_{n=0}^{p-1} \left(\left(e^{i\omega_m \tau} - 1 \right) e^{i\omega_m n\Delta t}\hat{b}^\dagger - \left(e^{-i\omega_m \tau} - 1 \right) e^{-i\omega_m n\Delta t}\hat{b} \right) \tag{3.47}$$

Next is the calculation of Ω_2, which is more impacted by the new $f(t)$ factor.

---

[7]For better readability and easier comparison in the coming calculations, the notation of $A(t)$ is still used to denote the time independent case expression. In this time dependent case, one will therefore use the same starting equations as before, simply replacing $A(t)$ by $A(t)f(t)$.

$$\Omega_2(p\Delta t) = \Omega_2(p\Delta t, 0) = \frac{1}{2} \int_0^{p\Delta t} dt \int_0^t dt' \ [A(t)f(t), A(t')f(t')] \tag{3.48}$$

$$= \frac{1}{2} \sum_{n=0}^{p-1} \int_{n\Delta t}^{n\Delta t + \tau} dt \int_0^t dt' \ [A(t), A(t')f(t')] \tag{3.49}$$

$$= \frac{1}{2} \sum_{n=0}^{p-1} \int_{n\Delta t}^{n\Delta t + \tau} dt \left(\sum_{m=0}^{n-1} \int_{m\Delta t}^{m\Delta t + \tau} dt' \ [A(t), A(t')] + \int_{n\Delta t}^t dt' \ [A(t), A(t')] \right) \tag{3.50}$$

The first set of simplifications for this are relatively straightforward and similar to the time independent case for Ω_2, details are included in Appendix C.4. The result of these simplifications gives

$$\Omega_2(p\Delta t) = i\frac{g^2(\hat{a}^\dagger \hat{a})^2}{\omega_m^2} \left(p\big(\omega_m\tau - \sin(\omega_m\tau)\big) + \big(1 - \cos(\omega_m\tau)\big) \sum_{n=0}^{p-1} \sum_{m=0}^{n-1} \sin\big(\omega_m(n-m)\Delta t\big) \right) \tag{3.51}$$

The next problem to solve in order to obtain a fully explicit formula is the problem of the sum of sines with angle in arithmetic progression. This problem is discussed in Appendix E, in which the following identity is proven

$$\sum_{k=0}^{n-1} \sin(a + kd) = \frac{\sin(nd/2)}{\sin(d/2)} \sin(a + (n-1)d/2) \tag{3.52}$$

Using this formula on the sum on the m index gives

$$\Omega_2(p\Delta t) = i\frac{g^2(\hat{a}^\dagger \hat{a})^2}{\omega_m^2} \left(p\big(\omega_m\tau - \sin(\omega_m\tau)\big) + \frac{1 - \cos(\omega_m\tau)}{\sin(\omega_m\Delta t/2)} \sum_{n=0}^{p-1} \sin(n\omega_m\Delta t) \sin\big((n+1)\omega_m\Delta t/2\big) \right) \tag{3.53}$$

Using the product-sum trigonometric identities, it is then possible to change this product of sines with n in their angle into a difference of cosines with n in their angle. Then, using the cosine version of the identity given in Equation 3.52, it is possible to obtain a fully explicit expression. Despite this possibility and the desire for a fully explicit formula, it will appear later that it is not useful to do this last step, which is why this last expression will be kept as is for now.

Knowing Ω_1 and Ω_2, and once again noting that all the following terms in the Magnus series are null ($\hat{a}^\dagger\hat{a}$ commutes with all operators in $A(t)$, and this is of course also true for $(\hat{a}^\dagger\hat{a})^2$), it is now possible to write the time evolution operator in interaction picture.

$$\hat{U}_p = e^{\Omega_1(p\Delta t) + \Omega_2(p\Delta t)} = e^{\Omega_1(p\Delta t)} e^{\Omega_2(p\Delta t)} \tag{3.54}$$

Where the exponential was easily split since $\Omega_2(p\Delta t)$ commutes with $\Omega_1(p\Delta t)$.

3.4.3 Splitting the Ω_1 Exponential

In order to find an expression similar to Equation 3.40, it is now necessary to examine the first exponential and to split it into a product

$$e^{\Omega_1(p\Delta t)} = \exp\left(\frac{g\hat{a}^\dagger\hat{a}}{\sqrt{2}\omega_m} \sum_{n=0}^{p-1} \left(\big(e^{i\omega_m\tau} - 1\big)e^{i\omega_m n\Delta t}\hat{b}^\dagger - \big(e^{-i\omega_m\tau} - 1\big)e^{-i\omega_m n\Delta t}\hat{b} \right) \right) \tag{3.55}$$

Since the arguments do not commute, the BCH formula must be used to split this sum inside the exponential in a product of exponentials. An important intermediate result is to compute the commutator of any two terms in that sum. Let the nth term in the sum be denoted as

$$A_n = \frac{g\hat{a}^\dagger\hat{a}}{\sqrt{2}\omega_m}\left(\left(e^{i\omega_m\tau}-1\right)e^{i\omega_m n\Delta t}\hat{b}^\dagger - \left(e^{-i\omega_m\tau}-1\right)e^{-i\omega_m n\Delta t}\hat{b}\right) \tag{3.56}$$

The exponential can therefore be simply written as

$$e^{\Omega_1(p\Delta t)} = \exp\left(\sum_{n=0}^{p-1}A_n\right) \tag{3.57}$$

The computation of the commutator of any two terms then reads (details in Appendix C.5)

$$[A_n, A_k] = 2i\frac{g^2(\hat{a}^\dagger\hat{a})^2}{\omega_m^2}\left(1-\cos(\omega_m\tau)\right)\sin\left(\omega_m(n-k)\Delta t\right) \tag{3.58}$$

This result is once again the commutator $(\hat{a}^\dagger\hat{a})^2$, which commutes with all other operators. As before, all the higher order commutators in the BCH formula vanish. Considering how higher order terms vanish, in order to split the last term of the sum from the rest of the exponential, one writes

$$e^{\Omega_1(p\Delta t)} = \exp\left(\sum_{n=0}^{p-1}A_n\right) = \exp\left(A_{p-1}\right)\exp\left(\sum_{n=0}^{p-2}A_n\right)\exp\left(-\frac{1}{2}\left[A_{p-1},\sum_{n=0}^{p-2}A_n\right]\right) \tag{3.59}$$

Replacing the result above, this gives

$$\exp\left(A_{p-1}\right)\exp\left(\sum_{n=0}^{p-2}A_n\right)\exp\left(-\sum_{n=0}^{p-2}i\frac{g^2(\hat{a}^\dagger\hat{a})^2}{\omega_m^2}\left(1-\cos(\omega_m\tau)\right)\sin\left(\omega_m(p-1-n)\Delta t\right)\right) \tag{3.60}$$

Taking a bit of time to think about this expression and how it would transform when splitting the other A_n terms from the main sum one by one, it is then possible to see the global result

$$e^{\Omega_1(p\Delta t)} = \left(\prod_{n=0}^{p-1}\exp\left(A_n\right)\right)\exp\left(-\sum_{k=1}^{p-1}\sum_{n=0}^{p-1-k}i\frac{g^2(\hat{a}^\dagger\hat{a})^2}{\omega_m^2}\left(1-\cos(\omega_m\tau)\right)\sin\left(\omega_m(p-k-n)\Delta t\right)\right) \tag{3.61}$$

where the exponential of the sum of A_n terms was finally completely split in a product of p exponentials with argument A_n. Using the previous identity for the sum of sines with angle in arithmetic progression, the second sum is computed to obtain

$$e^{\Omega_1(p\Delta t)} = \left(\prod_{n=0}^{p-1}\exp\left(A_n\right)\right)\exp\left(-i\frac{g^2(\hat{a}^\dagger\hat{a})^2}{\omega_m^2}\frac{1-\cos(\omega_m\tau)}{\sin(\omega_m\Delta t/2)}\right.$$
$$\left.\sum_{k=1}^{p-1}\sin\left((p-k)\omega_m\Delta t/2\right)\sin\left(\omega_m(p-k+1)\Delta t/2\right)\right) \tag{3.62}$$

where we note that the exponential in $(\hat{a}^\dagger\hat{a})^2$ can be rewritten as

$$\exp\left(-i\frac{g^2(\hat{a}^\dagger\hat{a})^2}{\omega_m^2}\frac{1-\cos(\omega_m\tau)}{\sin(\omega_m\Delta t/2)}\sum_{n=0}^{p-1}\sin\left(n\omega_m\Delta t/2\right)\sin\left((n+1)\omega_m\Delta t/2\right)\right) \tag{3.63}$$

where the order in which the sum is done was simply reversed, and the trivially null term $n=0$ was added. As always, given that it is a factor in $(\hat{a}^\dagger\hat{a})^2$, this factor commutes with everything in the above equations.

3.4.4 Second Interaction Picture Result and Approximations

Most remarkably, the rather complicated factor that was obtained after splitting the Ω_1 exponential *exactly* cancels the second part of $\Omega_2(p\Delta t)$ that was obtained[8] in Equation 3.53 !

The time evolution operator in this second interaction picture can then be written as

$$
\hat{U}_p = e^{\Omega_1(p\Delta t)}e^{\Omega_2(p\Delta t)} = \left(\prod_{n=0}^{p-1} \exp\left(A_n\right)\right)\exp\left(i\frac{g^2(\hat{a}^\dagger \hat{a})^2}{\omega_m^2}\left(p\big(\omega_m\tau - \sin(\omega_m\tau)\big)\right)\right)
$$

$$
\text{with} \qquad A_n = \left(\frac{g}{\omega_m}\hat{a}^\dagger\hat{a}\frac{(e^{i\omega_m\tau}-1)e^{i\omega_m n\Delta t}\hat{b}^\dagger - (e^{-i\omega_m\tau}-1)e^{-i\omega_m n\Delta t}\hat{b}}{\sqrt{2}}\right)
$$

(3.64)

Now, finally, the fact that τ was chosen to be very small can be considered. And only the highest order in $\omega_m\tau$ for the different operators in the expression is kept.

$$
\hat{U}_p = \left(\prod_{n=0}^{p-1} \exp\left(ig\tau\hat{a}^\dagger\hat{a}\frac{e^{i\omega_m n\Delta t}\hat{b}^\dagger + e^{-i\omega_m n\Delta t}\hat{b}}{\sqrt{2}}\right)\right)\exp\left(i\frac{g^2(\hat{a}^\dagger\hat{a})^2}{\omega_m^2}\frac{p(\omega_m\tau)^3}{6}\right)
$$

(3.65)

The final expression is then obtained considering that the third order in $\omega_m\tau$ for the $(\hat{a}^\dagger\hat{a})^2$ operator is sufficiently small to be neglected. Defining the strength of the interaction $\lambda = g\tau$, the angle $\theta = -\omega_m\Delta t$, and the operator $\hat{O} = \hat{a}^\dagger\hat{a}$, the final result is

$$
\hat{U}_p = \prod_{n=0}^{p-1} \exp\left(i\lambda\hat{O}\frac{e^{-in\theta}\hat{b}^\dagger + e^{in\theta}\hat{b}}{\sqrt{2}}\right)
$$

(3.66)

This is the identical[9] to the expression mentioned in [30] and is the main result of the above calculations. It is however not yet in a form which explicitly shows that this operator can be used to produce the Milburn gate, this will be shown in the next section by deriving the corresponding closed form expression.

Two final considerations are to be kept in mind about the above result.

Firstly, the expression found in Equation 3.66 includes a pi product symbol. While the pi product is generally defined from left to right (the first term is multiplied by the next term on its right side, and so on), it can be checked from Equation 3.59 that here however, this product was used as defined from the left (the second term multiplies the first one its left, and so on). The order of the terms in the above product is therefore the same as the order in which the associated operators would be applied ; $\hat{Z}_n...\hat{Z}_1\hat{Z}_0$.

Secondly, it can be useful to take note of the only two approximations that were made in the above. The first was to consider only the highest order in $\omega_m\tau$ for each operator, and the second was to neglect the impact of $(\hat{a}^\dagger\hat{a})^2(\omega_m\tau)^3$ when compared to $(\hat{a}^\dagger\hat{a})(\omega_m\tau)$.

3.4.5 First Interaction Picture and Schrödinger Picture Result

The final result in Equation 3.66 can already be interpreted relatively easily and used to understand that each factor in the product corresponds to an additional short interaction. However, each additional interaction is slightly different, since n changes for each additional term. The reader may wonder why that is, since all the short interactions are identical.

It is also not yet very clear from the expression what was the physical impact of the approximations that were done to derive Equation 3.66.

---

[8]And one can now see why keeping the sum on n instead of calculating it was an interesting choice, as we show that this sum cancels !

[9]There is actually a nuance between the two results, which lays in the definition of the pi product symbol. More details on this are given later.

The reason for this is because this expression is still in the second interaction picture. By going back to the first interaction picture (and even to the Schrödinger picture), it is possible to better interpret the expression, and explicitly see the impact of the approximations.

As explained in Equations 3.37, to transform the time evolution operator into the first interaction picture, one can just multiply by the free time evolution operator. A couple of algebraic manipulations can then be made to obtain a largely simplified the result.

$$\hat{U}(p\Delta t) = \hat{U}_{0,S,m}(p\Delta t)\hat{U}_p \tag{3.67}$$

$$= \exp\left(-i\omega_m \hat{b}^\dagger \hat{b} p\Delta t\right) \prod_{n=0}^{p-1} \exp\left(i\lambda\hat{O}\frac{e^{-in\theta}\hat{b}^\dagger + e^{in\theta}\hat{b}}{\sqrt{2}}\right) \tag{3.68}$$

$$= \prod_{n=0}^{p-1}\left(\exp\left(i\hat{b}^\dagger\hat{b}(n+1)\theta\right)\exp\left(i\lambda\hat{O}\frac{e^{-in\theta}\hat{b}^\dagger + e^{in\theta}\hat{b}}{\sqrt{2}}\right)\exp\left(-i\hat{b}^\dagger\hat{b}n\theta\right)\right) \tag{3.69}$$

$$= \prod_{n=0}^{p-1}\left(\exp\left(i\hat{b}^\dagger\hat{b}\theta\right)\exp\left(i\lambda\hat{O}\frac{e^{-in\theta}e^{i\hat{b}^\dagger\hat{b}n\theta}\hat{b}^\dagger e^{-i\hat{b}^\dagger\hat{b}n\theta} + e^{in\theta}e^{i\hat{b}^\dagger\hat{b}n\theta}\hat{b}e^{-i\hat{b}^\dagger\hat{b}n\theta}}{\sqrt{2}}\right)\right) \tag{3.70}$$

Once again making use of the BCH lemma introduced in Equation 2.18, one can compute

$$e^{i\hat{b}^\dagger\hat{b}n\theta}\hat{b}^\dagger e^{-i\hat{b}^\dagger\hat{b}n\theta} = \sum_{k=0}^{\infty}\frac{\left[\left(i\hat{b}^\dagger\hat{b}n\theta\right)^k, \hat{b}^\dagger\right]}{k!} = \sum_{k=0}^{\infty}\frac{(in\theta)^k\,\hat{b}^\dagger}{k!} = e^{in\theta}\hat{b}^\dagger \tag{3.71}$$

and similarly for the $\hat{b}$ term

$$e^{i\hat{b}^\dagger\hat{b}n\theta}\hat{b}e^{-i\hat{b}^\dagger\hat{b}n\theta} = e^{-in\theta}\hat{b} \tag{3.72}$$

When replacing back θ, $\hat{O}$, and λ by their original values, this then gives the very simple result

$$\hat{U}(p\Delta t) = \prod_{n=0}^{p-1}\left(\exp\left(-i\omega_m\hat{b}^\dagger\hat{b}\Delta t\right)\exp\left(ig\hat{a}^\dagger\hat{a}\frac{\hat{b}^\dagger + \hat{b}}{\sqrt{2}}\tau\right)\right) \tag{3.73}$$

$$= \left(e^{-i\hat{H}_{0,S,m}\Delta t/\hbar}e^{-i\hat{H}_{int,S}\tau/\hbar}\right)^p \tag{3.74}$$

$$= \left(\hat{U}_{0,S,m}(\Delta t)e^{-i\hat{H}_{int,S}\tau/\hbar}\right)^p \tag{3.75}$$

Directly, it is understood that the time evolution in the first interaction picture boils down to a simple interaction of duration τ during which the free mechanical evolution was neglected, followed by a free mechanical evolution of time Δt (instead of $\Delta t - \tau$). This resulting operator is then simply repeated p times (ie : the number of short interactions).

While this section could be seen as a bit of a mathematical step back from the expression that will lead to the final fully explicit geometric gate operator, it leads to extremely important results. Moving back to the previous pictures after the approximations were made in the more complex expressions and using this particular "pulse separated" expression enables to understand what these mathematical approximations mean in terms of actual physical behaviour. In addition, since it approximates the behaviour as something that precisely separates a purely mechanical time evolution from the rest, the expression derived in Equation 3.75 will be instrumental to adding dissipation to the system (which is the subject of Chapter 4). This "pulse separated" approach and its use for dissipation calculations constitutes an original result that was not found in the literature.

Physically, one realises that the two approximations that were done amount to

1. Neglect the free evolution of the systel during the interactions (*i.e.* neglect the free mechanical evolution during the short interactions).

2. Consider the mechanical system to evolve freely for a slightly longer time than the time between interactions. (*i.e.* Perform the following free mechanical evolution for time Δt instead of $\Delta t - \tau$).

For completeness, one can also take a look at the Schrödinger picture result. It simply adds the free optical evolution, which commutes with everything else anyway.

$$\hat{U}_S(p\Delta t) = \hat{U}_{0,S,f}(p\Delta t)\left(\hat{U}_{0,S,m}(\Delta t)e^{-i\hat{H}_{int,S}\tau/\hbar}\right)^p \tag{3.76}$$

3.5 Pulsed Geometric Gate closed-form expression

Section 3.4.4 derived the time evolution operator expression for the set of short interaction pulses in the second interaction picture. It lead to a product of exponentials with each exponential corresponding to one additional pulse. However, the expression obtained for $\hat{U}_p$ is not yet a closed form, and it is not trivial to recognise a geometric gate from this expression. It still includes a product of p exponentials. The objective of this section is to derive a closed form expression which will compute this large product, and which will explicitly show how the geometric gate arises in this system.

In order to reach this goal it will be useful to take advantage of the fact that each term in the product can be seen as a displacement operator, and use the previously derived mathematical tools linked to displacement operators.

Given the structure of the expression obtained for $\hat{U}_p$, it is possible to use the same notation as presented before for displacement operators. An "O-displacement" operator was previously defined as (see Section 2.3.5)

$$\hat{D}_O(\alpha) = e^{\hat{O}(\alpha\hat{a}^\dagger - \alpha^*\hat{a})} \tag{3.77}$$

where $\hat{O}$ is an operator which commutes with both the $\hat{a}^\dagger$ and the $\hat{a}$ operators. Looking back at Equation 3.66, one can directly see that each term can be seen as a single $\hat{O}$ displacement operator with the $\hat{b}^\dagger$ and $\hat{b}$ operators.

$$\hat{U}_p = \prod_{n=0}^{p-1} \exp\left(i\lambda\hat{O}\frac{e^{-in\theta}\hat{b}^\dagger + e^{in\theta}\hat{b}}{\sqrt{2}}\right) = \prod_{n=0}^{p-1} \hat{D}_O\left(\frac{i\lambda e^{-in\theta}}{\sqrt{2}}\right) \tag{3.78}$$

From the previous calculations, it is also known that displacement operators compose in the following way

$$\hat{D}_X(\alpha)\hat{D}_X(\beta) = \hat{D}_X(\alpha + \beta)\exp\left(i|\alpha||\beta|\sin(\arg\alpha - \arg\beta)\hat{X}^2\right) \tag{3.79}$$

Using this general result, one can then examine the result of the product of the set of $\hat{O}$ displacement operators

$$\hat{U}_p = \prod_{n=0}^{p-1} \hat{D}_O\left(\frac{i\lambda e^{-in\theta}}{\sqrt{2}}\right) = \hat{D}_O\left(\sum_{n=0}^{p-1}\frac{i\lambda e^{-in\theta}}{\sqrt{2}}\right)$$
$$\prod_{n=1}^{p-1}\exp\left(i\left|\frac{i\lambda e^{-in\theta}}{\sqrt{2}}\right|\left|\sum_{k=0}^{n-1}\frac{i\lambda e^{-ik\theta}}{\sqrt{2}}\right|\sin\left(\arg\left(\frac{i\lambda e^{-in\theta}}{\sqrt{2}}\right) - \arg\left(\sum_{k=0}^{n-1}\frac{i\lambda e^{-ik\theta}}{\sqrt{2}}\right)\right)\hat{O}^2\right) \tag{3.80}$$

As a first step, the product of $\hat{O}^2$ exponentials is set aside and denoted B.

$$\hat{U}_p = \hat{D}_O\left(\sum_{n=0}^{p-1}\frac{i\lambda e^{-in\theta}}{\sqrt{2}}\right)B \tag{3.81}$$

45

Examining the displacement operator itself and its argument, it is useful[10] to express this displacement operator in terms of the $\hat{X}$ and $\hat{P}$ operators (the quadrature operators). For this, let us come back to the expression of the displacement operator

$$\hat{D}_O(\alpha) = \exp\left(\hat{O}(\alpha\hat{b}^\dagger - \alpha^*\hat{b})\right)$$
$$= \exp\left(i\hat{O}(\sqrt{2}\alpha_{\mathcal{I}}\hat{X} - \sqrt{2}\alpha_{\mathcal{R}}\hat{P})\right) \tag{3.82}$$
$$= \exp\left(i\hat{O}(c_1\hat{X} - c_2\hat{P})\right)$$

where one keeps in mind that

$$\begin{cases} \alpha_{\mathcal{R}} = \mathrm{Re}\{\alpha\} \\ \alpha_{\mathcal{I}} = \mathrm{Im}\{\alpha\} \end{cases} \quad \text{and} \quad \begin{cases} \hat{X} = \left(\hat{b}^\dagger + \hat{b}\right)/\sqrt{2} \\ \hat{P} = i\left(\hat{b}^\dagger - \hat{b}\right)/\sqrt{2} \end{cases} \tag{3.83}$$

In the above, the two constants c_1 and c_2 were named, and need to be computed explicitly. Starting with c_1

$$c_1 = \sqrt{2}\alpha_{\mathcal{I}} = \sqrt{2}\,\mathrm{Im}\left\{\sum_{n=0}^{p-1} \frac{i\lambda e^{-in\theta}}{\sqrt{2}}\right\} \tag{3.84}$$
$$= \lambda\sum_{n=0}^{p-1} \cos(n\theta) \tag{3.85}$$
$$= \lambda\frac{\sin(p\theta/2)}{\sin(\theta/2)}\cos\left((p-1)\theta/2\right) \tag{3.86}$$

where the cosine version of the identity in Equation 3.52 (see Appendix E) was used. Very similarly for c_2, one writes

$$c_2 = \sqrt{2}\alpha_{\mathcal{R}} = \sqrt{2}\,\mathrm{Re}\left\{\sum_{n=0}^{p-1} \frac{i\lambda e^{-in\theta}}{\sqrt{2}}\right\} \tag{3.87}$$
$$= \lambda\sum_{n=0}^{p-1} \sin(n\theta) \tag{3.88}$$
$$= \lambda\frac{\sin(p\theta/2)}{\sin(\theta/2)}\sin\left((p-1)\theta/2\right) \tag{3.89}$$

The result can now be written as

$$\hat{U}_p = \exp\left(i\hat{O}(c_1\hat{X} - c_2\hat{P})\right)B \tag{3.90}$$

and the factor B is left to be examined. One can simplify

$$B = \prod_{n=1}^{p-1} \exp\left(i\left|\frac{i\lambda e^{-in\theta}}{\sqrt{2}}\right|\left|\sum_{k=0}^{n-1}\frac{i\lambda e^{-ik\theta}}{\sqrt{2}}\right|\sin\left(\arg\left(\frac{i\lambda e^{-in\theta}}{\sqrt{2}}\right) - \arg\left(\sum_{k=0}^{n-1}\frac{i\lambda e^{-ik\theta}}{\sqrt{2}}\right)\right)\hat{O}^2\right) \tag{3.91}$$

$$= \exp\left(\sum_{n=1}^{p-1} i\frac{\lambda^2}{2}\left|\sum_{k=0}^{n-1}e^{-ik\theta}\right|\sin\left(\arg\left(\frac{\lambda e^{-in\theta}}{\sqrt{2}}\right) + \frac{\pi}{2} - \frac{\pi}{2} - \arg\left(\sum_{k=0}^{n-1}\frac{\lambda e^{-ik\theta}}{\sqrt{2}}\right)\right)\hat{O}^2\right) \tag{3.92}$$

---

[10]While this will directly be used while simplifying the sum, the complex sum could be computed as is. The reason for expressing the displacement operator in terms of the quadrature operator is to make explicit the displacement in the phase space in the interpretation of the final result that will occur later. One may remember that one particularity of geometric gates is that they amount to a trivial displacement in the phase space.

$$= \exp\left(\sum_{n=1}^{p-1} i\frac{\lambda^2}{2} \left|\sum_{k=0}^{n-1} e^{-ik\theta}\right| \sin\left(-n\theta - \arg\left(\sum_{k=0}^{n-1} e^{-ik\theta}\right)\right)\hat{O}^2\right) \tag{3.93}$$

Where some trivial norms and arguments were computed, and the different exponential factors were merged in a single exponential (since their arguments commute). It is now useful to quickly consider the geometric sum that appears in Equation 3.93, as both its norm and argument are needed (details are included in Appendix C.6).

$$\sum_{k=0}^{n-1} e^{-ik\theta} = \frac{\sin(n\theta/2)}{\sin(\theta/2)} e^{-i(n-1)\theta/2} \tag{3.94}$$

In this form, it is now trivial to extract the norm and the argument, and rewrite Equation 3.93 as

$$B = \exp\left(\sum_{n=1}^{p-1} i\frac{\lambda^2}{2}\frac{\sin(n\theta/2)}{\sin(\theta/2)}\sin\left(-n\theta - \left(-(n-1)\theta/2\right)\right)\hat{O}^2\right) \tag{3.95}$$

$$= \exp\left(\sum_{n=1}^{p-1} i\frac{\lambda^2}{2}\frac{\sin(n\theta/2)}{\sin(\theta/2)}\sin\left(-(n+1)\theta/2\right)\hat{O}^2\right) \tag{3.96}$$

$$= \exp\left(ic_3\hat{O}^2\right) \tag{3.97}$$

To find an explicit form of this c_3 constant one writes

$$c_3 = \sum_{n=1}^{p-1} \frac{\lambda^2}{2}\frac{\sin(n\theta/2)}{\sin(\theta/2)}\sin\left(-(n+1)\theta/2\right) \tag{3.98}$$

$$= \frac{\lambda^2}{2\sin(\theta/2)}\sum_{n=1}^{p-1}\frac{1}{2}\left(\cos\left((2n+1)\theta/2\right) - \cos(-\theta/2)\right) \tag{3.99}$$

where one product-sum trigonometric identity was used, followed once again by one of the trigonometric sums proven in Appendix E. The final result can finally be written as

$$c_3 = \frac{\lambda^2}{4\sin(\theta/2)}\left(\frac{\sin(p\theta/2)}{\sin(\theta/2)}\cos\left(\theta/2 + (p-1)\theta/2\right) - \cos(\theta/2) - (p-1)\cos(\theta/2)\right) \tag{3.100}$$

$$= \frac{\lambda^2}{4\sin(\theta/2)}\left(\frac{\sin(p\theta/2)}{\sin(\theta/2)}\cos(p\theta/2) - p\cos(\theta/2)\right) \tag{3.101}$$

$$= -\lambda^2\frac{p\sin(\theta/2)\cos(\theta/2) - \sin(p\theta/2)\cos(p\theta/2)}{4\sin^2(\theta/2)} \tag{3.102}$$

$$= -\frac{\lambda^2}{2}\frac{p\sin(\theta) - \sin(p\theta)}{4\sin^2(\theta/2)} \tag{3.103}$$

Now that the analysis of the term in $\hat{O}^2$ is done, it is finally possible to write down the fully explicit form of the time evolution operator

$$\hat{U}_p = \exp\left(i\hat{O}(c_1\hat{X} - c_2\hat{P})\right)\exp\left(ic_3\hat{O}^2\right) \tag{3.104}$$

with

$$c_1 = \frac{\lambda}{2}\left(1 + \cos\left((p-1)\theta\right) + \sin\left((p-1)\theta\right)\cot(\theta/2)\right) \tag{3.105}$$

$$c_2 = \frac{\lambda}{2}\left(1 - \cos\left((p-1)\theta\right)\cot(\theta/2) + \sin\left((p-1)\theta\right)\right) \tag{3.106}$$

$$c_3 = -\frac{\lambda^2}{2}\frac{p\sin(\theta) - \sin(p\theta)}{4\sin^2(\theta/2)} \tag{3.107}$$

Where some additional equivalent expressions were used

$$c_1 = \lambda\frac{\sin(p\theta/2)}{\sin(\theta/2)}\cos\big((p-1)\theta/2\big) = \frac{\lambda}{2}\Big(1 + \cos\big((p-1)\theta\big) + \sin\big((p-1)\theta\big)\cot(\theta/2)\Big) \tag{3.108}$$

$$c_2 = \lambda\frac{\sin(p\theta/2)}{\sin(\theta/2)}\sin\big((p-1)\theta/2\big) = \frac{\lambda}{2}\Big(1 - \cos\big((p-1)\theta\big)\cot(\theta/2) + \sin\big((p-1)\theta\big)\Big) \tag{3.109}$$

These particular forms for c_1, c_2, and c_3 do not have particular advantages apart from the fact that they confirm the correctness of the result, since these are identical to the ones mentioned in [30][11]. The equivalence above for c_1 and c_2 is not especially difficult to obtain, and this is done in Appendix C.7.

This final result for $\hat{U}_p$ finally enables us to see the expression of a geometrical gate similar to the Milburn gate (and to the Sørensen-Mølmer gate). For some choices of p and θ (chosen via the choice of the number of pulses p and of the period of the interactions $\Delta t = -\theta/\omega_m$), the constants c_1 and c_2 can drop to zero, while c_3 is nonzero. This gives a gate identical to the one obtained before for the two geometric gates, with a closed loop in the phase space

$$\hat{U} = e^{ic_3\hat{O}^2} \tag{3.110}$$

While this particular gate has sometimes been referred to as the optomechanical version of "Milburn Gate" in this work, one could argue it should just be called a "geometric gate". Indeed, the phase space loop created by this system is not a rectangle, but rather a regular polygon (with number of sides equal to the number of pulses p) which can be inscribed in the circle corresponding to the Sørensen-Mølmer gate in Figure 2.5.

Building on the results that have been shown here, the following chapter introduces dissipation to the mechanical subsystem in the optomechanical device.

---

[11]The only difference between [30] and the results shown here is the sign of c_3. However, this is not a problem. Both of the results are actually correct, because they do not correspond to the same situation. Despite the seemingly identical expression for Equation 3.66, the two cases are not identical. The case examined in [30] was postulated (*i.e.* knowing the mathematical equivalence between the optomechanical behaviour and displacement operators, the author wrote this particular set of pulses). Importantly, the pi product symbol the author used was then defined as left to right (next term multiplied on the right). However, here, the final expression was obtained starting from a particular set of interaction pulses (with $f(t)$ defining when interaction were on or off), and the final result was the same expression but with the pi product symbol going from right to left (next term multiplied on the left). Considering a closed loop and using the representation in the phase space, one can easily see that this just amounts to one case where the loop is drawn anti-clockwise and one case where it is drawn clockwise. This indeed changes the sign of c_3, as shown in the theoretical sections of the previous chapter.

Chapter 4

Dissipation in Pulsed Optomechanical Geometric Gate

Now that the pulsed optomechanical geometric gate was studied, it is possible to introduce dissipation to the problem. The approach that will be used here is to keep the above results (and therefore the corresponding approximations), and to add mechanical dissipation to the free mechanical evolution of the first interaction picture expression (see Equation 3.75). After some theoretical points to set the mathematical framework needed and how exactly the above will be done, the full calculation will be made and generalised to an arbitrary number of pulse.

To the best knowledge of the author, the following results including dissipation to geometrical pulsed gates constitute original work and have not yet been shown in the literature.

4.1 Mathematical Framework for Dissipative Quantum Systems

While the behaviour of ideally isolated quantum systems can be computed in the brak-ket notations, dissipation phenomena benefits greatly from the density matrix formalism. Indeed, with dissipation to its environment, the state of the system of interest can no longer be seen as a pure state. The following introduces the density matrix approach to dissipative systems, as well as the master equation for dissipation and its solution.

4.1.1 Density Matrix Formalism

An introduction to density matrix formalism can be found in [8] and some of its results may be known by the reader. The general idea and its relation with dissipative systems are introduced here.

Fundamentally, the idea behind density matrix formalism can be summarised with the following. Let $|\psi\rangle$ be a quantum state (any such state can be called *pure*), the corresponding density matrix is writtent as $|\psi\rangle \langle\psi|$, and the expectation value of an observable is then defined as

$$\langle \hat{a} \rangle = \text{Tr}\left(\hat{\rho}\hat{a}\right) \tag{4.1}$$

This definition can be linked back to the usual formalism via

$$\text{Tr}\left(\hat{\rho}\hat{a}\right) = \sum_k \langle k| \hat{\rho}\hat{a} |k\rangle = \sum_k \langle k|\psi\rangle \langle\psi| \hat{a} |k\rangle = \langle\psi| \hat{a} \left(\sum_k |k\rangle \langle k|\right) |\psi\rangle = \langle\psi| \hat{a} |\psi\rangle \tag{4.2}$$

Where $|k\rangle$ are the elements of a complete orthonormal basis, and therefore $\sum_k |k\rangle \langle k| = \mathbb{1}$. Concerning the dynamics of density matrices, the equation which corresponds to Schrödinger's equation in density matrix formalism is

$$\frac{d}{dt}\hat{\rho} = -\frac{i}{\hbar}\left[\hat{H}, \hat{\rho}\right] \tag{4.3}$$

Once again, considering a pure state, one can easily show that this is still coherent with the usual formalism

$$\frac{d}{dt}\hat{\rho} = \frac{d}{dt}\left(|\psi\rangle\right)\langle\psi| + |\psi\rangle\frac{d}{dt}\left(\langle\psi|\right) \tag{4.4}$$

$$= -\frac{i}{\hbar}\hat{H}|\psi\rangle\langle\psi| + \frac{i}{\hbar}|\psi\rangle\langle\psi|\hat{H}^\dagger \tag{4.5}$$

$$= -\frac{i}{\hbar}\left(\hat{H}|\psi\rangle\langle\psi| - |\psi\rangle\langle\psi|\hat{H}\right) \tag{4.6}$$

$$= -\frac{i}{\hbar}\left[\hat{H}, \hat{\rho}\right] \tag{4.7}$$

From the above, it is confirmed that quantum mechanics can be expressed with the density matrix formalism, but it is not yet clear why would one use this new formalism. The reason for this is that density matrix formalism can be used for *mixed states* (defined in opposition with pure states). For this, it should be noted that a fully general density matrix can be written as $\sum_{k,l}\lambda_{kl}|k\rangle\langle l|$, which is a more general object than $|\psi\rangle\langle\psi|$. The density matrices which cannot be written as $|\psi\rangle\langle\psi|$ (*i.e.* split as a product of a ket and its corresponding bra) are said to describe *mixed* states. These states require density matrix formalism to be understood and used.

Without additional information, it would be natural to wonder why density matrices are not an actual quantum theory, since they seem to extend the space of states that can be treated. In reality, density matrices are not an extension of quantum mechanics, but rather a clever mathematical tool to consider particular systems. These "mixed states" come from the trace of a larger system. Let us consider a large system $|\psi\rangle$ composed of one subsystem $|\psi_s\rangle$ and its environment $|\psi_{env}\rangle$. Any state of the full system can then be written as a (pure) state

$$|\psi(t)\rangle = |\phi_s(t)\rangle \otimes |\psi_{env}(t)\rangle \tag{4.8}$$

Considering now that the subsystem is poorly isolated from its environment, and applying some time evolution on it. Since the subsystem is coupled to its environment, both will change (in the case of a dissipative subsystem, it will for instance lose energy to its environment). As usual, the full system after time evolution is still a pure state.

$$|\psi(t+\Delta t)\rangle = \hat{U}_c(\Delta t)|\psi(t)\rangle = |\phi_s(t+\Delta t)\rangle \otimes |\psi_{env}(t+\Delta t)\rangle \tag{4.9}$$

Where the c index on the time evolution operator was used to indicate that this operator couples the subsystem and its environment. This gives the density matrix

$$\hat{\rho}(t+\Delta t) = \Big(|\phi_s(t+\Delta t)\rangle \otimes |\psi_{env}(t+\Delta t)\rangle\Big)\Big(\langle\phi_s(t+\Delta t)| \otimes \langle\psi env(t+\Delta t)|\Big) \tag{4.10}$$

What will a measurement on the subsystem give ? Any observable of the subsystem will leave the environment invariant, they can therefore be written as operators of the form $\hat{a} \otimes \mathbb{1}$ acting on the full system. Using the previous expression, one gets the expectation value of the measurement $\hat{a}$ on the subsystem at time $t+\Delta t$ as

$$\langle\hat{a}\rangle = \mathrm{Tr}\left(\hat{a} \otimes \mathbb{1}\hat{\rho}(t+\Delta t)\right) = \mathrm{Tr}_s\left(\hat{a}\,\mathrm{Tr}_{env}\left(\rho(t\hat{+}\Delta t)\right)\right) = \mathrm{Tr}_s\left(\hat{a}\hat{\rho}_s(t+\Delta t)\right) \tag{4.11}$$

where a new smaller density matrix was defined

$$\rho_s(t+\Delta t) = \mathrm{Tr}_{env}\left(\hat{U}_c(\Delta t)\hat{\rho}(t)\hat{U}_c^\dagger(\Delta t)\right) \tag{4.12}$$

This new density matrix that can be used to compute any measurement made on the subsystem is then a fully general density matrix, it is no longer necessarily separable as $|\psi\rangle\langle\psi|$. Measurements on the subsystem can then be described by regular measurements on a "mixed state". This is how interaction between systems generate these "mixed state". As in the example, the typical use of this is to consider measurements on an imperfectly isolated system.

The main advantage of working in the density matrix formalism (and with mixed states), is then to entirely bypass the problem of calculating Equation 4.12, and directly find the differential equation that corresponds to the correct density matrix. If the result is a pure state, then the differential equation would be Equation 4.3, but if not, then Equation 4.3 will have to be modified to include new terms in addition to the commutator.

4.1.2 Mechanical Dissipation Master Equation and Solution

Following the previous section, it is understood that in order to avoid explicitly taking into account the environment in dissipative systems, one must work with density matrices and mixed states. For this, Equation 4.3 must be modified to be able to generate the mixed states that correspond to the dissipative system considered.

4.1.2.1 Master Equation

In the case of dissipation to the environment for a quantum mechanical oscillator, this differential equation can be written

$$\frac{d}{dt}\hat{\rho} = -\frac{i}{\hbar}\left[\hat{H}_{0,m,S},\hat{\rho}\right] + \frac{\gamma}{2}\left(2\hat{b}\hat{\rho}\hat{b}^\dagger - \hat{b}^\dagger\hat{b}\hat{\rho} - \hat{\rho}\hat{b}^\dagger\hat{b}\right) \tag{4.13}$$

where γ quantifies the strength of the dissipation and, as usual, $\hat{H}_{0,m,S}$ is the free Hamiltonian for the mechanical quantum oscillator in Schrödinger picture.

A quick qualitative understanding of these additional terms can be given by noting that the first term amounts to removing one excitation to the oscillator (this excitation is dissipated in the environment), and that the two additional terms ensure the necessary condition that the trace of the density matrix must remain time invariant

$$\frac{d}{dt}\left(\mathrm{Tr}\,\hat{\rho}\right) = \mathrm{Tr}\,\frac{d}{dt}\hat{\rho} = \mathrm{Tr}\left(-\frac{i}{\hbar}\left[\hat{H}_{0,m,S},\hat{\rho}\right] + \frac{\gamma}{2}\left(2\hat{b}\hat{\rho}\hat{b}^\dagger - \hat{b}^\dagger\hat{b}\hat{\rho} - \hat{\rho}\hat{b}^\dagger\hat{b}\right)\right) = 0 \tag{4.14}$$

where the cyclic property of the trace was used. Even if the above gives some understanding of the meaning behind the expression, the rigorous derivation is far more complex. In reality, the above terms are a simplified version of a (far) more complicated expression that is simplified via several approximations (these include the Born-Markov approximation, as well as assuming the environment to be at zero kelvin). Due to the length and complexity of the derivation, it will not be included here. For a general approach including this derivation, [47; 48; 49] can be consulted. Apart from finding its direct proof, this is also a well known result often used in the literature [50; 51; 52].

4.1.2.2 Interaction Picture and Solution

Fully solving Equation 4.13 seems challenging, fortunately, it is possible to simplify it by moving to the interaction picture with respect to the free mechanical propagation. The transformation of the density matrix to this interaction picture being $\hat{\rho}_I(t) = \hat{U}_{0,m,S}^{-1}(t)\hat{\rho}(t)\hat{U}_{0,m,S}(t)$, the differential equation becomes

$$\frac{d\hat{\rho}_I}{dt} = \frac{d}{dt}\left(\hat{U}_{0,m,S}^{-1}\hat{\rho}\hat{U}_{0,m,S}\right) \tag{4.15}$$

$$= \frac{d}{dt}\left(\hat{U}_{0,m,S}^{-1}\right)\hat{\rho}\hat{U}_{0,m,S} + \hat{U}_{0,m,S}^{-1}\frac{d\hat{\rho}}{dt}\hat{U}_{0,m,S} + \hat{U}_{0,m,S}^{-1}\hat{\rho}\frac{d}{dt}\left(\hat{U}_{0,m,S}\right) \tag{4.16}$$

$$= \hat{U}_{0,m,S}^{-1}\left(\frac{i}{\hbar}\hat{H}_{0,m,S}\hat{\rho} + \frac{d\hat{\rho}}{dt} + \frac{-i}{\hbar}\hat{\rho}\hat{H}_{0,m,S}\right)\hat{U}_{0,m,S} \tag{4.17}$$

$$= \hat{U}_{0,m,S}^{-1}\left(\frac{\gamma}{2}\left(2\hat{b}\hat{\rho}\hat{b}^\dagger - \hat{b}^\dagger\hat{b}\hat{\rho} - \hat{\rho}\hat{b}^\dagger\hat{b}\right)\right)\hat{U}_{0,m,S} \tag{4.18}$$

$$= \frac{\gamma}{2}\left(2\hat{U}_{0,m,S}^{-1}\hat{b}\hat{\rho}\hat{b}^\dagger\hat{U}_{0,m,S} - \hat{b}^\dagger\hat{b}\hat{\rho}_I - \hat{\rho}_I\hat{b}^\dagger\hat{b}\right) \tag{4.19}$$

For the two last terms, $\hat{H}_{0,m,S}$ trivially commutes with $\hat{b}^\dagger \hat{b}$, so they simply gave the same terms with $\hat{\rho}_I$ instead of $\hat{\rho}$. Proving the same behaviour for the first term necessitates a bit more thought, it is done in Appendix F.1. The final result is then

$$\frac{d\hat{\rho}_I}{dt} = \frac{\gamma}{2}\left(2\hat{b}\hat{\rho}_I\hat{b}^\dagger - \hat{b}^\dagger\hat{b}\hat{\rho}_I - \hat{\rho}_I\hat{b}^\dagger\hat{b}\right) \tag{4.20}$$

The solution of the remaining differential equation, while not easily proven, is well known in the literature. Let us suppose a particular density matrix to be written at time $t = 0$ in the coherent state basis as

$$\rho_I(0) = |\lambda_i\rangle\langle\lambda_j| \tag{4.21}$$

with the time evolution given by Equation 4.20, the solution for $\rho_I(t)$ is given by

$$\rho_I(t) = \langle\lambda_i|\lambda_j\rangle^{1-e^{-\gamma t}}\left|\lambda_i e^{-\gamma t/2}\right\rangle\left\langle\lambda_j e^{-\gamma t/2}\right| \tag{4.22}$$

Once again, due to its length, the demonstration of this solution will not be included here. For reference, this solution is used in [50; 51], some intermediate results needed to prove it are given in [52] and elements in [53] can be used to better understand the mathematical tools used for the proof.

4.2 Application to the Pulsed Optomechanical System

This section is the core of the developments made to compute the density matrix resulting from the pulsed interactions including dissipation. The result after p interaction pulses with dissipation is written $\hat{\rho}_p = \hat{\rho}(p\Delta t)$.

The first subsection will present the general approach to the calculation. The following will compute $\hat{\rho}_1$, $\hat{\rho}_2$, and $\hat{\rho}_3$. Finally, a general expression for any number of pulses $\hat{\rho}_p$ will be derived by two different methods.

4.2.1 Calculation Method

The starting state considered is $|\alpha\rangle_f \otimes |0\rangle_m$. Where both the optical (index f) and the mechanical (index m) states are expressed in the coherent state basis. This in turn leads to the starting density matrix

$$\hat{\rho}_0 = |\alpha\rangle\langle\alpha|_f \otimes |0\rangle\langle0|_m \tag{4.23}$$

As previously mentioned, the whole approach to introducing dissipation is to use the expression previously obtained for the first interaction picture time evolution operator in Equation 3.75. The result is reminded here

$$\hat{U}(p\Delta t) = \left(\hat{U}_{0,S,m}(\Delta t)e^{-i\hat{H}_{int,S}\tau/\hbar}\right)^p \tag{4.24}$$

Introducing dissipation to this only impacts the above by replacing the free mechanical propagation in $\hat{U}_{0,S,m}(\Delta t)$ by the free propagation with dissipation. The reason behind this approach is that the previous approximations of the pulsed interactions led to neglecting any change in the mechanical system during the interaction. Previously, this only implied neglecting free mechanical propagation, but now that dissipation is introduced, there is no reason to try to introduce dissipation during the short interaction. In short, the present approach takes advantage of the previous approximations instead of completely starting from zero again.

As a summary, a single pulse on some $\hat{\rho}_n$ can be computed as

1. Apply the interaction pulse

$$e^{-i\hat{H}_{int,S}\tau/\hbar} = \exp\left(ig\tau\hat{a}^\dagger\hat{a}\frac{\hat{b}^\dagger + \hat{b}}{\sqrt{2}}\right) = \hat{U}_{int} \tag{4.25}$$

on the density matrix, the result is then named

$$\hat{\rho}_{n+\tau} = \hat{U}_{int}\hat{\rho}_n\hat{U}_{int}^{-1} \tag{4.26}$$

To do this, the optical state is written in the Fock eigenbasis in order to simplify the number operator $\hat{a}^\dagger\hat{a} = \hat{N}$ with its corresponding eigenstate, and the remaining of the operator $\hat{U}_{int}$ becomes a displacement operator on the mechanical state in the coherent state basis.

2. Next, the resulting $\hat{\rho}_{n+\tau}$ is transformed to be in the interaction picture with respect to the free mechanical evolution. However, since nothing depends on absolute time in Equation 4.24 (only time intervals are used), the time can be redefined at $t = 0$ when starting this step, the transformation is therefore trivial !

$$\hat{\rho}_{I,n+\tau} = \hat{U}_{0,S,m}^{-1}(0)\hat{\rho}_{n+\tau}\hat{U}_{0,S,m}(0) = \hat{\rho}_{n+\tau} \tag{4.27}$$

Since one remembers that Equation 3.75 was in the first interaction picture, this new interaction picture transformation done for the duration of the dissipation will also be called "second interaction picture".

3. The effect of dissipation during the time Δt can now be computed on the second interaction picture $\hat{\rho}_{I,n+\tau}$ via Equation 4.22 where t is simply replaced by Δt, the result is named $\hat{\rho}_{I,n+\Delta t}$.

4. The resulting density matrix can now be transformed back in the first interaction picture, the time elapsed since the first transformation at $t = 0$ being Δt, the result is

$$\hat{\rho}_{n+1} = \hat{U}_{0,S,m}(\Delta t)\hat{\rho}_{I,n+\Delta t}\hat{U}_{0,S,m}^{-1}(\Delta t) = \hat{\rho}((n+1)\Delta t) \tag{4.28}$$

Now that all the mathematical details are covered, the next section jumps into the actual calculation. Since the step 2 was shown above to be trivial thanks to some redefinition of t, the following only mentions three steps. Below, the three remaining steps are named "interaction pulse", "dissipative time evolution", and "interaction picture inverse transformation".

4.2.2 Calculation of $\hat{\rho}_1$

Starting from $\hat{\rho}_0$, the optical states are expressed in the Fock eigenbasis in order to apply the interaction operator $\hat{U}_{int}$. One may want to look back at Section 2.3.2 and Equation 2.75 for the expression of a coherent state in the Fock basis.

The starting density matrix can therefore be written

$$\hat{\rho}_0 = |\alpha\rangle\langle\alpha|_f \otimes |0\rangle\langle0|_m = e^{-|\alpha|^2}\sum_{n=0}^{\infty}\sum_{k=0}^{\infty}\frac{\alpha^n(\alpha^*)^k}{\sqrt{n!k!}}|n\rangle\langle k|_f \otimes |0\rangle\langle0|_m \tag{4.29}$$

where $|n\rangle\langle k|_f$ are Fock basis states.

It can be noted that this section treating $\hat{\rho}_1$ will be more detailed than the ones for the next pulses, as it will be possible to use some of the results of this first pulse to simplify the calculation of the next ones (*e.g.* it will be shown here that the "interaction picture inverse transformation" step is very easily realised, and does not really require its own subsection). In addition, for clarity, everything will be written out explicitly for this first pulse. Later however, due to the length of the expressions, keeping everything written explicitly will do more harm than good, and new notations will be introduced to improve readability.

4.2.2.1 Interaction Pulse

Applying the interaction pulse, the result is calculated as

$$\hat{\rho}_{0+\tau} = \hat{U}_{int}\hat{\rho}_0\hat{U}_{int}^{-1} \tag{4.30}$$

$$= \exp\left(ig\tau\hat{a}^\dagger\hat{a}\frac{\hat{b}^\dagger + \hat{b}}{\sqrt{2}}\right) e^{-|\alpha|^2} \sum_{n=0}^\infty \sum_{k=0}^\infty \frac{\alpha^n(\alpha^*)^k}{\sqrt{n!k!}} |n\rangle\langle k|_f \otimes |0\rangle\langle 0|_m \exp\left(-ig\tau\hat{a}^\dagger\hat{a}\frac{\hat{b}^\dagger + \hat{b}}{\sqrt{2}}\right) \quad (4.31)$$

$$= e^{-|\alpha|^2} \sum_{n=0}^\infty \sum_{k=0}^\infty \frac{\alpha^n(\alpha^*)^k}{\sqrt{n!k!}} |n\rangle\langle k|_f \otimes \left(\exp\left(ig\tau n\frac{\hat{b}^\dagger + \hat{b}}{\sqrt{2}}\right)|0\rangle\langle 0|_m \exp\left(-ig\tau k\frac{\hat{b}^\dagger + \hat{b}}{\sqrt{2}}\right)\right) \quad (4.32)$$

$$= e^{-|\alpha|^2} \sum_{n=0}^\infty \sum_{k=0}^\infty \frac{\alpha^n(\alpha^*)^k}{\sqrt{n!k!}} |n\rangle\langle k|_f \otimes \left(\hat{D}\left(\frac{ig\tau n}{\sqrt{2}}\right)|0\rangle\langle 0|_m \hat{D}\left(-\frac{ig\tau k}{\sqrt{2}}\right)\right) \quad (4.33)$$

$$= e^{-|\alpha|^2} \sum_{n=0}^\infty \sum_{k=0}^\infty \frac{\alpha^n(\alpha^*)^k}{\sqrt{n!k!}} |n\rangle\langle k|_f \otimes \left(\hat{D}\left(\frac{ig\tau n}{\sqrt{2}}\right)|0\rangle\langle 0|_m \hat{D}^\dagger\left(\frac{ig\tau k}{\sqrt{2}}\right)\right) \quad (4.34)$$

$$= e^{-|\alpha|^2} \sum_{n=0}^\infty \sum_{k=0}^\infty \frac{\alpha^n(\alpha^*)^k}{\sqrt{n!k!}} |n\rangle\langle k|_f \otimes \left|\frac{ig\tau n}{\sqrt{2}}\right\rangle\left\langle\frac{ig\tau k}{\sqrt{2}}\right|_m \quad (4.35)$$

4.2.2.2 Dissipative Time Evolution

Applying the result of Equation 4.22 on $\hat{\rho}_{0+\tau}$ gives

$$\hat{\rho}_{I,0+\Delta t} = e^{-|\alpha|^2} \sum_{n=0}^\infty \sum_{k=0}^\infty \frac{\alpha^n(\alpha^*)^k}{\sqrt{n!k!}} \left\langle\frac{ig\tau n}{\sqrt{2}}\bigg|\frac{ig\tau k}{\sqrt{2}}\right\rangle^{1-e^{-\gamma\Delta t}} |n\rangle\langle k|_f \otimes$$

$$\left|\frac{ig\tau n}{\sqrt{2}}e^{-\gamma\Delta t/2}\right\rangle\left\langle\frac{ig\tau k}{\sqrt{2}}e^{-\gamma\Delta t/2}\right|_m \quad (4.36)$$

In order to write this explicitly, this requires computing the overlap of the two coherent states. The result for this overlap was proven in Equation 2.76, which is reminded here for convenience

$$\langle\beta|\alpha\rangle = e^{\beta^*\alpha - \frac{1}{2}(|\beta|^2 + |\alpha|^2)} \quad (4.37)$$

$$\left\langle\frac{ig\tau n}{\sqrt{2}}\bigg|\frac{ig\tau k}{\sqrt{2}}\right\rangle = \exp\left(\frac{-ig\tau n}{\sqrt{2}}\frac{ig\tau k}{\sqrt{2}} - \frac{(g\tau n)^2}{4} - \frac{(g\tau k)^2}{4}\right) = \exp\left(-\frac{g^2\tau^2}{4}(n-k)^2\right) \quad (4.38)$$

The simplified result for $\hat{\rho}_{I,0+\Delta t}$ therefore gives

$$\hat{\rho}_{I,0+\Delta t} = e^{-|\alpha|^2} \sum_{n=0}^\infty \sum_{k=0}^\infty \frac{\alpha^n(\alpha^*)^k}{\sqrt{n!k!}} |n\rangle\langle k|_f \otimes \exp\left(-\frac{g^2\tau^2}{4}(n-k)^2\left(1-e^{-\gamma\Delta t}\right)\right)$$

$$\left|\frac{ig\tau n}{\sqrt{2}}e^{-\gamma\Delta t/2}\right\rangle\left\langle\frac{ig\tau k}{\sqrt{2}}e^{-\gamma\Delta t/2}\right|_m \quad (4.39)$$

4.2.2.3 Interaction Picture Inverse Transformation

The inverse transformation in order to go back to the first interaction picture is written

$$\hat{\rho}_1 = \hat{U}_{0,S,m}(\Delta t)\hat{\rho}_{I,0+\Delta t}\hat{U}_{0,S,m}^{-1}(\Delta t) = \exp\left(-i\omega_m\hat{b}^\dagger\hat{b}\Delta t\right)\hat{\rho}_{I,0+\Delta t}\exp\left(i\omega_m\hat{b}^\dagger\hat{b}\Delta t\right) \quad (4.40)$$

where one immediately notices a slight problem. No relation was derived concerning the effect of this type of operator in $\hat{b}^\dagger\hat{b}$ on a coherent state. While for the optical case it was possible and easy to move to the Fock eigenbasis, it is not convenient to do it for the mechanical state. As seen above, every pulse will apply displacement operators on the mechanical states, so moving to the energy eigenstate basis would make the calculation of the next pulse very cumbersome. However, there is actually a very nice general result that can be derived by temporarily switching to the energy eigenbasis. Considering some general coherent state, one can write

$$\exp\left(-i\omega_m \hat{b}^\dagger \hat{b} \Delta t\right)|\alpha\rangle = \exp\left(-i\omega_m \hat{b}^\dagger \hat{b} \Delta t\right)\exp\left(-\frac{|\alpha|^2}{2}\right)\sum_{n=0}^{\infty}\frac{\alpha^n}{\sqrt{n!}}|n\rangle \tag{4.41}$$

$$= \sum_{n=0}^{\infty}\exp\left(-\frac{|\alpha|^2}{2}\right)\exp\left(-i\omega_m n\Delta t\right)\frac{\alpha^n}{\sqrt{n!}}|n\rangle \tag{4.42}$$

$$= \sum_{n=0}^{\infty}\exp\left(-\frac{|\alpha\exp(-i\omega_m\Delta t)|^2}{2}\right)\frac{(\alpha\exp\left(-i\omega_m\Delta t\right))^n}{\sqrt{n!}}|n\rangle \tag{4.43}$$

$$= \left|\alpha e^{-i\omega_m\Delta t}\right\rangle \tag{4.44}$$

This incredibly simple result then makes all the interaction picture inverse transformations very easy to perform. All interaction picture inverse transformations are then simply equivalent to adding the phase $\exp\left(-i\omega_m\Delta t\right)$ to the coherent state. In the coming sections to compute $\hat{\rho}_2$ and $\hat{\rho}_3$, there will be no need to dedicate a subsection to this transformation

4.2.2.4 Result for $\hat{\rho}_1$

$$\hat{\rho}_1 = e^{-|\alpha|^2}\sum_{n=0}^{\infty}\sum_{k=0}^{\infty}\frac{\alpha^n(\alpha^*)^k}{\sqrt{n!k!}}|n\rangle\langle k|_f \otimes S_1(n,k)\left|\frac{ig\tau n}{\sqrt{2}}e^{-i\omega_m\Delta t - \gamma\Delta t/2}\right\rangle\left\langle\frac{ig\tau k}{\sqrt{2}}e^{-i\omega_m\Delta t - \gamma\Delta t/2}\right|_m \tag{4.45}$$

where a first "scaling factor" was named $S_1(n,k)$. It is very convenient to name these kinds of functions of n and k in order to shorten the notations. As it will not be changed by the next pulses, at least one instance of the factor $S_1(n,k)$ will be found in any $\hat{\rho}_p$ with $p \geq 1$

$$S_1(n,k) = \exp\left(-\frac{g^2\tau^2}{4}(n-k)^2\left(1-e^{-\gamma\Delta t}\right)\right) \tag{4.46}$$

4.2.3 Calculation of $\hat{\rho}_2$

Starting from $\hat{\rho}_1$, the calculation for $\hat{\rho}_2$ can be done. The crucial difference from the previous case is that now the mechanical state is not the ground state anymore. A phase term will therefore be generated by the composition of displacement operators. As shown by the first case, the step for the interaction picture inverse transformation is very easily done and no subsection will be dedicated to that step from now on.

4.2.3.1 Interaction Pulse

Making use of the similarity with the calculation for $\hat{\rho}_1$, the first few steps can be skipped. It can be directly written that the interaction pulse amounts to the same two displacement operators as in the previous case (in n on the left and in k on the right).

$$\hat{\rho}_{1+\tau} = \hat{U}_{int}\hat{\rho}_1\hat{U}_{int}^{-1} \tag{4.47}$$

$$= e^{-|\alpha|^2}\sum_{n=0}^{\infty}\sum_{k=0}^{\infty}\frac{\alpha^n(\alpha^*)^k}{\sqrt{n!k!}}|n\rangle\langle k|_f \otimes S_1(n,k)$$

$$\left(\hat{D}\left(\frac{ig\tau n}{\sqrt{2}}\right)\left|\frac{ig\tau n}{\sqrt{2}}e^{-i\omega_m\Delta t - \gamma\Delta t/2}\right\rangle\left\langle\frac{ig\tau k}{\sqrt{2}}e^{-i\omega_m\Delta t - \gamma\Delta t/2}\right|_m\hat{D}^\dagger\left(\frac{ig\tau k}{\sqrt{2}}\right)\right) \tag{4.48}$$

Seeing the speed at which the length of the expressions increase, it appears both desirable and inevitable to introduce new notations. In the following, the coherent states of the mechanical system will follow the same convention as the one used for $\hat{\rho}$. For instance, the above coherent state in the mechanical part will be written (after this interaction pulse) $|\psi_{1+\tau}(n)\rangle$, as it is the coherent state after one full

pulse and the interaction of the second pulse. Conveniently, it can be easily checked that it will always be possible to use the same expression for $\langle \psi_{1+\tau}(k) |$ (just replacing n with k and taking the hermitian conjugate). One can then write

$$\hat{\rho}_{1+\tau} = e^{-|\alpha|^2} \sum_{n=0}^{\infty} \sum_{k=0}^{\infty} \frac{\alpha^n (\alpha^*)^k}{\sqrt{n!k!}} |n\rangle \langle k|_f \otimes S_1(n,k) \left(\hat{D}\left(\frac{ig\tau n}{\sqrt{2}}\right) |\psi_1(n)\rangle \langle \psi_1(k)|_m \hat{D}^\dagger\left(\frac{ig\tau k}{\sqrt{2}}\right) \right) \quad (4.49)$$

Before moving on to compute $|\psi_{1+\tau}\rangle$, one remembers that from the developments in Section 2.3.4 and Equation 2.86, acting with a displacement operator on a coherent state that is not the ground state generates an additional phase. As a reminder

$$\hat{D}(\beta) |\alpha\rangle = \hat{D}(\beta)\hat{D}(\alpha) |0\rangle = e^{(\beta\alpha^* - \beta^*\alpha)/2} \hat{D}(\alpha + \beta) |0\rangle = e^{(\beta\alpha^* - \beta^*\alpha)/2} |\alpha + \beta\rangle \quad (4.50)$$

By expecting a new phase factor to be generated, one can compute $C(n) |\psi_{1+\tau}(n)\rangle$ where $C(n)$ is one of the two phase factors generated. Since a displacement is applied on both $|\psi_1(n)\rangle$ and $\langle \psi_1(k)|$, each will generate a part of the final phase factor.

$$C(n) |\psi_{1+\tau}(n)\rangle = \hat{D}\left(\frac{ig\tau n}{\sqrt{2}}\right) |\psi_1(n)\rangle \quad (4.51)$$

$$= \hat{D}\left(\frac{ig\tau n}{\sqrt{2}}\right) \left| \frac{ig\tau n}{\sqrt{2}} e^{-i\omega_m \Delta t - \gamma \Delta t/2} \right\rangle \quad (4.52)$$

$$= \exp\left(\frac{1}{2} \frac{ig\tau n}{\sqrt{2}} \frac{-ig\tau n}{\sqrt{2}} e^{i\omega_m \Delta t - \gamma \Delta t/2} - \frac{1}{2} \frac{-ig\tau n}{\sqrt{2}} \frac{ig\tau n}{\sqrt{2}} e^{-i\omega_m \Delta t - \gamma \Delta t/2} \right)$$
$$\left| \frac{ig\tau n}{\sqrt{2}} \left(1 + e^{-i\omega_m \Delta t - \gamma \Delta t/2} \right) \right\rangle \quad (4.53)$$

$$= \exp\left(i \frac{g^2 \tau^2}{2} n^2 e^{-\gamma \Delta t/2} \sin(\omega_m \Delta t) \right) \left| \frac{ig\tau n}{\sqrt{2}} \left(1 + e^{-i\omega_m \Delta t - \gamma \Delta t/2} \right) \right\rangle \quad (4.54)$$

The complex conjugate of this phase factor with k instead of n will be generated by the displacement acted on the right on $\langle \psi_1(k)|$. Choosing to name the total phase $P_2(n,k) = C(n)C^*(k)$ (the index 2 being added since it was obtained in the second pulse), the result after the interaction can be written

$$\hat{\rho}_{1+\tau} = e^{-|\alpha|^2} \sum_{n=0}^{\infty} \sum_{k=0}^{\infty} \frac{\alpha^n (\alpha^*)^k}{\sqrt{n!k!}} |n\rangle \langle k|_f \otimes S_1(n,k) P_2(n,k) |\psi_{1+\tau}(n)\rangle \langle \psi_{1+\tau}(k)|_m \quad (4.55)$$

with the new definitions

$$P_2(n,k) = \exp\left(i \frac{g^2 \tau^2}{2} (n^2 - k^2) e^{-\gamma \Delta t/2} \sin(\omega_m \Delta t) \right) \quad (4.56)$$

$$|\psi_{1+\tau}(n)\rangle = \left| \frac{ig\tau n}{\sqrt{2}} \left(1 + e^{-i\omega_m \Delta t - \gamma \Delta t/2} \right) \right\rangle \quad (4.57)$$

4.2.3.2 Dissipative Time Evolution

Applying the dissipative time evolution (once again, see Equation 4.22) after the trivial transformation to the second interaction picture, $\hat{\rho}_{I,1+\Delta t}$ is calculated as

$$\hat{\rho}_{I,1+\Delta t} = e^{-|\alpha|^2} \sum_{n=0}^{\infty} \sum_{k=0}^{\infty} \frac{\alpha^n (\alpha^*)^k}{\sqrt{n!k!}} |n\rangle \langle k|_f \otimes S_1(n,k) P_2(n,k) \langle \psi_{1+\tau}(n)|\psi_{1+\tau}(k)\rangle^{1 - e^{-\gamma \Delta t}}$$
$$\left| \psi_{1+\tau}(n) e^{-\gamma \Delta t/2} \right\rangle \left\langle \psi_{1+\tau}(k) e^{-\gamma \Delta t/2} \right|_m \quad (4.58)$$

The new scaling factor for this pulse is then calculated

$$S_2(n,k) = \langle \psi_{1+\tau}(n)|\psi_{1+\tau}(k)\rangle^{1-e^{-\gamma\Delta t}} \tag{4.59}$$

$$= \left\langle \frac{ig\tau n}{\sqrt{2}}\left(1 + e^{-i\omega_m\Delta t - \gamma\Delta t/2}\right)\middle|\frac{ig\tau k}{\sqrt{2}}\left(1 + e^{-i\omega_m\Delta t - \gamma\Delta t/2}\right)\right\rangle^{1-e^{-\gamma\Delta t}} \tag{4.60}$$

$$= \exp\left(-\frac{g^2\tau^2}{4}(n-k)^2\left(1 - e^{-\gamma\Delta t}\right)\frac{1 - e^{-\gamma\Delta t}2\cos(2\omega_m\Delta t) + e^{-2\gamma\Delta t}}{1 - e^{-\gamma\Delta t/2}2\cos(\omega_m\Delta t) + e^{-\gamma\Delta t}}\right) \tag{4.61}$$

Although not especially complex, the calculation between 4.60 and 4.61 is a bit long, it is included in Appendix F.2. The result after the dissipation in this second interaction picture appears as

$$\hat{\rho}_{I,1+\Delta t} = e^{-|\alpha|^2}\sum_{n=0}^{\infty}\sum_{k=0}^{\infty}\frac{\alpha^n(\alpha^*)^k}{\sqrt{n!k!}}|n\rangle\langle k|_f \otimes S_1(n,k)S_2(n,k)P_2(n,k)|\psi_{I,1+\Delta t}(n)\rangle\langle\psi_{I,1+\Delta t}(k)|_m \tag{4.62}$$

with the new definitions

$$|\psi_{I,1+\Delta t}(n)\rangle = \left|\frac{ig\tau n}{\sqrt{2}}\left(1 + e^{-i\omega_m\Delta t - \gamma\Delta t/2}\right)e^{-\gamma\Delta t/2}\right\rangle \tag{4.63}$$

$$S_2(n,k) = \exp\left(-\frac{g^2\tau^2}{4}(n-k)^2\left(1 - e^{-\gamma\Delta t}\right)\frac{1 - e^{-\gamma\Delta t}2\cos(2\omega_m\Delta t) + e^{-2\gamma\Delta t}}{1 - e^{-\gamma\Delta t/2}2\cos(\omega_m\Delta t) + e^{-\gamma\Delta t}}\right) \tag{4.64}$$

4.2.3.3 Result for $\hat{\rho}_2$

Since reverting to the first interaction picture just boils down to adding the $e^{-i\omega_m\Delta t}$ phase *inside* the coherent mechanical states, the result for $\hat{\rho}_2$ can be written

$$\hat{\rho}_2 = e^{-|\alpha|^2}\sum_{n=0}^{\infty}\sum_{k=0}^{\infty}\frac{\alpha^n(\alpha^*)^k}{\sqrt{n!k!}}|n\rangle\langle k|_f \otimes S_1(n,k)S_2(n,k)P_2(n,k)|\psi_2(n)\rangle\langle\psi_2(k)|_m \tag{4.65}$$

The new definitions (when compared to the result for $\hat{\rho}_1$) are reminded below

$$S_2(n,k) = \exp\left(-\frac{g^2\tau^2}{4}(n-k)^2\left(1 - e^{-\gamma\Delta t}\right)\frac{1 - e^{-\gamma\Delta t}2\cos(2\omega_m\Delta t) + e^{-2\gamma\Delta t}}{1 - e^{-\gamma\Delta t/2}2\cos(\omega_m\Delta t) + e^{-\gamma\Delta t}}\right) \tag{4.66}$$

$$P_2(n,k) = \exp\left(i\frac{g^2\tau^2}{2}(n^2 - k^2)e^{-\gamma\Delta t/2}\sin(\omega_m\Delta t)\right) \tag{4.67}$$

$$|\psi_2(n)\rangle = \left|\frac{ig\tau n}{\sqrt{2}}\left(e^M + e^{2M}\right)\right\rangle \qquad \text{with} \qquad M = -i\omega_m\Delta t - \gamma\Delta t/2 \tag{4.68}$$

4.2.4 Calculation of $\hat{\rho}_3$

4.2.4.1 Interaction Pulse

$$\hat{\rho}_{2+\tau} = e^{-|\alpha|^2}\sum_{n=0}^{\infty}\sum_{k=0}^{\infty}\frac{\alpha^n(\alpha^*)^k}{\sqrt{n!k!}}|n\rangle\langle k|_f \otimes S_1(n,k)S_2(n,k)P_2(n,k)$$

$$\left(\hat{D}\left(\frac{ig\tau n}{\sqrt{2}}\right)|\psi_2(n)\rangle\langle\psi_2(k)|_m\hat{D}^{\dagger}\left(\frac{ig\tau k}{\sqrt{2}}\right)\right) \tag{4.69}$$

As for the previous case, two phase factors are generated by the actions of the displacement operators on the mechanical states.

For the first state and some phase factor $C(n)$,

$$C(n)\left|\psi_{2+\tau}\right\rangle = \hat{D}\left(\frac{ig\tau n}{\sqrt{2}}\right)\left|\psi_2(n)\right\rangle \tag{4.70}$$

$$= \hat{D}\left(\frac{ig\tau n}{\sqrt{2}}\right)\left|\frac{ig\tau n}{\sqrt{2}}\left(1+e^M\right)e^M\right\rangle \tag{4.71}$$

$$= \exp\left(i\frac{g^2\tau^2}{2}n^2\left(e^{-\gamma\Delta t/2}\sin(\omega_m\Delta t) + e^{-\gamma\Delta t}\sin(2\omega_m\Delta t)\right)\right)$$

$$\left|\frac{ig\tau n}{\sqrt{2}}\left(1+\left(1+e^M\right)e^M\right)\right\rangle \tag{4.72}$$

where the notation $M = -i\omega_m\Delta t - \gamma\Delta t/2$ was used. Details between Equation 4.71 and 4.72 are included in Appendix F.3. The phase factor is then given by $P_3(n,k) = C(n)C^*(k)$, and the result after the interaction is written

$$\hat{\rho}_{2+\tau} = e^{-|\alpha|^2}\sum_{n=0}^{\infty}\sum_{k=0}^{\infty}\frac{\alpha^n(\alpha^*)^k}{\sqrt{n!k!}}\left|n\right\rangle\left\langle k\right|_f \otimes S_1(n,k)S_2(n,k)P_2(n,k)P_3(n,k)\left|\psi_{2+\tau}(n)\right\rangle\left\langle\psi_{2+\tau}(k)\right|_m \tag{4.73}$$

with the new definitions

$$P_3(n,k) = \exp\left(i\frac{g^2\tau^2}{2}(n^2-k^2)\left(e^{-\gamma\Delta t/2}\sin(\omega_m\Delta t) + e^{-\gamma\Delta t}\sin(2\omega_m\Delta t)\right)\right) \tag{4.74}$$

$$\left|\psi_{2+\tau}(n)\right\rangle = \left|\frac{ig\tau n}{\sqrt{2}}\left(1+e^M+e^{2M}\right)\right\rangle \qquad \text{with} \qquad M = -i\omega_m\Delta t - \gamma\Delta t/2 \tag{4.75}$$

4.2.4.2   Dissipative Time Evolution

Similarly to the previous cases, $\hat{\rho}_{I,2+\Delta t}$ can be written

$$\hat{\rho}_{I,2+\Delta t} = e^{-|\alpha|^2}\sum_{n=0}^{\infty}\sum_{k=0}^{\infty}\frac{\alpha^n(\alpha^*)^k}{\sqrt{n!k!}}\left|n\right\rangle\left\langle k\right|_f \otimes S_1(n,k)S_2(n,k)P_2(n,k)P_3(n,k)$$

$$\left\langle\psi_{2+\tau}(n)|\psi_{2+\tau}(k)\right\rangle^{1-e^{-\gamma\Delta t}}\left|\psi_{2+\tau}(n)e^{-\gamma\Delta t/2}\right\rangle\left\langle\psi_{2+\tau}(k)e^{-\gamma\Delta t/2}\right|_m \tag{4.76}$$

$$= e^{-|\alpha|^2}\sum_{n=0}^{\infty}\sum_{k=0}^{\infty}\frac{\alpha^n(\alpha^*)^k}{\sqrt{n!k!}}\left|n\right\rangle\left\langle k\right|_f \otimes \prod_{j=1}^{3}S_j(n,k)\prod_{l=2}^{3}P_l(n,k)\left|\psi_{I,2+\Delta t}(n)\right\rangle\left\langle\psi_{I,2+\Delta t}(k)\right|_m \tag{4.77}$$

which uses the new definition ($\left|\psi_{I,2+\Delta t}\right\rangle$ is not shown anymore, as seen above, it is trivial to define it by using $\left|\psi_{2+\tau}\right\rangle$). The details of the calculation for $S_3(n,k)$ are available in Appendix F.4, and give

$$S_3(n,k) = \left\langle\psi_{2+\tau}(n)|\psi_{2+\tau}(k)\right\rangle^{1-e^{-\gamma\Delta t}} \tag{4.78}$$

$$= \exp\left(-\frac{g^2\tau^2}{4}(n-k)^2\left(1-e^{-\gamma\Delta t}\right)\frac{1-e^{-3\gamma\Delta t/2}2\cos(3\omega_m\Delta t)+e^{-3\gamma\Delta t}}{1-e^{-\gamma\Delta t/2}2\cos(\omega_m\Delta t)+e^{-\gamma\Delta t}}\right) \tag{4.79}$$

4.2.4.3   Result for $\hat{\rho}_3$

After the easy transformation to get back to the first interaction picture, the result for $\hat{\rho}_3$ can now be written

$$\hat{\rho}_3 = e^{-|\alpha|^2}\sum_{n=0}^{\infty}\sum_{k=0}^{\infty}\frac{\alpha^n(\alpha^*)^k}{\sqrt{n!k!}}\left|n\right\rangle\left\langle k\right|_f \otimes \prod_{j=1}^{3}S_j(n,k)\prod_{l=2}^{3}P_l(n,k)\left|\psi_3(n)\right\rangle\left\langle\psi_3(k)\right|_m \tag{4.80}$$

58

with the associated new (with respect to the $\hat{\rho}_2$) definitions.

$$P_3(n,k) = \exp\left(i\frac{g^2\tau^2}{2}(n^2 - k^2)\left(e^{-\gamma\Delta t/2}\sin(\omega_m\Delta t) + e^{-\gamma\Delta t}\sin(2\omega_m\Delta t)\right)\right) \tag{4.81}$$

$$S_3(n,k) = \exp\left(-\frac{g^2\tau^2}{4}(n-k)^2\left(1 - e^{-\gamma\Delta t}\right)\frac{1 - e^{-3\gamma\Delta t/2}2\cos(3\omega_m\Delta t) + e^{-3\gamma\Delta t}}{1 - e^{-\gamma\Delta t/2}2\cos(\omega_m\Delta t) + e^{-\gamma\Delta t}}\right) \tag{4.82}$$

$$|\psi_3(n)\rangle = \left|\frac{ig\tau n}{\sqrt{2}}\left(e^M + e^{2M} + e^{3M}\right)\right\rangle \qquad \text{with} \qquad M = -i\omega_m\Delta t - \gamma\Delta t/2 \tag{4.83}$$

4.3 Generalisation to p Number of Pulses

Seeing the repeating patterns in the calculations that were made in the above, it appears clear that a general formula for any number of pulses must exist. The following derives this formula from two approaches. First, the formula will be derived in an intuitive manner, by making an educated guess on the basis of the evolution of the different parts of $\hat{\rho}_1$, $\hat{\rho}_2$, and $\hat{\rho}_3$. Next, a rigorous proof will be presented by using induction on the pulse number and mechanical state, and using the result to deduce the other factors.

4.3.1 Educated Guess From Calculated Results

Thanks to the calculations made for $\hat{\rho}_1$, $\hat{\rho}_2$, and $\hat{\rho}_3$, it is actually possible to intuitively see the form the generalised formula should take without much effort.

4.3.1.1 Mechanical States

From the previous calculations, the mechanical state after each full pulse appeared as

$$|\psi_1(n)\rangle = \left|\frac{ig\tau n}{\sqrt{2}}e^M\right\rangle, \quad |\psi_2(n)\rangle = \left|\frac{ig\tau n}{\sqrt{2}}\left(e^M + e^{2M}\right)\right\rangle, \quad |\psi_3(n)\rangle = \left|\frac{ig\tau n}{\sqrt{2}}\left(e^M + e^{2M} + e^{3M}\right)\right\rangle \tag{4.84}$$

with $M = -i\omega_m\Delta t - \gamma\Delta t/2$. The behaviour of the state after p full pulses therefore seems to be following

$$|\psi_p(n)\rangle = \left|\frac{ig\tau n}{\sqrt{2}}\sum_{j=1}^{p} e^{jM}\right\rangle \qquad \text{with} \qquad M = -i\omega_m\Delta t - \gamma\Delta t/2 \tag{4.85}$$

4.3.1.2 Total Scaling Factor

In the calculation of the three first pulses, the three scaling factors that were derived are

$$S_1(n,k) = \exp\left(-\frac{g^2\tau^2}{4}(n-k)^2\left(1 - e^{-\gamma\Delta t}\right)\right) \tag{4.86}$$

$$S_2(n,k) = \exp\left(-\frac{g^2\tau^2}{4}(n-k)^2\left(1 - e^{-\gamma\Delta t}\right)\frac{1 - e^{-\gamma\Delta t}2\cos(2\omega_m\Delta t) + e^{-2\gamma\Delta t}}{1 - e^{-\gamma\Delta t/2}2\cos(\omega_m\Delta t) + e^{-\gamma\Delta t}}\right) \tag{4.87}$$

$$S_3(n,k) = \exp\left(-\frac{g^2\tau^2}{4}(n-k)^2\left(1 - e^{-\gamma\Delta t}\right)\frac{1 - e^{-3\gamma\Delta t/2}2\cos(3\omega_m\Delta t) + e^{-3\gamma\Delta t}}{1 - e^{-\gamma\Delta t/2}2\cos(\omega_m\Delta t) + e^{-\gamma\Delta t}}\right) \tag{4.88}$$

After p full pulses, these factors are multiplied, giving a total scaling factor

$$S_{tot,p}(n,k) = \prod_{j=1}^{p} S_j(n,k) \tag{4.89}$$

From the first three scaling factors, the total scaling factor also seems easily generalisable

$$S_{tot,p}(n,k) = \exp\left(-\frac{g^2\tau^2}{4}(n-k)^2\left(1-e^{-\gamma\Delta t}\right)\sum_{j=1}^{p}\frac{1-e^{-j\gamma\Delta t/2}2\cos(j\omega_m\Delta t)+e^{-j\gamma\Delta t}}{1-e^{-\gamma\Delta t/2}2\cos(\omega_m\Delta t)+e^{-\gamma\Delta t}}\right) \quad (4.90)$$

It should be noted here that while the pattern is very easy to see here, it is mainly thanks to how some of the algebra was simplified. The use of geometric sums instead of distributing terms in a set of trigonometric functions is the key that enabled the great similarity between $S_2(n,k)$ and $S_3(n,k)$. One can look back at Appendix F.3 and F.4 to understand how the particular way the equations were simplified led to the simple result seen here. If another approach was taken, the results would still be equivalent, but the pattern between the different scaling factors would have been a lot harder to notice. In some way, the way some factors were simplified anticipated some results of the more rigorous proof that will be done in Section 4.3.2.

4.3.1.3 Total Phase Factor

Similarly to the previous cases, the list of the obtained phase factor is

$$P_1(n,k) = 1 \quad (4.91)$$

$$P_2(n,k) = \exp\left(i\frac{g^2\tau^2}{2}(n^2-k^2)e^{-\gamma\Delta t/2}\sin\left(\omega_m\Delta t\right)\right) \quad (4.92)$$

$$P_3(n,k) = \exp\left(i\frac{g^2\tau^2}{2}(n^2-k^2)\left(e^{-\gamma\Delta t/2}\sin(\omega_m\Delta t)+e^{-\gamma\Delta t}\sin(2\omega_m\Delta t)\right)\right) \quad (4.93)$$

With the total phase factor after p pulses

$$P_{tot,p}(n,k) = \prod_{j=1}^{p}P_j(n,k) \quad (4.94)$$

Here, the first phase factor $P_1(n,k) = 1$ was added, to complete the list and underline the fact that the first full pulse does not lead to any additional phase. From the above, it seems the phase factor that is acquired at pulse number p can be written

$$P_p(n,k) = \exp\left(i\frac{g^2\tau^2}{2}(n^2-k^2)\sum_{j=1}^{p-1}e^{-j\gamma\Delta t/2}\sin\left(j\omega_m\Delta t\right)\right) \quad (4.95)$$

Then, the total phase factor after p would be

$$P_{tot,p}(n,k) = \prod_{s=1}^{p}\exp\left(i\frac{g^2\tau^2}{2}(n^2-k^2)\sum_{j=1}^{s-1}e^{-j\gamma\Delta t/2}\sin\left(j\omega_m\Delta t\right)\right) \quad (4.96)$$

$$= \exp\left(i\frac{g^2\tau^2}{2}(n^2-k^2)\sum_{s=1}^{p}\sum_{j=1}^{s-1}e^{-j\gamma\Delta t/2}\sin\left(j\omega_m\Delta t\right)\right) \quad (4.97)$$

$$= \exp\left(i\frac{g^2\tau^2}{2}(n^2-k^2)\sum_{j=1}^{p-1}(p-j)e^{-j\gamma\Delta t/2}\sin\left(j\omega_m\Delta t\right)\right) \quad (4.98)$$

4.3.2 Proof of the General Result for p Pulses

While the results derived from the intuitive approach seems nice, there is no rigorous proof the conclusions above are correct yet. These are just patterns that appeared for the first three pulses that

were calculated. Some may think that the correctness of the above is highly likely, but examples exist where patterns on a first few terms are actually misleading[1]. The following proves this rigorously.

The central part of the proof to show the result of any number of pulses on the starting density matrix $\hat{\rho}_0 = |\alpha\rangle \langle\alpha|_f \otimes |0\rangle \langle0|_m$ is an induction proof done to understand the mechanical state after any number of pulses. Once this is done, the different factors for the scaling and phase of the result can be directly computed for any number of pulses.

4.3.2.1 Proof by Induction for the Mechanical State

Proving that the mechanical state after p pulses can be written as

$$|\psi_p(n)\rangle = \left| \frac{ig\tau n}{\sqrt{2}} \sum_{j=1}^{p} e^{jM} \right\rangle \qquad \text{with} \qquad M = -i\omega_m \Delta t - \gamma \Delta t/2 \qquad (4.99)$$

is quite easy. For this, one just needs to carefully consider the different operations that are done on the mechanical state. Starting with some mechanical coherent state $|\alpha\rangle$, the different operations give

1. An interaction pulse amounts to applying a displacement operator, giving a result proportional to

$$\left| \alpha + \frac{ig\tau n}{\sqrt{2}} \right\rangle \qquad (4.100)$$

2. The trivial transformation to the second interaction picture does not change the state.

3. The dissipation induces a scaling of the mechanical sate, the results being now proportional to

$$\left| \left(\alpha + \frac{ig\tau n}{\sqrt{2}} \right) e^{-\gamma \Delta t/2} \right\rangle \qquad (4.101)$$

4. Finally, the inverse transformation to get back to the first interaction picture adds a phase

$$\left| \left(\alpha + \frac{ig\tau n}{\sqrt{2}} \right) e^{-i\omega_m \Delta t - \gamma \Delta t/2} \right\rangle = \left| \left(\alpha + \frac{ig\tau n}{\sqrt{2}} \right) e^{M} \right\rangle \qquad (4.102)$$

Now considering that $\alpha = \frac{ig\tau n}{\sqrt{2}} \sum_{j=1}^{p} e^{jM}$ for some p, then after one more pulse, the result is

$$
\begin{aligned}
\left| \left(\alpha + \frac{ig\tau n}{\sqrt{2}} \right) e^{M} \right\rangle &= \left| \left(\frac{ig\tau n}{\sqrt{2}} \sum_{j=1}^{p} e^{jM} + \frac{ig\tau n}{\sqrt{2}} \right) e^{M} \right\rangle \\
&= \left| \left(\frac{ig\tau n}{\sqrt{2}} \sum_{j=0}^{p} e^{jM} \right) e^{M} \right\rangle \qquad (4.103) \\
&= \left| \frac{ig\tau n}{\sqrt{2}} \sum_{j=1}^{p+1} e^{jM} \right\rangle
\end{aligned}
$$

Since the formula matches with the starting state (*i.e.* $|0\rangle$), all the requirements for the proof by induction are met. The mechanical state expression in Equation 4.99 is proven.

---

[1]The discussion following the presentation of the Magnus series is actually a very good example of this, see Equation 3.12 and the associated discussion.

4.3.2.2 Total Scaling Factor

Staying general, the scaling factor S_p acquired during pulse number p, is always obtained due to the dissipative time evolution, more precisely, it comes from the factor

$$S_p(n,k) = \left\langle \psi_{I,(p-1)+\tau}(n) \middle| \psi_{I,(p-1)+\tau}(k) \right\rangle^{1-e^{-\gamma\Delta t}} \tag{4.104}$$

Thanks to the previous expression proven for $|\psi_p(n)\rangle$, and to the knowledge that the only change from it to obtain $|\psi_{I,p+\tau}\rangle$ is to add the displacement $ig\tau n/\sqrt{2}$. It then follows that

$$\left|\psi_{I,(p-1)+\tau}(n)\right\rangle = \left|\frac{ig\tau n}{\sqrt{2}}\sum_{j=1}^{p-1}e^{jM} + \frac{ig\tau n}{\sqrt{2}}\right\rangle = \left|\frac{ig\tau n}{\sqrt{2}}\sum_{j=0}^{p-1}e^{jM}\right\rangle \tag{4.105}$$

The scaling factor for the pth pulse can then be written

$$S_p(n,k) = \left\langle \frac{ig\tau n}{\sqrt{2}}\sum_{j=0}^{p-1}e^{jM} \middle| \frac{ig\tau k}{\sqrt{2}}\sum_{j=0}^{p-1}e^{jM} \right\rangle^{1-e^{-\gamma\Delta t}} \tag{4.106}$$

$$= \left\langle \frac{ig\tau n}{\sqrt{2}}\frac{1-e^{pM}}{1-e^{M}} \middle| \frac{ig\tau k}{\sqrt{2}}\frac{1-e^{pM}}{1-e^{M}} \right\rangle^{1-e^{-\gamma\Delta t}} \tag{4.107}$$

$$= \exp\left(\frac{-ig\tau n}{\sqrt{2}}\frac{1-e^{pM^*}}{1-e^{M^*}}\frac{ig\tau k}{\sqrt{2}}\frac{1-e^{pM}}{1-e^{M}} - \frac{1}{2}\left|\frac{ig\tau n}{\sqrt{2}}\frac{1-e^{pM}}{1-e^{M}}\right|^2 \right.$$

$$\left. - \frac{1}{2}\left|\frac{ig\tau k}{\sqrt{2}}\frac{1-e^{pM}}{1-e^{M}}\right|^2 \right)^{1-e^{-\gamma\Delta t}} \tag{4.108}$$

$$= \exp\left(-\frac{g^2\tau^2}{4}(n-k)^2\frac{1-e^{pM^*}}{1-e^{M^*}}\frac{1-e^{pM}}{1-e^{M}}\left(1-e^{-\gamma\Delta t}\right) \right) \tag{4.109}$$

$$= \exp\left(-\frac{g^2\tau^2}{4}(n-k)^2\left(1-e^{-\gamma\Delta t}\right)\frac{1-e^{-p\gamma\Delta t/2}2\cos(p\omega_m\Delta t)+e^{-p\gamma\Delta t}}{1-e^{-\gamma\Delta t/2}2\cos(\omega_m\Delta t)+e^{-\gamma\Delta t}} \right) \tag{4.110}$$

The total scaling factor is then easy to compute, and the result exactly proves the educated guess made in Equation 4.90.

$$S_{tot,p} = \prod_{j=1}^{p}S_j(n,k) \tag{4.111}$$

$$= \exp\left(-\frac{g^2\tau^2}{4}(n-k)^2\left(1-e^{-\gamma\Delta t}\right)\sum_{j=1}^{p}\frac{1-e^{-j\gamma\Delta t/2}2\cos(j\omega_m\Delta t)+e^{-j\gamma\Delta t}}{1-e^{-\gamma\Delta t/2}2\cos(\omega_m\Delta t)+e^{-\gamma\Delta t}} \right) \tag{4.112}$$

4.3.2.3 Total Phase Factor

The origin of the phase factor $P_p(n,k)$ is the result of the displacement operator applied on the density matrix by the interaction. It can be written as

$$\hat{D}\left(\frac{ig\tau n}{\sqrt{2}}\right)|\psi_p(n)\rangle = C(n)|\psi_{p+\tau}(n)\rangle \tag{4.113}$$

where $C(n)$ is used to obtain the actual phase factor via $P_p(n,k) = C(n)C^*(k)$. This is easily understood from all the calculations above, or by simply writing

$$\hat{D}\left(\frac{ig\tau n}{\sqrt{2}}\right)|\psi_p(n)\rangle\langle\psi_p(k)|\hat{D}\left(-\frac{ig\tau k}{\sqrt{2}}\right) = \hat{D}\left(\frac{ig\tau n}{\sqrt{2}}\right)|\psi_p(n)\rangle\left(\hat{D}\left(\frac{ig\tau k}{\sqrt{2}}\right)|\psi_p(k)\rangle\right)^{\dagger} \tag{4.114}$$

$$= C(n) |\psi_{p+\tau}(n)\rangle \left(C(k) |\psi_{p+\tau}(k)\rangle \right)^\dagger \tag{4.115}$$

$$= C(n)C^*(k) |\psi_{p+\tau}(n)\rangle \langle\psi_{p+\tau}(k)| \tag{4.116}$$

To calculate $P_p(n, k)$, $C(n)$ is obtained as generated by the pth interaction on $|\psi_{p-1}\rangle$.

$$\hat{D}\left(\frac{ig\tau n}{\sqrt{2}}\right) |\psi_{p-1}(n)\rangle = \hat{D}\left(\frac{ig\tau n}{\sqrt{2}}\right) \left| \frac{ig\tau n}{\sqrt{2}} \sum_{j=1}^{p-1} e^{jM} \right\rangle \tag{4.117}$$

As before, the formula used is the one that was first proven in Equation 2.86.

$$C(n) = \exp\left(\frac{1}{2} \frac{ig\tau n}{\sqrt{2}} \frac{-ig\tau n}{\sqrt{2}} \sum_{j=1}^{p-1} e^{jM^*} - \frac{1}{2} \frac{-ig\tau n}{\sqrt{2}} \frac{ig\tau n}{\sqrt{2}} \sum_{j=1}^{p-1} e^{jM} \right) \tag{4.118}$$

$$= \exp\left(\frac{g^2\tau^2}{4} n^2 \sum_{j=1}^{p-1} \left(e^{jM^*} - e^{jM} \right) \right) \tag{4.119}$$

$$= \exp\left(i\frac{g^2\tau^2}{2} n^2 \sum_{j=1}^{p-1} e^{-ij\gamma\Delta t/2} \sin(j\omega_m\Delta t) \right) \tag{4.120}$$

This directly lead to the exact same factor given as the educated guess in Equation 4.95.

$$P_p(n, k) = C(n)C^*(k) = \exp\left(i\frac{g^2\tau^2}{2} (n^2 - k^2) \sum_{j=1}^{p-1} e^{-ij\gamma\Delta t/2} \sin(j\omega_m\Delta t) \right) \tag{4.121}$$

As a direct consequence, the same total phase factor is also proven

$$P_{tot,p}(n, k) = \exp\left(i\frac{g^2\tau^2}{2} (n^2 - k^2) \sum_{j=1}^{p-1} (p-j) e^{-j\gamma\Delta t/2} \sin(j\omega_m\Delta t) \right) \tag{4.122}$$

4.3.3 Final Result

The pulsed interaction applied for a number p of pulses on the starting state $|\alpha\rangle_f \otimes |0\rangle_m$ while taking into account mechanical dissipation generates a mixed state. This mixed state which includes particular scaling and phase factors can then be represented by the density matrix

$$\hat{\rho}_p = e^{-|\alpha|^2} \sum_{n=0}^{\infty} \sum_{k=0}^{\infty} \frac{\alpha^n (\alpha^*)^k}{\sqrt{n!k!}} S_{tot,p}(n, k) P_{tot,p}(n, k) |n\rangle \langle k|_f \otimes |\psi_p(n)\rangle \langle\psi_p(k)|_m \tag{4.123}$$

with

$$S_{tot,p} = \exp\left(-\frac{g^2\tau^2}{4} (n-k)^2 \left(1 - e^{-\gamma\Delta t}\right) \sum_{j=1}^{p} \frac{1 - e^{-j\gamma\Delta t/2} 2\cos(j\omega_m\Delta t) + e^{-j\gamma\Delta t}}{1 - e^{-\gamma\Delta t/2} 2\cos(\omega_m\Delta t) + e^{-\gamma\Delta t}} \right) \tag{4.124}$$

$$P_{tot,p}(n, k) = \exp\left(i\frac{g^2\tau^2}{2} (n^2 - k^2) \sum_{j=1}^{p-1} (p-j) e^{-j\gamma\Delta t/2} \sin(j\omega_m\Delta t) \right) \tag{4.125}$$

$$|\psi_p(n)\rangle = \left| \frac{ig\tau n}{\sqrt{2}} \sum_{j=1}^{p} e^{jM} \right\rangle \qquad \text{with} \qquad M = -i\omega_m\Delta t - \gamma\Delta t/2 \tag{4.126}$$

4.4 Interpretation and Consistency Check

The final result that was just obtained for the pulsed system with dissipation in the first interaction picture is a relatively long and complex expression. It is therefore of interest to both interpret it and dedicate some time to discuss its correctness.

4.4.1 Interpretation

The first fundamental fact that can be noted from the final expression with dissipation is that the dissipation influences all the different factors present. The final mechanical state, its scaling, and the geometric phase are all impacted.

Accurately quantifying the different impacts this has on the gate operation would require additional theoretical developments, which will unfortunately not be done in this work. However, a qualitative discussion of the different impacts on the result is given below.

4.4.1.1 Final Mechanical State and Closed Loops

The final mechanical state is influenced by γ in the M factor, and this impact grows with the number of pulses. One can check that for each additional displacement in the phase space, the factor $\exp(-j\gamma\Delta/2)$ appears, with j the number of said displacement. Thinking in the phase space, this has the impact of slightly decreasing the amplitude of each displacement. If there is little dissipation (*i.e.* γ is small), it leads $s = \exp(-\gamma\Delta/2)$ to be only slightly below 1. However, the effect of this "shortening factor" actually grows exponentially with the number of pulses. The amplitude of the displacement due to the pulse number 100 will then be shortened by the factor s^{100}.

This is an especially interesting result if the objective is to obtain a closed loop in the phase space. Considering a gate with 8 pulses with parameters chosen to obtain a closed loop, the ideal result will be a regular octagon inscribed in a circle (one can refer to Figure 2.5 for a representation of this circle). In a non ideal situation however (*i.e.* with non negligible dissipation), this octagon will not be closed at the origin anymore. Instead, its sides will have decreasing length and the corresponding open shape[2] will be inscribed in a spiral going inward (*i.e.* the distance from the center of the ideal circle decreases with additional steps). This spiralling phenomenon comes from the fact that, while the amplitude of the displacements is decreased, the progression in the angle at which they are added stays ideal (since this angle comes from the factor $ij\omega_m\Delta t$).

Interestingly, because of the spiralling phenomenon, the idea of simply "adding more pulses" will never solve the problem of closing the loop. However, a progressive and precise control of either Δt or ω_m would enable the control of the angle of the next displacement. If this control is precisely tuned according to the amount of dissipation, this would make closing the loop theoretically possible.

With a set of experimental parameters, a few lines of code, and the above theoretical results, this behaviour and the complex shapes that result from it could easily be calculated and represented.

4.4.1.2 Total Scaling and Total Phase Factors

As can be understood from its origin in the calculations and from the fact that it goes to one if $\gamma = 0$, it is easily understood that the scaling factor $S_{tot,p}$ is a direct consequence of introducing dissipation in the system. This factor can be relatively hard to interpret without additional theoretical developments, because it depends on the number of photons variable[3] (n and k), which is summed over all the Fock states.

A few things can nonetheless be noted. As his name suggests, this factor reduces the amplitude for elements according to the strength of the dissipation. It also particularly impacts the elements of the

---

[2]By "open shape" what is meant here is the geometrical object resulting from adding different segments at different angles one after the other.

[3]These variables were also present in the final mechanical states, but were multiplied by zero if the loop was closed, which conveniently made their discussion less central.

density matrix that are far from its diagonal (*i.e.* since it includes the factor $(n - k)^2$). In fact, it leaves invariant the elements of the density matrix for which $n = k$. This behaviour of only keeping the diagonal elements transforms the state that was originally a pure and coherent state into a statistical mixture. This phenomenon means a loss of quantum coherence, and the impossibility of using the result for additional operations relying on quantum interference.

Concerning the phase factor, most has already been said via the talk concerning the impact of dissipation on the path in the phase space. As discussed in Section 2.3.4, a difference in the path in the phase space will lead to different factors for the area associated with each step, it is therefore expected to find the "shortening factor" $s^j = \exp(-\gamma \Delta t/2)$ in the phase factor. It can also be noted that both this factor and the scaling factor are second order in the photon number variables, and the phase is multiplied by $n^2 - k^2$, which means that this phase factor will grow with the number of photons, and be null on the diagonal. Since the scaling factor decreases all the off-diagonal elements, the chance of being able to observe any geometric phase at all is also decreased by the dissipation.

4.4.2 Correctness of the Final Result

It is reasonable to already have relatively high confidence in the correctness of the final result thanks to how it was obtained. Indeed, it is always reassuring to derive the same result by using two approaches. While the general proof confirmed the fact that the same patterns indeed repeated themselves for any number of pulses p, it also exactly matched the direct calculations done for the three first pulses (*i.e.* $\hat{\rho}_1$, $\hat{\rho}_2$, and $\hat{\rho}_3$).

There is however one more consistency check that could be done, which is to verify that the final result also matches the final result of Chapter 3, where the problem was examined without dissipation. This is done here.

4.4.2.1 Consistency Check with Chapter 3

It is useful to note that trying to exactly make the value of c_1, c_2 and c_3 (see Equation 3.104, these parameters corresponded to the fully explicit version of $\hat{U}_p$) appear from the dissipative case with $\gamma = 0$ would be very long and of little interest. In the following, as soon as the equivalence can be proven, using the fully explicit version of $\hat{U}_p$ or not has no importance.

Rewriting the final result of this chapter in the case of $\gamma = 0$ gives

$$\hat{\rho}_{p,\gamma=0} = e^{-|\alpha|^2} \sum_{n=0}^{\infty} \sum_{k=0}^{\infty} \frac{\alpha^n (\alpha^*)^k}{\sqrt{n!k!}} P_{tot,p,\gamma=0}(n,k) |n\rangle \langle k|_f \otimes |\psi_p(n)\rangle \langle \psi_p(k)|_{m,\gamma=0} \tag{4.127}$$

with

$$P_{tot,p,\gamma=0}(n,k) = \exp\left(i \frac{g^2 \tau^2}{2} (n^2 - k^2) \sum_{j=1}^{p-1} (p-j) \sin\left(j\omega_m \Delta t\right) \right) \tag{4.128}$$

$$|\psi_p(n)\rangle_{\gamma=0} = \left| \frac{ig\tau n}{\sqrt{2}} \sum_{j=1}^{p} e^{-ij\omega_m \Delta t} \right\rangle \tag{4.129}$$

Starting by checking the final mechanical state, it is crucial to remember that the last results of Chapter 3 are in the second interaction picture. And not any second interaction picture, but the second interaction picture with $t = 0$ defined at the start of the first pulse. As mentioned in the reminder about interaction picture (see Section 3.2.1), comparing results obtained in different interaction pictures is a common mistake. In this choice for the origin of time, the resulting density matrix that is obtained in this section is at $t = p\Delta t$, and so one can move the state $|\psi_p\rangle$ to the same second interaction picture using

$$\hat{U}_{0,S,m}^{-1}(p\Delta t)\,|\psi_p\rangle = e^{i\omega_m p\Delta t \hat{b}^\dagger \hat{b}}\left|\frac{ig\tau n}{\sqrt{2}}\sum_{j=1}^{p}e^{-ij\omega_m \Delta t}\right\rangle \tag{4.130}$$

$$= \left|\frac{ig\tau n}{\sqrt{2}}\sum_{j=1}^{p}e^{i(p-j)\omega_m \Delta t}\right\rangle \tag{4.131}$$

$$= \left|\frac{ig\tau n}{\sqrt{2}}\sum_{j=0}^{p-1}e^{ij\omega_m \Delta t}\right\rangle \tag{4.132}$$

Now, one could use the final expression of Chapter 3 (see Equation 3.104), but this expression was made fully explicit via a relatively long set of developments. To compare it with this result, using the final version of $\hat{U}_p$ would actually make everything way harder than using one of the earlier results, before c_1 and c_2 were calculated. In this case, the best version to use is Equation 3.78, the expression in terms of product of displacement operators easily gives that the total operator will be proportional to the general displacement

$$\hat{U}_p \propto \hat{D}_O\left(\sum_{n=0}^{p-1}\frac{i\lambda e^{-in\theta}}{\sqrt{2}}\right) = \hat{D}_O\left(\frac{ig\tau}{\sqrt{2}}\sum_{j=0}^{p-1}e^{ij\omega_m \Delta t}\right) \tag{4.133}$$

where one remembers that $\theta = -\omega_m \Delta t$, $\lambda = g\tau$, and $\hat{O} = \hat{a}^\dagger \hat{a}$. It immediately appears that acting with this operator on the starting state $|\alpha\rangle_f \otimes |0\rangle_m$ will indeed give the mechanical state mentioned above in Equation 4.132 (similarly to before, the coherent state α is decomposed in its Fock basis with a sum on n, and the action of $\hat{O}$ on this state is simply $\hat{a}^\dagger \hat{a}\,|n\rangle = n\,|n\rangle$, which multiplies the displacement amplitude of the displacement operator by n, and gives 4.132).

The next and final problem is to prove that the phase factor in Equation 4.128 would also be obtained by applying the operator

$$e^{ic_3 \hat{O}^2} \qquad \text{with} \qquad \hat{O} = \hat{a}^\dagger \hat{a} \tag{4.134}$$

on the starting density matrix $\hat{\rho}_0 = |\alpha\rangle\langle\alpha|_f \otimes |0\rangle\langle0|_m$ (where c_3 is given back in Equation 3.107). As for the previous case, one can dramatically shorten the proof by starting from one of the first expressions for this operator, before it was made fully explicit. In chapter 3, this operator was first named B, and before being simplified in the above form, it was written (see Equation 3.96)

$$B = \exp\left(\sum_{n=1}^{p-1}i\frac{\lambda^2}{2}\frac{\sin(n\theta/2)}{\sin(\theta/2)}\sin\left(-(n+1)\theta/2\right)\hat{O}^2\right) \tag{4.135}$$

$$= \exp\left(\sum_{n=1}^{p-1}i\frac{g^2\tau^2}{2}\frac{\sin(n\omega_m\Delta t/2)}{\sin(\omega_m\Delta t/2)}\sin\left((n+1)\omega_m\Delta t/2\right)\hat{O}^2\right) \tag{4.136}$$

when used on $\hat{\rho}_0$, the operator $\hat{O}^2$ will simply lead to the factor $n^2 - k^2$ (following the Fock space decomposition of the optical states, and since the operator only acts on the optical states the interaction picture transformation on the mechanical states has no impact on this result). Now back to $P_{tot,p,\gamma=0}(n,k)$, let us use its form right before the sum on all phase factors is computed and do the first sum (using the trigonometric sums developed and proven in Appendix E), in Equation 4.97 (using $\gamma = 0$).

$$P_{tot,p,\gamma=0}(n,k) = \exp\left(i\frac{g^2\tau^2}{2}(n^2 - k^2)\sum_{s=1}^{p}\sum_{j=1}^{s-1}\sin\left(j\omega_m\Delta t\right)\right) \tag{4.137}$$

$$= \exp\left(i\frac{g^2\tau^2}{2}(n^2 - k^2)\sum_{s=1}^{p}\frac{\sin(s\omega_m\Delta t/2)}{\sin(\omega_m\Delta t/2)}\sin\left(\frac{s-1}{2}\omega_m\Delta t\right)\right) \tag{4.138}$$

$$= \exp\left(i\frac{g^2\tau^2}{2}(n^2 - k^2)\sum_{s=0}^{p-1}\frac{\sin((s+1)\omega_m\Delta t/2)}{\sin(\omega_m\Delta t/2)}\sin\left(s\omega_m\Delta t/2\right)\right) \tag{4.139}$$

$$= \exp\left(i\frac{g^2\tau^2}{2}(n^2 - k^2)\sum_{s=1}^{p-1}\frac{\sin((s+1)\omega_m\Delta t/2)}{\sin(\omega_m\Delta t/2)}\sin\left(s\omega_m\Delta t/2\right)\right) \tag{4.140}$$

replacing $\hat{O}^2$ by $n^2 - k^2$ as explained above, this shows that the two expressions are indeed identical !

The last consistency check is therefore successful. The expression derived to include mechanical dissipation is indeed equivalent to the the case without dissipation when $\gamma = 0$.

Chapter 5

Conclusion

The present conclusion summarises the achievements of the different chapters of this dissertation, and presents some ideas for future work.

5.1 Dissertation Overview

This document started with a general introduction to the field, contextualising the present work and setting the objectives of the different chapters.

The approach taken to introduce the subject was to start with a general introduction to the concepts and ideas of quantum computing. Through this, the subject of quantum gates and the relevance of the associated scientific research today was underlined. Geometric phase quantum gates, which are the main object of this work, were then introduced in this context by presenting their advantages over other quantum gates and qualitatively presenting the current state of the associated research.

In order to move on to a mathematically precise understanding of geometric phase gates and later go into optomechanical systems and even dissipation phenomena, a lot of ground had to be covered in the second chapter. This was done by deriving the Milburn gate in the context of trapped ions. By introducing and proving the expressions for the Milburn gate, which is the simplest geometric phase quantum gate, this chapter was used to give all the tools necessary to approach quantum geometric gates in general. In addition, it also lead to a broader understanding of the context in terms of other gates, such as the Cirac-Zoller gate and the Sørensen-Mølmer gate. Importantly, this chapter derived a set of general results that are not limited to trapped ions applications (such as coherent states and their behaviour, the coherent state overcomplete basis, quantum displacement operators, and their phase space behaviour and interpretation, including phase space loops.).

In the third chapter the optomechanical system that is central to this work was first studied. First examining a time independent optomechanical interaction, the analysis was then pushed to the time dependent regime of pulsed short interactions. This pulsed interaction was shown to result in a general "pulsed geometric quantum gate" of p successive displacements. By tuning its parameters, this result was linked to both the Milburn gate and the Sørensen-Mølmer gate. In order to obtain these results, this chapter also introduced some additional mathematical tools, such as the Magnus expansion and the use of nested interaction picture transformations. The final result of this chapter was shown in different pictures and expressions for different purposes. One of these expression was a fully simplified and explicit formula in the second interaction picture, which was confirmed by identical results found in the literature. Another expression in the first interaction picture was manipulated to obtain a "pulse separated form". This second expression was instrumental in the interpretation of the approximations made, and in the introduction of dissipation in the next chapter.

The fourth and final chapter introduced dissipation to the optomechanical system, and started with a general description of the necessary mathematical framework for the problem (such as density matrices and the dissipation master equation). The approach to the dissipative nature of the mechanical system

relied on one of the particular mathematical forms for the gate presented in the previous chapter (the first interaction picture pulse separated version). First, direct calculations were used to compute the density matrix resulting from one, two, and three successive pulses. With these results, a pattern was extracted and an educated guess was presented for the result for any number of successive pulses. Thanks to the precise understanding of the mathematical behaviour of the different objects and operators at play throughout these calculations, this educated guess was then confirmed via a general rigorous proof. A final consistency check was then made on the final result to verify it matched the results of the previous chapter in the limit case $\gamma = 0$. The final result obtained was also criticised and some of the implications of dissipation on the gate operation were presented.

To the best knowledge of the author, the results of the last chapter concerning the impact of dissipation on pulsed geometric quantum gates in optomechanical systems constitute original work, and these results have not yet been derived in the literature. Similarly, the approach using the first interaction picture pulse separated expression that was demonstrated in the third chapter was also never seen in any of the consulted literature.

5.2 Future Work

The possibilities for future work are numerous. The first and most obvious thing that could be developed further is to continue to study the final result for dissipation. This final result could be used to compute Q-function, state fidelity, purity, and other practical indicators of performance of the gate. Unfortunately, the time and length of the present dissertation are limited, and it could not be done in this document. An additional possibility would be to study some of the points that were underlined in the interpretation of the result of the final chapter. Both the accurate computation of the geometrical shape generated in the phase space due to dissipation and the further study of the idea of controlled time pulses/mechanical frequency to counteract dissipation may be interesting.

Another aspect that could be pushed further is the study and contextualisation of the optomechanical system and its applications. Here, the subject of geometric gates was introduced via a discussion on quantum computing, followed by the presentation of such gates on trapped ions. The understanding and the mathematical tools acquired were then put to use on a particular pulsed optomechanical system. However, as mentioned at the beginning of the associated chapter, this device has several applications that are not directly linked to quantum computing, such as in sensing applications. A study of practical systems that directly use this type of optomechanical device would be interesting, especially if coupled to more experimental considerations and data. As the above work was mainly theoretical, a study of its results when used with experimental values for the different parameters would be very interesting.

A final direction in which future work could be taken would be to further discuss the assumptions and approximations made in this work, and their quality. For instance, one remembers that the master equation for dissipation presented in Chapter 4 assumes an environment cooled to the ground state. This condition is of course not ideally reproduced in practical applications. It would then be interesting to consider whether adapting the value for γ is sufficient or not to consider the imperfect experimental conditions.

Appendix A

Calculation Details for Chapter 2

This appendix groups a set of short proofs and developments assisting in the calculations made in Chapter 2. These were taken out of the main text in order to improve readability and clarity. Instead of opening half-page parentheses in a main development to solve each small mathematical hurdle, these small proofs are included here.

A.1 Equation 2.15

Using the matrix forms of the Pauli matrices, and of the σ_+ and σ_- matrices (reminded below)

$$\sigma_x = \begin{pmatrix} 0 & 1 \\ 1 & 0 \end{pmatrix} \qquad \sigma_y = \begin{pmatrix} 0 & -i \\ i & 0 \end{pmatrix} \qquad \sigma_z = \begin{pmatrix} 1 & 0 \\ 0 & -1 \end{pmatrix} \qquad \sigma_+ = \begin{pmatrix} 0 & 1 \\ 0 & 0 \end{pmatrix} \qquad \sigma_- = \begin{pmatrix} 0 & 0 \\ 1 & 0 \end{pmatrix} \quad (A.1)$$

one can easily show the following simple identities

$$\sigma_x = \sigma_+ + \sigma_- \tag{A.2}$$
$$\sigma_-(\sigma_z)^n = \sigma_- \tag{A.3}$$
$$\sigma_+(\sigma_z)^n = (-1)^n \sigma_+ \tag{A.4}$$
$$\tag{A.5}$$

With these and a simple Taylor expansion, all that is necessary to complete the small proof is to write

$$\sigma_x e^{-i\omega_0 \sigma_z t} = (\sigma_+ + \sigma_-) \sum_{n=0}^{\infty} \frac{(-i\omega_0 \sigma_z t)^n}{n!} \tag{A.6}$$

$$= \sigma_- \sum_{n=0}^{\infty} \frac{(-i\omega_0 t)^n}{n!} + \sigma_+ \sum_{n=0}^{\infty} \frac{(i\omega_0 t)^n}{n!} \tag{A.7}$$

$$= \sigma_- e^{-i\omega_0 t} + \sigma_+ e^{i\omega_0 t} \tag{A.8}$$

A.2 BCH Lemma Proof

$$e^{\hat{X}} \hat{Y} e^{-\hat{X}} = \sum_{n=0}^{\infty} \frac{[(\hat{X})^n, \hat{Y}]}{n!} \qquad \text{with} \qquad [(\hat{X})^n, Y] = \underbrace{[\hat{X}, ...[\hat{X}, [\hat{X}, \hat{Y}]]...]}_{n \text{ times}} \quad \text{and} \quad [(\hat{X})^0, \hat{Y}] = \hat{Y} \quad (A.9)$$

Starting from the operator function $\hat{F}(\epsilon) = e^{\epsilon \hat{X}} \hat{Y} e^{-\epsilon \hat{X}}$, which is the starting expression if $\epsilon = 1$, its Taylor expansion around zero is

$$F(\epsilon) = \sum_{n=0}^{\infty} \left. \frac{d^n F(\epsilon)}{d\epsilon} \right|_{\epsilon=0} \frac{\epsilon^n}{n!} \tag{A.10}$$

Taking a bite of time to compute the different derivatives at $\epsilon = 0$, one can find

$$\left. \frac{d^0 F(\epsilon)}{d\epsilon} \right|_{\epsilon=0} = F(0) = \hat{Y} \tag{A.11}$$

$$\left. \frac{dF(\epsilon)}{d\epsilon} \right|_{\epsilon=0} = \left(\hat{X} e^{\epsilon \hat{X}} \hat{Y} e^{-\epsilon \hat{X}} + e^{\epsilon \hat{X}} \hat{Y} (-\hat{X}) e^{-\epsilon \hat{X}} \right) \Big|_{\epsilon=0} = [\hat{X}, F(\epsilon)] \big|_{\epsilon=0} = [\hat{X}, \hat{Y}] \tag{A.12}$$

$$\left. \frac{d^2 F(\epsilon)}{d\epsilon} \right|_{\epsilon=0} = \left. [\hat{X}, \frac{dF(\epsilon)}{d\epsilon}] \right|_{\epsilon=0} = [\hat{X}, [\hat{X}, \hat{Y}]] \tag{A.13}$$

It then easily appears that

$$\left. \frac{d^n F(\epsilon)}{d\epsilon} \right|_{\epsilon=0} = [(\hat{X})^n, \hat{Y}] \tag{A.14}$$

as it was defined above (it is important to remember that the definition of this commutator "with brackets" defined above is not the usual commutator expression $[(\hat{X})^n, \hat{Y}] \neq [\hat{X}^n, \hat{Y}]$).

Then, to conclude the proof, evaluating Equation A.10 at $\epsilon = 1$ exactly gives the result.

$$e^{\hat{X}} \hat{Y} e^{-\hat{X}} = \sum_{n=0}^{\infty} \frac{[(\hat{X})^n, \hat{Y}]}{n!} \tag{A.15}$$

A.3 Collective Spin Pulse with full notations

Here, the result of a "$\pi/2$ collective spin pulse in y" on the starting state $|-N/2\rangle$ (which corresponds to all ions being in the z ground state) is demonstrated. Instead of taking advantage of the symmetry in this problem in order to only consider a single spin pulse, the following uses the general approach. To easily follow the next calculation, it can be of use to keep Table 2.1 in mind. This $\pi/2$ pulse is obtained by setting $\tau = \frac{\pi}{2\Omega}$

$$\hat{U}_{\hat{J}_y}(\tau) |-N/2\rangle = \hat{U}_{\hat{J}_y}(\tau) |ggg...gg\rangle_z = e^{-i\hat{H}_I \tau/\hbar} \bigotimes_{i=1}^{N} |g\rangle^{(i)} \tag{A.16}$$

$$= e^{-i\Omega \sum_{i=1}^{N} \frac{1}{2}\hat{\sigma}_y^{(i)} \tau} \bigotimes_{i=1}^{N} \frac{|g\rangle_y^{(i)} + |e\rangle_y^{(i)}}{\sqrt{2}} \tag{A.17}$$

$$= \prod_{i=1}^{N} e^{-i\Omega \frac{1}{2}\hat{\sigma}_y^{(i)} \tau} \bigotimes_{i=1}^{N} \frac{|g\rangle_y^{(i)} + |e\rangle_y^{(i)}}{\sqrt{2}} \tag{A.18}$$

$$= \bigotimes_{i=1}^{N} \frac{e^{\frac{i\Omega\tau}{2}} |g\rangle_y^{(i)} + e^{\frac{-i\Omega\tau}{2}} |e\rangle_y^{(i)}}{\sqrt{2}} \tag{A.19}$$

$$= \bigotimes_{i=1}^{N} \frac{\frac{1+i}{\sqrt{2}} |g\rangle_y^{(i)} + \frac{1-i}{\sqrt{2}} |e\rangle_y^{(i)}}{\sqrt{2}} \tag{A.20}$$

$$= \bigotimes_{i=1}^{N} \frac{|g\rangle^{(i)} + i^2 |e\rangle^{(i)}}{\sqrt{2}} \tag{A.21}$$

$$= \bigotimes_{i=1}^{N} |g\rangle_x^{(i)} = |-N/2\rangle_x \tag{A.22}$$

All the notations used in the above were previously defined, except the notation $|\phi\rangle^{(i)}$ that was introduced to denote a state of the ith ion. As expected, the result is the same as the one shown when considering only the operation on a single ion and consider all ions to behave in the same way (see Section 2.2.4.3).

A.4 Coherent States Overlap

The overlap is easily calculated starting from the expression of coherent states in the energy eigenbasis, given in Equation 2.75.

$$\langle\beta|\alpha\rangle = \left(e^{-\frac{1}{2}|\beta|^2}\sum_{k=0}^{\infty}\frac{\beta^k}{\sqrt{k!}}|k\rangle\right)^{\dagger}e^{-\frac{1}{2}|\alpha|^2}\sum_{n=0}^{\infty}\frac{\alpha^n}{\sqrt{n!}}|n\rangle \tag{A.23}$$

$$= e^{-\frac{1}{2}(|\beta|^2+|\alpha|^2)}\sum_{k=0}^{\infty}\sum_{n=0}^{\infty}\frac{(\beta^*)^k}{\sqrt{k!}}\frac{\alpha^n}{\sqrt{n!}}\langle k|n\rangle \tag{A.24}$$

$$= e^{-\frac{1}{2}(|\beta|^2+|\alpha|^2)}\sum_{n=0}^{\infty}\frac{(\beta^*\alpha)^n}{n!} \tag{A.25}$$

$$= e^{\beta^*\alpha-\frac{1}{2}(|\beta|^2+|\alpha|^2)} \tag{A.26}$$

A.5 Proof of Equation 2.104

This section shows two approaches to prove

$$e^{i\kappa_p\hat{P}\hat{J}_z}\hat{X}e^{-i\kappa_p\hat{P}\hat{J}_z} = \hat{X} + \kappa_p\hat{J}_z \tag{A.27}$$

Using only the most basic mathematical tools, one can show this via

$$e^{i\kappa_p\hat{P}\hat{J}_z}\hat{X}e^{-i\kappa_p\hat{P}\hat{J}_z} = \left(\left[e^{i\kappa_p\hat{P}\hat{J}_z},\hat{X}\right] + \hat{X}e^{i\kappa_p\hat{P}\hat{J}_z}\right)e^{-i\kappa_p\hat{P}\hat{J}_z} \tag{A.28}$$

$$= \sum_{n=0}^{\infty}\left[\frac{\left(i\kappa_p\hat{P}\hat{J}_z\right)^n}{n!},\hat{X}\right]e^{-i\kappa_p\hat{P}\hat{J}_z} + \hat{X} \tag{A.29}$$

Remembering that $\hat{J}_z$ and $\hat{P}$ commute, it follows that

$$\sum_{n=0}^{\infty}\left[\frac{\left(i\kappa_p\hat{P}\hat{J}_z\right)^n}{n!},\hat{X}\right]e^{-i\kappa_p\hat{P}\hat{J}_z} + \hat{X} = \sum_{n=1}^{\infty}\frac{\left(i\kappa_p\hat{J}_z\right)^n}{n!}\left[\hat{P}^n,\hat{X}\right]e^{-i\kappa_p\hat{P}\hat{J}_z} + \hat{X} \tag{A.30}$$

By induction, it is easy to show that $[\hat{P}^n,\hat{X}] = -ni\hat{P}^{n-1}$ (knowing $[\hat{X},\hat{P}] = i$). It can be important to note that the start of the sum was moved to $n = 1$ (since the commutator is zero if $n = 0$) the final result is then shown, since

$$e^{i\kappa_p\hat{P}\hat{J}_z}\hat{X}e^{-i\kappa_p\hat{P}\hat{J}_z} = \sum_{n=1}^{\infty}\frac{\left(i\kappa_p\hat{J}_z\right)^n}{n!}(-i)n\hat{P}^{n-1}e^{-i\kappa_p\hat{P}\hat{J}_z} + \hat{X}$$

$$= i\kappa_p\hat{J}_z\sum_{n-1=0}^{\infty}\frac{\left(i\kappa_p\hat{J}_z\right)^{n-1}}{(n-1)!}(-i)\hat{P}^{n-1}e^{-i\kappa_p\hat{P}\hat{J}_z} + \hat{X} \tag{A.31}$$

$$= \kappa_p\hat{J}_z e^{i\kappa_p\hat{P}\hat{J}_z}e^{-i\kappa_p\hat{P}\hat{J}_z} + \hat{X} \tag{A.32}$$

$$= \hat{X} + \kappa_p \hat{J}_z \tag{A.33}$$

There is also a more efficient and interesting way to compute this by using the lemma associated with the BCH formula (first mentioned in Equation 2.18, and proven in Appendix A.2). From a general point of view, one can immediately simplify the first expression as

$$e^{i\kappa_p \hat{P}\hat{J}_z} \hat{X} e^{-i\kappa_p \hat{P}\hat{J}_z} = \sum_{n=0}^{\infty} \frac{[(i\kappa_p \hat{P}\hat{J}_z)^n, \hat{X}]}{n!} \tag{A.34}$$

Since any commutator of $\hat{X}$ and $\hat{P}$ that is of order higher than 1 gives zero, the result appears immediately.

$$e^{i\kappa_p \hat{P}\hat{J}_z} \hat{X} e^{-i\kappa_p \hat{P}\hat{J}_z} = \frac{[(i\kappa_p \hat{P}\hat{J}_z)^0, \hat{X}]}{0!} + \frac{[(i\kappa_p \hat{P}\hat{J}_z)^1, \hat{X}]}{1!} \tag{A.35}$$

$$= \hat{X} + \kappa_p \hat{J}_z \tag{A.36}$$

In this last step, while the notations may seem ambiguous, one remembers that the BCH lemma used the definition $[(\hat{X})^0, \hat{Y}] = \hat{Y} \neq [\mathbb{1}, \hat{Y}] = 0$ (see Equation 2.18 and Appendix A.2).

Appendix B

Conditional Displacement Operator Interpretation

This appendix aims to prove the impact of the displacement operator on a general quantum state instead of on a coherent state.

Using

$$\hat{a} = \frac{\hat{X} + i\hat{P}}{\sqrt{2}} \tag{B.1}$$

Let us now denote a ket for a general one-dimensional system and express it in the position and momentum bases. First examining the Fourier transform of the wavefunction expressed in its position basis, one gets

$$|\psi\rangle = \int \frac{dp}{2\pi} \; \tilde{\psi}(p) \, |p\rangle = \int \frac{dp}{2\pi} \int dx \; \psi(x) e^{-\frac{ixp}{\hbar}} \, |p\rangle \tag{B.2}$$

Then let us consider a purely real choice for α. Then,

$$\hat{D}(\alpha_{\mathcal{R}}) \, |\psi\rangle = e^{\alpha_{\mathcal{R}} \hat{a}^\dagger - \alpha_{\mathcal{R}}^* \hat{a}} \int \frac{dp}{2\pi} \int dx \; \psi(x) e^{-\frac{ixp}{\hbar}} \, |p\rangle \tag{B.3}$$

$$= e^{\alpha_{\mathcal{R}}(\hat{a}^\dagger - \hat{a})} \int \frac{dp}{2\pi} \int dx \; \psi(x) e^{-\frac{ixp}{\hbar}} \, |p\rangle \tag{B.4}$$

$$= e^{-i\sqrt{2}\alpha_{\mathcal{R}}\hat{P}} \int \frac{dp}{2\pi} \int dx \; \psi(x) e^{-\frac{ixp}{\hbar}} \, |p\rangle \tag{B.5}$$

$$= e^{-i\alpha_{\mathcal{R}}\sqrt{\frac{2}{\hbar m\omega}}\hat{p}} \int \frac{dp}{2\pi} \int dx \; \psi(x) e^{-\frac{ixp}{\hbar}} \, |p\rangle \tag{B.6}$$

$$= \int \frac{dp}{2\pi} \int dx \; \psi(x) e^{-\frac{i(x+\sqrt{2}/\sqrt{\hbar m\omega}\alpha_{\mathcal{R}})p}{\hbar}} \, |p\rangle \tag{B.7}$$

$$= \int \frac{dp}{2\pi} \int dx \; \psi(x - \sqrt{2}/\sqrt{\hbar^3 m\omega}\alpha_{\mathcal{R}}) e^{-\frac{ixp}{\hbar}} \, |p\rangle \tag{B.8}$$

$$= \int dx \; \psi(x - \sqrt{2}/\sqrt{\hbar^3 m\omega}\alpha_{\mathcal{R}}) \, |x\rangle \tag{B.9}$$

Once this is obtained, let us compute the expectation value of the position for this new "real displaced" wavefunction.

$$\langle \hat{x} \rangle_{\alpha_{\mathcal{R}}} = \langle \psi | \, \hat{D}^\dagger(\alpha_{\mathcal{R}}) \hat{x} \hat{D}(\alpha_{\mathcal{R}}) \, |\psi\rangle \tag{B.10}$$

$$= \int dx' \int dx \; \left| \psi(x - \sqrt{2}/\sqrt{\hbar^3 m\omega}\alpha_{\mathcal{R}}) \right|^2 \langle x' | \, \hat{x} \, |x\rangle \tag{B.11}$$

$$= \int dx \; x \left| \psi(x - \sqrt{2}/\sqrt{\hbar^3 m\omega}\alpha_{\mathcal{R}}) \right|^2 \tag{B.12}$$

$$= \int dx \ (x + \sqrt{2}/\sqrt{\hbar^3 m\omega}\alpha_\mathcal{R})|\psi(x)|^2 \tag{B.13}$$

$$= \langle\psi|\, \hat{x}\,|\psi\rangle + \int dx \ \sqrt{2}/\sqrt{\hbar^3 m\omega}\alpha_\mathcal{R}|\psi(x)|^2 \tag{B.14}$$

$$= \langle\hat{x}\rangle + \sqrt{2}/\sqrt{\hbar^3 m\omega}\alpha_\mathcal{R} \tag{B.15}$$

And this exactly shows that a displacement operator with α being real corresponds to a shift in the expectation value of the position (proportional to $\sqrt{2}\alpha$) of this general state.

Now moving on to the imaginary case ($\alpha = i\alpha_\mathcal{I}$),

$$|\psi\rangle = \int dx \ \psi(x)\,|x\rangle = \int dx \int \frac{dp}{2\pi} \ \tilde{\psi}(p)e^{\frac{ixp}{\hbar}}\,|x\rangle \tag{B.16}$$

$$\hat{D}(i\alpha_\mathcal{I})\,|\psi\rangle = e^{i\alpha_\mathcal{I}\hat{a}^\dagger - (i\alpha_\mathcal{I})^*\hat{a}}\int dx \int \frac{dp}{2\pi} \ \tilde{\psi}(p)e^{\frac{ixp}{\hbar}}\,|x\rangle \tag{B.17}$$

$$= e^{i\alpha_\mathcal{I}(\hat{a}^\dagger + \hat{a})}\int dx \int \frac{dp}{2\pi} \ \tilde{\psi}(p)e^{\frac{ixp}{\hbar}}\,|x\rangle \tag{B.18}$$

$$= e^{i\sqrt{2}\alpha_\mathcal{I}\hat{X}}\int dx \int \frac{dp}{2\pi} \ \psi(p)e^{\frac{ixp}{\hbar}}\,|x\rangle \tag{B.19}$$

$$= e^{i\alpha_\mathcal{I}\sqrt{\frac{2m\omega}{\hbar}}\hat{x}}\int dx \int \frac{dp}{2\pi} \ \tilde{\psi}(p)e^{\frac{ixp}{\hbar}}\,|x\rangle \tag{B.20}$$

$$= \int dx \int \frac{dp}{2\pi} \ \tilde{\psi}(p)e^{\frac{ix(P + \sqrt{2m\hbar\omega}\alpha_\mathcal{I})}{\hbar}}\,|x\rangle \tag{B.21}$$

$$= \int \frac{dP}{2\pi}\tilde{\psi}(p - \sqrt{2m\hbar\omega}\alpha_\mathcal{I})\,|p\rangle \tag{B.22}$$

Without doing the computation that was done above for the position, one can directly see that this will result in a shift of the expectation value of the momentum by $+\sqrt{2m\hbar\omega}\alpha_\mathcal{I}$. It is therefore confirmed that whatever the wavefunction of the system $\hat{D}(\alpha)$ acts upon, it leads to a displacement in the phase space of position and momentum. In addition, this is done with the complex part of α corresponding to the displacement in the $\hat{p}$ direction, and the real part corresponding to the displacement in the $\hat{x}$ direction. Since the actual position and momentum space were used here (instead of the adimensional ones), the shift in the phase space is not of $\sqrt{2}\alpha$, but of factors proportional to $\sqrt{2}\alpha$. As shown above, if one uses the phase space of the quadratures of the creation and annihilation operators (ie : $\hat{X}$ and $\hat{P}$), the displacement is of length $\sqrt{2}|\alpha|$ and in the direction $\arg\alpha$.

Appendix C

Calculation Details for Chapter 3

This appendix groups a set of short proofs and developments assisting in the calculations made in Chapter 3.

C.1 Composition of Magnus Expansion Solutions

However, as will be shown later, only the second order of the Magnus expansion will be used in this report, due to the higher order commutators included in the later terms. Following this, the approach taken here is to only show the above property at this order.

Before starting the proof, it is interesting to note a few facts. Given that the case of interest is the case where only Ω_1 and Ω_2 are non zero, it follows that $[A(t_1), A(t_2)]$ commutes with $A(t_3)$. In turn, this means that Ω_1 commutes with Ω_2. And this also means that $\Omega_2(t_1, t_2)$ commutes with $\Omega_2(t_3, t_4)$ (and all these properties are true for all possible choices of t_1, t_2, t_3, and t_4). Keeping these facts in mind helps greatly in splitting and merging the many exponentials without using the Baker-Campbell-Hausdorff (BCH) formula.

$$\hat{U}(t_2, t_1)\hat{U}(t_1, t_0) = e^{\Omega_1(t_2,t_1)+\Omega_2(t_2,t_1)}e^{\Omega_1(t_1,t_0)+\Omega_2(t_1,t_0)} \tag{C.1}$$

$$= e^{\Omega_1(t_2,t_1)}e^{\Omega_1(t_1,t_0)}e^{\Omega_2(t_2,t_1)+\Omega_2(t_1,t_0)} \tag{C.2}$$

Now using the BCH formula to merge the first two exponentials, one obtains

$$e^{\Omega_1(t_2,t_1)}e^{\Omega_1(t_1,t_0)} = e^{\Omega_1(t_2,t_1)+\Omega_1(t_1,t_0)+\frac{1}{2}[\Omega_1(t_2,t_1),\Omega_1(t_1,t_0)]+HOC} \tag{C.3}$$

Once again, since the commutators of order 3 and above in A vanish, the higher order commutators vanish in the BCH formula. The only nonzero commutator can then be computed as

$$\frac{1}{2}[\Omega_1(t_2, t_1), \Omega_1(t_1, t_0)] = \frac{1}{2}\left[\int_{t_1}^{t_2} dt\, A(t), \int_{t_0}^{t_1} dt'\, A(t')\right] = \frac{1}{2}\int_{t_1}^{t_2} dt \int_{t_0}^{t_1} dt'\, [A(t), A(t')] \tag{C.4}$$

which shows that this term behaves in the same manner as Ω_2 regarding its commutation relations. Thanks to this, it is now possible to merge the remaining exponentials without using the BCH formula, and obtain the final result

$$\hat{U}(t_2, t_1)\hat{U}(t_1, t_0) = e^{\Omega_1(t_2,t_1)+\Omega_1(t_1,t_0)+\frac{1}{2}[\Omega_1(t_2,t_1),\Omega_1(t_1,t_0)]+\Omega_2(t_2,t_1)+\Omega_2(t_1,t_0)} \tag{C.5}$$

The first two terms easily simplify as

$$\Omega_1(t_2, t_1) + \Omega_1(t_1, t_0) = \int_{t_0}^{t_2} dt\, A(t) = \Omega_1(t_2, t_0) \tag{C.6}$$

And the last three give

$$\frac{1}{2}[\Omega_1(t_2,t_1),\Omega_1(t_1,t_0)] + \Omega_2(t_2,t_1) + \Omega_2(t_1,t_0)$$

$$= \frac{1}{2}\int_{t_1}^{t_2} dt \int_{t_0}^{t_1} dt' \, [A(t),A(t')] + \frac{1}{2}\int_{t_1}^{t_2} dt \int_{t_1}^{t} dt' \, [A(t),A(t')] + \frac{1}{2}\int_{t_0}^{t_1} dt \int_{t_0}^{t} dt' \, [A(t),A(t')] \quad (C.7)$$

$$= \frac{1}{2}\int_{t_1}^{t_2} dt \int_{t_0}^{t} dt' \, [A(t),A(t')] + \frac{1}{2}\int_{t_0}^{t_1} dt \int_{t_0}^{t} dt' \, [A(t),A(t')] \qquad (C.8)$$

$$= \frac{1}{2}\int_{t_0}^{t_2} dt \int_{t_0}^{t} dt' \, [A(t),A(t')] = \Omega_2(t_2,t_0) \qquad (C.9)$$

Which then shows

$$\hat{U}(t_2,t_1)\hat{U}(t_1,t_0) = e^{\Omega_1(t_2,t_0)+\Omega_2(t_2,t_0)} = \hat{U}(t_2,t_0) \qquad (C.10)$$

This confirms that the time evolution operator obtained via the Magnus expansion has indeed the expected behaviour (for operators with vanishing third order commutators). As usual, the following can then be written

$$|\psi(t_2)\rangle = \hat{U}(t_2,t_1)|\psi(t_1)\rangle = \hat{U}(t_2,t_1)\hat{U}(t_1,0)|\psi(0)\rangle = \hat{U}(t_2,0)|\psi(0)\rangle \qquad (C.11)$$

in which $\hat{U}(t_2,0)$ is sometimes shortened as $\hat{U}(t_2)$.

C.2 Details on the Optomechanical $\hat{H}_{int,S}$

The following gives a very qualitative way to understand the interaction Hamiltonian in the optomechanical system. Surprisingly, the result can easily be obtained by a very classical approach to the problem.

$$\hat{H}_{int,S} = -\hbar g \hat{a}^\dagger \hat{a} \frac{\hat{b}^\dagger + \hat{b}}{\sqrt{2}} \qquad (C.12)$$

Remembering Chapter 2, the $(\hat{b}^\dagger + \hat{b})/\sqrt{2}$ factor corresponds to the (dimensionless) position operator for the side of the optical cavity that is linked to the mechanical oscillator (*i.e.* : the (dimensionless) position of the mechanical oscillator $\hat{X}$). In addition, $\hat{a}^\dagger \hat{a} = \hat{N}$ is the operator for the number of photons in the optical state. The above interaction Hamiltonian therefore simply corresponds to supposing

1. The (outgoing) force applied on the sides an optical cavity by the field are proportional to the number of photons in the cavity.

2. If the mechanical oscillator moves the side of an optical cavity by the distance given by $\hat{X}$ while this force is applied, it produces (or absorbs) work. Therefore, the total energy of the system decreases by the product of this force and the distance.

Of course, this depends on the conventions used for which direction is positive or negative for the mechanical oscillator, and the proportionality constant between photon number and force is hard to calculate. But this can all be included in the g factor, and be experimentally (or theoretically) determined. In this case, since g is considered to be a positive constant for the strength of the interaction, and since the sign of the Hamiltonian is negative, then the axis for $\hat{X}$ was chosen pointing to the left in Figure 3.1.

More details and rigorous derivations can be found in the literature, but this very qualitative and classical interpretation is already a good way to understand the meaning behind this interaction Hamiltonian.

C.3 Time Independent Ω_2 Calculation Details

When showing the details of the calculation, $\Omega_2(t, t_0)$ in Equation 3.32 is obtained via

$$A(t) = \frac{-i}{\hbar}\hat{H}_I(t) = ig\hat{a}^\dagger\hat{a}\frac{e^{i\omega_m t}\hat{b}^\dagger + e^{-i\omega_m t}\hat{b}}{\sqrt{2}} \tag{C.13}$$

$$\Omega_2(t, t_0) = \frac{1}{2}\int_{t_0}^{t} dt_1 \int_{t_0}^{t_1} dt_2 \; [A(t_1), A(t_2)] \tag{C.14}$$

$$= -\frac{g^2(\hat{a}^\dagger\hat{a})^2}{4}\int_{t_0}^{t} dt_1 \int_{t_0}^{t_1} dt_2 \; [e^{i\omega_m t_1}\hat{b}^\dagger + e^{-i\omega_m t_1}\hat{b}, e^{i\omega_m t_2}\hat{b}^\dagger + e^{-i\omega_m t_2}\hat{b}] \tag{C.15}$$

$$= -\frac{g^2(\hat{a}^\dagger\hat{a})^2}{4}\int_{t_0}^{t} dt_1 \int_{t_0}^{t_1} dt_2 \; \Big(-e^{i\omega_m(t_1-t_2)} + e^{-i\omega_m(t_1-t_2)} \Big) \tag{C.16}$$

$$= \frac{g^2(\hat{a}^\dagger\hat{a})^2}{2}\int_{t_0}^{t} dt_1 \int_{t_0}^{t_1} dt_2 \; i\sin\big(\omega_m(t_1-t_2)\big) \tag{C.17}$$

$$= i\frac{g^2(\hat{a}^\dagger\hat{a})^2}{2}\int_{t_0}^{t} dt_1 \left[\frac{\cos\big(\omega_m(t_1-t_2)\big)}{\omega_m}\right]_{t_0}^{t_1} \tag{C.18}$$

$$= i\frac{g^2(\hat{a}^\dagger\hat{a})^2}{2\omega_m}\int_{t_0}^{t} dt_1 \; \Big(1 - \cos\big(\omega_m(t_1-t_0)\big)\Big) \tag{C.19}$$

$$= i\frac{g^2(\hat{a}^\dagger\hat{a})^2}{2\omega_m}\left[t_1 - \frac{\sin\big(\omega_m(t_1-t_0)\big)}{\omega_m}\right]_{t_0}^{t} \tag{C.20}$$

$$= i\frac{g^2(\hat{a}^\dagger\hat{a})^2}{2\omega_m}\left(t - t_0 - \frac{\sin\big(\omega_m(t-t_0)\big)}{\omega_m}\right) \tag{C.21}$$

C.4 Time Dependent Ω_2 Calculation Details

The following includes the details for the first set of simplifications made to compute Ω_2 in the time dependent case. It includes the calculations that are necessary in order to obtain Equation 3.51 from Equation 3.50.

In order to get the expression for $[A(t), A(t')]$ and some of the first integrals, one can refer to the time independent calculation in the previous section.

$$\Omega_2(p\Delta t) = \frac{1}{2}\sum_{n=0}^{p-1}\int_{n\Delta t}^{n\Delta t+\tau} dt \left(\sum_{m=0}^{n-1}\int_{m\Delta t}^{m\Delta t+\tau} dt' \; [A(t), A(t')] + \int_{n\Delta t}^{t} dt' \; [A(t), A(t')]\right) \tag{C.22}$$

$$= i\frac{g^2(\hat{a}^\dagger\hat{a})^2}{2}\sum_{n=0}^{p-1}\int_{n\Delta t}^{n\Delta t+\tau} dt \left(\sum_{m=0}^{n-1}\left[\frac{\cos\big(\omega_m(t-t')\big)}{\omega_m}\right]_{m\Delta t}^{m\Delta t+\tau} + \left[\frac{\cos\big(\omega_m(t-t')\big)}{\omega_m}\right]_{n\Delta t}^{t}\right) \tag{C.23}$$

$$= i\frac{g^2(\hat{a}^\dagger\hat{a})^2}{2\omega_m}\sum_{n=0}^{p-1}\int_{n\Delta t}^{n\Delta t+\tau} dt \bigg(\sum_{m=0}^{n-1}\Big(\cos\big(\omega_m(t-m\Delta t-\tau)\big)$$
$$-\cos\big(\omega_m(t-m\Delta t)\big)\Big) + 1 - \cos\big(\omega_m(t-n\Delta t)\big)\bigg) \tag{C.24}$$

$$= i\frac{g^2(\hat{a}^\dagger\hat{a})^2}{2\omega_m}\sum_{n=0}^{p-1}\left(\sum_{m=0}^{n-1}\left(\left[\frac{\sin\left(\omega_m(t-m\Delta t-\tau)\right)}{\omega_m}\right]_{n\Delta t}^{n\Delta t+\tau}\right.\right.$$
$$\left.\left.-\left[\frac{\sin\left(\omega_m(t-m\Delta t)\right)}{\omega_m}\right]_{n\Delta t}^{n\Delta t+\tau}\right)+\left[t-\frac{\sin\left(\omega_m(t-n\Delta t)\right)}{\omega_m}\right)\right]_{n\Delta t}^{n\Delta t+\tau}\right) \quad \text{(C.25)}$$

$$= i\frac{g^2(\hat{a}^\dagger\hat{a})^2}{2\omega_m^2}\sum_{n=0}^{p-1}\left(\sum_{m=0}^{n-1}\left(\sin\left(\omega_m(n-m)\Delta t\right)-\sin\left(\omega_m(n-m)\Delta t-\omega_m\tau\right)\right.\right.$$
$$\left.\left.-\sin\left(\omega_m(n-m)\Delta t+\omega_m\tau\right)+\sin\left(\omega_m(n-m)\Delta t\right)\right)+\omega_m\tau-\sin(\omega_m\tau)\right) \quad \text{(C.26)}$$

$$= i\frac{g^2(\hat{a}^\dagger\hat{a})^2}{2\omega_m^2}\sum_{n=0}^{p-1}\left(\sum_{m=0}^{n-1}\left(2\sin\left(\omega_m(n-m)\Delta t\right)-2\sin\left(\omega_m(n-m)\Delta t\right)\cos(\omega_m\tau)\right)\right.$$
$$\left.+\omega_m\tau-\sin(\omega_m\tau)\right) \quad \text{(C.27)}$$

$$= i\frac{g^2(\hat{a}^\dagger\hat{a})^2}{\omega_m^2}\sum_{n=0}^{p-1}\left(\left(1-\cos(\omega_m\tau)\right)\sum_{m=0}^{n-1}\sin\left(\omega_m(n-m)\Delta t\right)+\omega_m\tau-\sin(\omega_m\tau)\right) \quad \text{(C.28)}$$

$$= i\frac{g^2(\hat{a}^\dagger\hat{a})^2}{\omega_m^2}\left(p\left(\omega_m\tau-\sin(\omega_m\tau)\right)+\left(1-\cos(\omega_m\tau)\right)\sum_{n=0}^{p-1}\sum_{m=0}^{n-1}\sin\left(\omega_m(n-m)\Delta t\right)\right) \quad \text{(C.29)}$$

where the basic trigonometric identity $\sin(A+B)+\sin(A-B)=2\sin(A)\cos(B)$ was used to obtain Equation C.27.

C.5   Equation 3.58 Details

The commutator of any two terms in the sum from the exponential

$$e^{\Omega_1(p\Delta t)}=\exp\left(\sum_{n=0}^{p-1}A_n\right) \quad \text{(C.30)}$$

with

$$A_n=\frac{g\hat{a}^\dagger\hat{a}}{\sqrt{2}\omega_m}\left(\left(e^{i\omega_m\tau}-1\right)e^{i\omega_m n\Delta t}\hat{b}^\dagger-\left(e^{-i\omega_m\tau}-1\right)e^{-i\omega_m n\Delta t}\hat{b}\right) \quad \text{(C.31)}$$

can be computed as

$$[A_n,A_k]=\frac{g^2(\hat{a}^\dagger\hat{a})^2}{2\omega_m^2}\left[\left(e^{i\omega_m\tau}-1\right)e^{i\omega_m n\Delta t}\hat{b}^\dagger-\left(e^{-i\omega_m\tau}-1\right)e^{-i\omega_m n\Delta t}\hat{b},\right.$$
$$\left.\left(e^{i\omega_m\tau}-1\right)e^{i\omega_m k\Delta t}\hat{b}^\dagger-\left(e^{-i\omega_m\tau}-1\right)e^{-i\omega_m k\Delta t}\hat{b}\right] \quad \text{(C.32)}$$

$$=\frac{g^2(\hat{a}^\dagger\hat{a})^2}{2\omega_m^2}\left(\left[\left(e^{i\omega_m\tau}-1\right)e^{i\omega_m n\Delta t}\hat{b}^\dagger,-\left(e^{-i\omega_m\tau}-1\right)e^{-i\omega_m k\Delta t}\hat{b}\right]\right.$$
$$\left.-\left[\left(e^{-i\omega_m\tau}-1\right)e^{-i\omega_m n\Delta t}\hat{b},\left(e^{i\omega_m\tau}-1\right)e^{i\omega_m k\Delta t}\hat{b}^\dagger\right]\right) \quad \text{(C.33)}$$

$$=\frac{g^2(\hat{a}^\dagger\hat{a})^2}{2\omega_m^2}\left(\left(2-2\cos(\omega_m\tau)\right)e^{i\omega_m(n-k)\Delta t}-\left(2-2\cos(\omega_m\tau)\right)e^{-i\omega_m(n-k)\Delta t}\right) \quad \text{(C.34)}$$

$$=2i\frac{g^2(\hat{a}^\dagger\hat{a})^2}{\omega_m^2}\left(1-\cos(\omega_m\tau)\right)\sin\left(\omega_m(n-k)\Delta t\right) \quad \text{(C.35)}$$

C.6 Equation 3.94

Equation 3.94 is simply proved by

$$\sum_{k=0}^{n-1} e^{-ik\theta} = \frac{1 - e^{-in\theta}}{1 - e^{-i\theta}} \tag{C.36}$$

$$= \frac{1 - e^{-in\theta} - e^{i\theta} + e^{-i(n-1)\theta}}{1 + 1 - e^{i\theta} - e^{-i\theta}} \tag{C.37}$$

$$= \frac{e^{i(n-1)\theta/2} - e^{-i(n+1)\theta/2} - e^{i(n+1)\theta/2} + e^{-i(n-1)\theta/2}}{2 - 2\cos(\theta)} e^{-i(n-1)\theta/2} \tag{C.38}$$

$$= \frac{\cos\left(\frac{n-1}{2}\theta\right) - \cos\left(\frac{n+1}{2}\theta\right)}{1 - \cos(\theta)} e^{-i(n-1)\theta/2} \tag{C.39}$$

$$= \frac{2\sin(n\theta/2)\sin(\theta/2)}{1 - \cos(\theta)} e^{-i(n-1)\theta/2} \tag{C.40}$$

$$= \frac{\sin(n\theta/2)}{\sin(\theta/2)} e^{-i(n-1)\theta/2} \tag{C.41}$$

where some simple trigonometric identities were used.

C.7 Equations 3.108 and 3.109

The proof of the equivalence mentioned in Equation 3.108 and 3.109 is given here. This can be a bit frustrating to show if one starts in the wrong direction. But using the mathematical trick of writing $\sin(p\theta/2)$ as $\sin\left((p-1)\theta/2 + \theta/2\right)$, followed by using some basic trigonometric identities makes the proof simple and short.

$$c_1 = \lambda \frac{\sin(p\theta/2)}{\sin(\theta/2)} \cos\left((p-1)\theta/2\right) \tag{C.42}$$

$$= \lambda \frac{\sin\left((p-1)\theta/2\right)\cos(\theta/2) + \sin(\theta/2)\cos\left((p-1)\theta/2\right)}{\sin(\theta/2)} \cos\left((p-1)\theta/2\right) \tag{C.43}$$

$$= \lambda \left(\sin\left((p-1)\theta/2\right) \cos\left((p-1)\theta/2\right) \cot(\theta/2) + \cos^2\left((p-1)\theta/2\right) \right) \tag{C.44}$$

$$= \frac{\lambda}{2} \left(1 + \cos\left((p-1)\theta\right) + \sin\left((p-1)\theta\right) \cot(\theta/2) \right) \tag{C.45}$$

$$c_2 = \lambda \frac{\sin(p\theta/2)}{\sin(\theta/2)} \sin\left((p-1)\theta/2\right) \tag{C.46}$$

$$= \lambda \frac{\sin\left((p-1)\theta/2\right)\cos(\theta/2) + \sin(\theta/2)\cos\left((p-1)\theta/2\right)}{\sin(\theta/2)} \sin\left((p-1)\theta/2\right) \tag{C.47}$$

$$= \lambda \left(\sin^2\left((p-1)\theta/2\right) \cot(\theta/2) + \cos\left((p-1)\theta/2\right) \sin\left((p-1)\theta/2\right) \right) \tag{C.48}$$

$$= \frac{\lambda}{2} \left(1 - \cos\left((p-1)\theta\right) \cot(\theta/2) + \sin\left((p-1)\theta\right) \right) \tag{C.49}$$

Appendix D

Magnus expansion and usual exponential solution

This short appendix is destined to the reader who first encountered the Magnus expansion in the above, and who wonders how and why does the usual solution not work in the case of non trivial time dependent commutation relations. As stated before, a full proof of the Magnus expansion is not provided here (see [45] in this case), but a short counter arguments can be easily made to show how the usual exponential solution is indeed a simplification of a more general case.

The main and most convincing counter argument to be made is to simply show that the usual exponential solution doesn't solve the problem for a simple case. Let us consider $[A(t_1), A(t_2)] = C(t_1, t_2)$ with $C(t_1, t_2)$ a simple two variable function.

The equation being

$$\frac{\partial f}{\partial t} = A(t)f(t), \tag{D.1}$$

let us examine the derivative of the usual solution (written $f_u(t)$)

$$\frac{\partial}{\partial t} f_u(t) = \frac{\partial}{\partial t} f(t_0) \exp\left(\int_{t_0}^{t} dt' A(t')\right) = f(t_0) \frac{\partial}{\partial t}\left(\exp\left(\int_{t_0}^{t_1} dt'' A(t'') + \int_{t_1}^{t} dt' A(t')\right)\right) \tag{D.2}$$

While this last manipulation seems trivial and unnecessary, the crucial point is to note that now, if one wishes to split the exponential, one has to use the BCH formula (as $[A(t_1), A(t_2)] \neq 0$). Since $C(t_1, t_2)$ commutes with $A(t')$ for any t') however, the only the first term of the BCH formula contributes.

$$\frac{\partial}{\partial t} f_u(t) = f(t_0) \frac{\partial}{\partial t}\left(\exp\left(\int_{t_0}^{t_1} dt'' A(t'')\right) \exp\left(\int_{t_1}^{t} dt' A(t')\right) \right.$$
$$\left. \exp\left(-\frac{1}{2}\int_{t_0}^{t_1} dt'' \int_{t_1}^{t} dt' [A(t''), A(t')]\right)\right) \tag{D.3}$$

$$= f(t_0) \exp\left(\int_{t_0}^{t_1} dt'' A(t'')\right)\left(A(t) \exp\left(\int_{t_1}^{t} dt' A(t')\right)\right.$$
$$\exp\left(-\frac{1}{2}\int_{t_0}^{t_1} dt'' \int_{t_1}^{t} dt' [A(t''), A(t')]\right) - \frac{1}{2}\left(\int_{t_0}^{t_1} dt'' [A(t''), A(t)]\right)$$
$$\left. \exp\left(\int_{t_1}^{t} dt' A(t')\right) \exp\left(-\frac{1}{2}\int_{t_0}^{t_1} dt'' \int_{t_1}^{t} dt' [A(t''), A(t')]\right)\right) \tag{D.4}$$

81

$$= f(t_0) \exp\left(\int_{t_0}^{t} dt' \, A(t')\right) \exp\left(-\frac{1}{2} \int_{t_0}^{t_1} dt'' \int_{t_1}^{t} dt' [A(t''), A(t')]\right) \left(A(t) - \right.$$

$$\left. \frac{1}{2} \left(\int_{t_0}^{t_1} dt'' [A(t''), A(t)]\right)\right) \quad \text{(D.5)}$$

$$= f_u(t) \exp\left(-\frac{1}{2} \int_{t_0}^{t_1} dt'' \int_{t_1}^{t} dt' [A(t''), A(t')]\right) \left(A(t) - \frac{1}{2} \left(\int_{t_0}^{t_1} dt'' [A(t''), A(t)]\right)\right) \quad \text{(D.6)}$$

$$= A(t) f_u(t) \qquad \text{only if} \qquad [A(t_1), A(t_2)] = 0 \; \forall \; t_1, t_2 \in \mathbb{R} \quad \text{(D.7)}$$

And it is easily shown that in this particular case, once more, $f_u(t)$ is the solution only if $[A(t_1), A(t_2)] = C(t_1, t_2) = 0$. One of the main takeaways from this development is to realise that the Magnus expansion problem is closely related to the BCH problem.

Appendix E

Trigonometric Sum

The objective of this short appendix section is to prove the following two identities solving the sum of the two basic trigonometric functions with their angle in arithmetic progression.

$$\sum_{k=0}^{n-1} \sin(a + kd) = \frac{\sin(nd/2)}{\sin(d/2)} \sin\left(a + \frac{n-1}{2}d\right) \tag{E.1}$$

$$\sum_{k=0}^{n-1} \cos(a + kd) = \frac{\sin(nd/2)}{\sin(d/2)} \cos\left(a + \frac{n-1}{2}d\right) \tag{E.2}$$

Starting with the first identity (for a sum of sines), one proceeds by simply expressing the terms with complex exponentials and using geometric sums

$$\sum_{k=0}^{n-1} \sin(a + kd) = \frac{1}{2i} \sum_{k=0}^{n-1} e^{i(a+kd)} - e^{-i(a+kd)} \tag{E.3}$$

$$= \frac{1}{2i} \left(e^{ia} \frac{1 - e^{ind}}{1 - e^{id}} - e^{-ia} \frac{1 - e^{-ind}}{1 - e^{-id}} \right) \tag{E.4}$$

$$= \frac{1}{2i} \frac{e^{ia} - e^{-i(d-a)} - e^{i(nd+a)} + e^{i\left((n-1)d+a\right)} - e^{-ia} + e^{i(d-a)} + e^{-i(nd+a)} - e^{-i\left((n-1)d+a\right)}}{1 - e^{id} - e^{-id} + 1} \tag{E.5}$$

$$= \frac{1}{2i} \frac{2i\sin(a) + 2i\sin(d-a) - 2i\sin(nd+a) + 2i\sin\left((n-1)d+a\right)}{2 - 2\cos(d)} \tag{E.6}$$

$$= \frac{\sin(a) + \sin(d-a) - \sin(nd+a) + \sin\left((n-1)d+a\right)}{4\sin^2(d/2)} \tag{E.7}$$

Since they will often be used (and are also used in the main chapters above) let us very quickly remind the sum-product trigonometric identities.

$$\sin(a) + \sin(b) = 2\sin\left(\frac{a+b}{2}\right)\cos\left(\frac{a-b}{2}\right) \tag{E.8}$$

$$\sin(a) - \sin(b) = 2\cos\left(\frac{a+b}{2}\right)\sin\left(\frac{a-b}{2}\right) \tag{E.9}$$

$$\cos(a) + \cos(b) = 2\cos\left(\frac{a+b}{2}\right)\cos\left(\frac{a-b}{2}\right) \tag{E.10}$$

$$\cos(a) - \cos(b) = -2\sin\left(\frac{a+b}{2}\right)\sin\left(\frac{a-b}{2}\right) \tag{E.11}$$

Using the two sine sum-product identities, one obtains

$$\sin(a) + \sin(d - a) = 2\sin(d/2)\cos(a - d/2) \tag{E.12}$$

$$\sin\big(a + (n-1)d\big) - \sin(a + nd) = 2\cos(a + nd - d/2)\sin(-d/2) \tag{E.13}$$

Equation E.7 therefore reduces to

$$\sum_{k=0}^{n-1}\sin(a + kd) = \frac{2\sin(d/2)\cos(a - d/2) + 2\cos(a + nd - d/2)\sin(-d/2)}{4\sin^2(d/2)} \tag{E.14}$$

$$= \frac{\cos(a - d/2) - \cos(a + nd - d/2)}{2\sin(d/2)} \tag{E.15}$$

$$= \frac{-2\sin\big(a + \frac{n-1}{2}d\big)\sin(-nd/2)}{2\sin(d/2)} \tag{E.16}$$

$$= \frac{\sin(nd/2)}{\sin(d/2)}\sin\left(a + \frac{n-1}{2}d\right) \tag{E.17}$$

where the cosine sum-product identity was used (reminded in Equation E.10), and where we finally obtain the desired result. Moving on to the proof of the cosine identity in Equation E.2, it is actually very simple to obtain when starting from the previous identity. One has

$$\sum_{k=0}^{n-1}\cos(a + kd) = \sum_{k=0}^{n-1}\sin\left(a + kd + \frac{\pi}{2}\right) \tag{E.18}$$

$$= \frac{\sin(nd/2)}{\sin(d/2)}\sin\left(a + \frac{\pi}{2} + \frac{n-1}{2}d\right) \tag{E.19}$$

$$= \frac{\sin(nd/2)}{\sin(d/2)}\cos\left(a + \frac{n-1}{2}d\right) \tag{E.20}$$

which proves the second identity.

Appendix F

Calculation Details for Chapter 3

This appendix groups a set of short proofs and developments assisting in the calculations made in Chapter 3.

F.1 Equation 4.19 to 4.20

In this section $\hat{U}_{0,m,S}$ will be shortened as $\hat{U}$ in order to improve readability. The necessary equivalence to go from Equation 4.19 to 4.20 is

$$\hat{U}^{-1}\hat{b}\hat{\rho}\hat{b}^{\dagger}\hat{U} = \hat{b}\hat{\rho}_I\hat{b}^{\dagger} \tag{F.1}$$

This is relatively easy to prove, it requires the intermediate results

$$\hat{U}^{-1}\hat{b}\hat{U} = e^{-i\omega_m t}\hat{b} \tag{F.2}$$

$$\hat{U}^{-1}\hat{b}^{\dagger}\hat{U} = e^{i\omega_m t}\hat{b}^{\dagger} \tag{F.3}$$

which are both easily obtained by using the BCH lemma (see Equation 2.18, or Appendix A.2)

$$\hat{U}^{-1}\hat{b}\hat{U} = e^{i\omega_m \hat{b}^{\dagger}\hat{b}t}\hat{b}e^{-i\omega_m \hat{b}^{\dagger}\hat{b}t} = \sum_{n=0}^{\infty}\frac{\left[\left(i\omega_m\hat{b}^{\dagger}\hat{b}t\right)^n,\hat{b}\right]}{n!} = \sum_{n=0}^{\infty}\frac{(-i\omega_m t)^n}{n!}\hat{b} = e^{-i\omega_m t}\hat{b} \tag{F.4}$$

$$\hat{U}^{-1}\hat{b}^{\dagger}\hat{U} = e^{i\omega_m \hat{b}^{\dagger}\hat{b}t}\hat{b}^{\dagger}e^{-i\omega_m \hat{b}^{\dagger}\hat{b}t} = \sum_{n=0}^{\infty}\frac{\left[\left(i\omega_m\hat{b}^{\dagger}\hat{b}t\right)^n,\hat{b}^{\dagger}\right]}{n!} = \sum_{n=0}^{\infty}\frac{(i\omega_m t)^n}{n!}\hat{b} = e^{i\omega_m t}\hat{b}^{\dagger} \tag{F.5}$$

where it can be useful to remember equation 3.26. Finally, the proof can be written as

$$\hat{U}^{-1}\hat{b}\hat{\rho}\hat{b}^{\dagger}\hat{U} = \hat{U}^{-1}\hat{b}\hat{U}\hat{U}^{-1}\hat{\rho}\hat{U}\hat{U}^{-1}\hat{b}^{\dagger}\hat{U} \tag{F.6}$$

$$= e^{-i\omega_m t}\hat{b}\hat{U}^{-1}\hat{\rho}\hat{U}e^{i\omega_m t}\hat{b}^{\dagger} \tag{F.7}$$

$$= \hat{b}\hat{\rho}_I\hat{b}^{\dagger} \tag{F.8}$$

F.2 Equation 4.60 to 4.61, Calculation of $S_2(n,k)$

The second scaling factor (*i.e.* the exponential factor originating from the dissipation during the second pulse) is computed using Equation 2.76 (reminded in Equation 4.37).

$$S_2(n,k) = \langle\psi_{1+\tau}(n)|\psi_{1+\tau}(k)\rangle^{1-e^{-\gamma\Delta t}} \tag{F.9}$$

$$= \left\langle \frac{ig\tau n}{\sqrt{2}} \left(1 + e^{-i\omega_m \Delta t - \gamma \Delta t/2}\right) \middle| \frac{ig\tau k}{\sqrt{2}} \left(1 + e^{-i\omega_m \Delta t - \gamma \Delta t/2}\right) \right\rangle^{1 - e^{-\gamma \Delta t}} \tag{F.10}$$

From now on, it will be useful to use the notation

$$M = -i\omega_m \Delta t - \gamma \Delta t/2 \tag{F.11}$$

using it, the calculation of the second scaling factor becomes

$$S_2(n,k) = \left\langle \frac{ig\tau n}{\sqrt{2}} \left(1 + e^M\right) \middle| \frac{ig\tau k}{\sqrt{2}} \left(1 + e^M\right) \right\rangle^{1 - e^{-\gamma \Delta t}} \tag{F.12}$$

$$= \exp\left(\frac{-ig\tau n}{\sqrt{2}} \left(1 + e^{M^*}\right) \frac{ig\tau k}{\sqrt{2}} \left(1 + e^M\right) - \frac{1}{2} \left| \frac{ig\tau n}{\sqrt{2}} \left(1 + e^M\right) \right|^2 \right.$$

$$\left. - \frac{1}{2} \left| \frac{ig\tau k}{\sqrt{2}} \left(1 + e^M\right) \right|^2 \right)^{1 - e^{\gamma \Delta t}} \tag{F.13}$$

$$= \exp\left(-\frac{g^2 \tau^2}{4}(n-k)^2 \left(1 + e^{M^*}\right)\left(1 + e^M\right)\left(1 - e^{-\gamma \Delta t}\right) \right) \tag{F.14}$$

There are now two ways to progress. The first is to directly compute the product including M as

$$\left(1 + e^{M^*}\right)\left(1 + e^M\right) = \left(1 + e^{i\omega_m \Delta t - \gamma \Delta t/2}\right)\left(1 + e^{-i\omega_m \Delta t - \gamma \Delta t/2}\right) = 1 + e^{-\gamma \Delta t/2} 2\cos(\omega_m \Delta t) + e^{-\gamma \Delta t} \tag{F.15}$$

The second approach is to see each sum $1 + e^M$ as a two term geometric sum. It may seem like needlessly complicating the expression at first, but this approach will be extremely useful for the cases with more pulses, and it is therefore preferred here.

$$\left(1 + e^{M^*}\right)\left(1 + e^M\right) = \frac{1 - e^{2M^*}}{1 - e^{M^*}} \frac{1 - e^{2M}}{1 - e^M} \tag{F.16}$$

$$= \frac{1 - e^{-\gamma \Delta t} 2\cos(2\omega_m \Delta t) + e^{-2\gamma \Delta t}}{1 - e^{-\gamma \Delta t/2} 2\cos(\omega_m \Delta t) + e^{-\gamma \Delta t}} \tag{F.17}$$

Using this second approach, the simplified second scaling factor is

$$S_2(n,k) = \exp\left(-\frac{g^2 \tau^2}{4}(n-k)^2 \left(1 - e^{-\gamma \Delta t}\right) \frac{1 - e^{-\gamma \Delta t} 2\cos(2\omega_m \Delta t) + e^{-2\gamma \Delta t}}{1 - e^{-\gamma \Delta t/2} 2\cos(\omega_m \Delta t) + e^{-\gamma \Delta t}} \right) \tag{F.18}$$

F.3   Equation 4.71 to 4.72

In a way very similar to what was done in Section 4.2.3.1, the following computes the phase factor and mechanical state after the third interaction. The phase factor $P_3(n,k)$, is obtained via $C(n)C^*(k)$ with $C(n)$ obtained below

$$C(n)\left|\psi_{2+\tau}\right\rangle = \hat{D}\left(\frac{ig\tau n}{\sqrt{2}}\right)\left| \frac{ig\tau n}{\sqrt{2}} \left(1 + e^{-i\omega_m \Delta t - \gamma \Delta t/2}\right) e^{-i\omega_m \Delta t - \gamma \Delta t/2} \right\rangle \tag{F.19}$$

$$= \hat{D}\left(\frac{ig\tau n}{\sqrt{2}}\right)\left| \frac{ig\tau n}{\sqrt{2}} \left(1 + e^M\right) e^M \right\rangle \quad \text{with} \quad M = -i\omega_m \Delta t - \gamma \Delta t/2 \tag{F.20}$$

The effect on the mechanical state is simply

$$\hat{D}\left(\frac{ig\tau n}{\sqrt{2}}\right)\left| \frac{ig\tau n}{\sqrt{2}} \left(1 + e^M\right) e^M \right\rangle \propto \left| \frac{ig\tau n}{\sqrt{2}} \left(1 + \left(1 + e^M\right) e^M\right) \right\rangle = \left|\psi_{2+\tau}\right\rangle \tag{F.21}$$

86

The phase $C(n)$ is then given by (β corresponding to the displacement and α to the coherent state on which it is acted)

$$C(n) = \exp\left((\beta\alpha^* - \beta^*\alpha)/2\right) \tag{F.22}$$

$$= \exp\left(\frac{1}{2}\frac{ig\tau n}{\sqrt{2}}\frac{-ig\tau n}{\sqrt{2}}\left(1 + e^{M^*}\right)e^{M^*} - \frac{1}{2}\frac{-ig\tau n}{\sqrt{2}}\frac{ig\tau n}{\sqrt{2}}\left(1 + e^M\right)e^M\right) \tag{F.23}$$

$$= \exp\left(\frac{g^2\tau^2}{4}n^2\left(e^{M^*} + e^{2M^*} - e^M - e^{2M}\right)\right) \tag{F.24}$$

$$= \exp\left(i\frac{g^2\tau^2}{4}n^2\left(2e^{-\gamma\Delta t/2}\sin(\omega_m\Delta t) + 2e^{-\gamma\Delta t}\sin(2\omega_m\Delta t)\right)\right) \tag{F.25}$$

F.4 Calculation of $S_3(n,k)$

The result given in Equation 4.79 is proven here.

$$S_3(n,k) = \langle\psi_{2+\tau}(n)|\psi_{2+\tau}(k)\rangle^{1-e^{-\gamma\Delta t}} \tag{F.26}$$

$$= \left\langle\frac{ig\tau n}{\sqrt{2}}\left(1 + e^M + e^{2M}\right)\middle|\frac{ig\tau k}{\sqrt{2}}\left(1 + e^M + e^{2M}\right)\right\rangle^{1-e^{-\gamma\Delta t}} \tag{F.27}$$

$$= \exp\left(\frac{-ig\tau n}{\sqrt{2}}\left(1 + e^{M^*} + e^{2M^*}\right)\frac{ig\tau k}{\sqrt{2}}\left(1 + e^M + e^{2M}\right) - \frac{1}{2}\left|\frac{ig\tau n}{\sqrt{2}}\left(1 + e^M + e^{2M}\right)\right|^2\right.$$

$$\left.- \frac{1}{2}\left|\frac{ig\tau k}{\sqrt{2}}\left(1 + e^M + e^{2M}\right)\right|^2\right)^{1-e^{-\gamma\Delta t}} \tag{F.28}$$

$$= \exp\left(-\frac{g^2\tau^2}{4}(n-k)^2\left(1 + e^{M^*} + e^{2M^*}\right)\left(1 + e^M + e^{2M}\right)\left(1 - e^{-\gamma\Delta t}\right)\right) \tag{F.29}$$

Remembering that $M = -i\omega_m\Delta t - \gamma\Delta t/2$ and simplifying the result using geometric sums

$$\left(1 + e^{M^*} + e^{2M^*}\right)\left(1 + e^M + e^{2M}\right) = \frac{1 - e^{3M^*}}{1 - e^{M^*}}\frac{1 - e^{3M}}{1 - e^M} \tag{F.30}$$

$$= \frac{1 - e^{-3\gamma\Delta t/2}2\cos(3\omega_m\Delta t) + e^{-3\gamma\Delta t}}{1 - e^{-\gamma\Delta t/2}2\cos(\omega_m\Delta t) + e^{-\gamma\Delta t}} \tag{F.31}$$

Putting this result in the previous expression, the third scaling factor is obtained, as used in Equation 4.79.

$$S_3(n,k) = \exp\left(-\frac{g^2\tau^2}{4}(n-k)^2\left(1 - e^{-\gamma\Delta t}\right)\frac{1 - e^{-3\gamma\Delta t/2}2\cos(3\omega_m\Delta t) + e^{-3\gamma\Delta t}}{1 - e^{-\gamma\Delta t/2}2\cos(\omega_m\Delta t) + e^{-\gamma\Delta t}}\right) \tag{F.32}$$

Bibliography

[1] IEEE, "International roadmap for devices and systems$^{\text{TM}}$," 2020.

[2] IEEE, "International technology roadmap for semiconductors$^{\text{TM}}$ 2.0," 2015.

[3] T. N. Theis and H.-S. P. Wong, "The end of moore's law: A new beginning for information technology," *Computing in Science Engineering*, vol. 19, no. 2, pp. 41–50, 2017.

[4] T. Kawahara, K. Ito, R. Takemura, and H. Ohno, "Spin-transfer torque ram technology: Review and prospect," *Microelectronics Reliability*, vol. 52, 04 2012.

[5] J. R. Tucker, C. Wang, and P. S. Carney, "Silicon field-effect transistor based on quantum tunneling," *Applied Physics Letters*, vol. 65, no. 5, pp. 618–620, 1994.

[6] A. Seabaugh, "The tunneling transistor," *IEEE Spectrum*, vol. 50, no. 10, pp. 35–62, 2013.

[7] A. Montanaro, "Quantum algorithms: an overview," *npj Quantum Information*, vol. 2, p. 15023, Jan 2016.

[8] M. Kim, *PHYS97080 : Quantum Information Lecture Notes*. Autumn 2020.

[9] R. P. Feynman, "Simulating physics with computers," *International Journal of Theoretical Physics*, vol. 21, pp. 467–488, Jun 1982.

[10] G. Milburn, "Simulating nonlinear spin models in an ion trap," Aug 1999.

[11] H.-P. Cheng, E. Deumens, J. K. Freericks, C. Li, and B. A. Sanders, "Application of quantum computing to biochemical systems: A look to the future," *Frontiers in Chemistry*, vol. 8, p. 1066, 2020.

[12] J. A. Jones and M. Mosca, "Implementation of a quantum algorithm on a nuclear magnetic resonance quantum computer," *The Journal of Chemical Physics*, vol. 109, p. 1648–1653, Aug 1998.

[13] W. S. Warren, N. Gershenfeld, and I. Chuang, "The usefulness of nmr quantum computing," *Science*, vol. 277, no. 5332, pp. 1688–1690, 1997.

[14] S. Gulde, M. Riebe, G. P. T. Lancaster, C. Becher, J. Eschner, H. Häffner, F. Schmidt-Kaler, I. L. Chuang, and R. Blatt, "Implementation of the deutsch–jozsa algorithm on an ion-trap quantum computer," *Nature*, vol. 421, pp. 48–50, Jan 2003.

[15] K. Ono, T. Mori, and S. Moriyama, "High-temperature operation of a silicon qubit," *Scientific Reports*, vol. 9, p. 469, Jan 2019.

[16] I. Pikovski, M. R. Vanner, M. Aspelmeyer, M. S. Kim, and C. Brukner, "Probing planck-scale physics with quantum optics," *Nature Physics*, vol. 8, p. 393–397, Mar 2012.

[17] W. H. P. Nielsen, Y. Tsaturyan, C. B. Møller, E. S. Polzik, and A. Schliesser, "Multimode optomechanical system in the quantum regime," *Proceedings of the National Academy of Sciences*, vol. 114, no. 1, pp. 62–66, 2017.

[18] S. Allen, J. Kim, D. L. Moehring, and C. R. Monroe, "Reconfigurable and programmable ion trap quantum computer," in *2017 IEEE International Conference on Rebooting Computing (ICRC)*, pp. 1–3, 2017.

[19] L. Vandersypen, H. Bluhm, J. Clarke, A. Dzurak, R. Ishihara, A. Morello, D. Reilly, L. Schreiber, and M. Veldhorst, "Interfacing spin qubits in quantum dots and donors - hot, dense and coherent," *npj Quantum Information*, vol. 3, 12 2016.

[20] N. C. Jones, R. Van Meter, A. G. Fowler, P. L. McMahon, J. Kim, T. D. Ladd, and Y. Yamamoto, "Layered architecture for quantum computing," *Physical Review X*, vol. 2, Jul 2012.

[21] S.-L. Zhu and P. Zanardi, "Geometric quantum gates that are robust against stochastic control errors," *Physical Review A*, vol. 72, Aug 2005.

[22] C. Zhang, T. Chen, S. Li, X. Wang, and Z.-Y. Xue, "High-fidelity geometric gate for silicon-based spin qubits," *Physical Review A*, vol. 101, May 2020.

[23] T. J. Proctor and V. Kendon, "Hybrid quantum computing with ancillas," *Contemporary Physics*, vol. 57, no. 4, pp. 459–476, 2016.

[24] M. V. Berry, "Quantal phase factors accompanying adiabatic changes," *Proceedings of the Royal Society of London. A. Mathematical and Physical Sciences*, vol. 392, no. 1802, pp. 45–57, 1984.

[25] P. Zanardi and M. Rasetti, "Holonomic quantum computation," *Physics Letters A*, vol. 264, p. 94–99, Dec 1999.

[26] A. Ekert, M. Ericsson, P. Hayden, H. Inamori, J. A. Jones, D. K. L. Oi, and V. Vedral, "Geometric quantum computation," *Journal of Modern Optics*, vol. 47, no. 14-15, pp. 2501–2513, 2000.

[27] L.-N. Ji, C.-Y. Ding, T. Chen, and Z.-Y. Xue, "Noncyclic geometric quantum gates with smooth paths via invariant-based shortcuts," *Advanced Quantum Technologies*, vol. 4, no. 6, p. 2100019, 2021.

[28] S. Li, J. Xue, T. Chen, and Z. Xue, "High-fidelity geometric quantum gates with short paths on superconducting circuits," *Advanced Quantum Technologies*, vol. 4, p. 2000140, Mar 2021.

[29] Z. S. Wang, C. Wu, X.-L. Feng, L. C. Kwek, C. H. Lai, C. H. Oh, and V. Vedral, "Nonadiabatic geometric quantum computation," *Phys. Rev. A*, vol. 76, p. 044303, Oct 2007.

[30] Y. Ma and M. Kim, "Connection and difference between sørensen-mølmer gate and milburn gate," 2020.

[31] C. F. Roos, "Ion trap quantum gates with amplitude-modulated laser beams," *New Journal of Physics*, vol. 10, p. 013002, Jan 2008.

[32] Y.-Y. Huang, Y.-K. Wu, F. Wang, P.-Y. Hou, W.-B. Wang, W.-G. Zhang, W.-Q. Lian, Y.-Q. Liu, H.-Y. Wang, H.-Y. Zhang, L. He, X.-Y. Chang, Y. Xu, and L.-M. Duan, "Experimental realization of robust geometric quantum gates with solid-state spins," *Phys. Rev. Lett.*, vol. 122, p. 010503, Jan 2019.

[33] J. Eschner, G. Morigi, F. Schmidt-Kaler, and R. Blatt, "Laser cooling of trapped ions," *J. Opt. Soc. Am. B*, vol. 20, pp. 1003–1015, May 2003.

[34] C. Champenois, "Trapping and cooling of ions," *DEA, ecole de Physique des Houches, ecole predocotorale sur les atomes froids et la condensation de Bose-Einstein*, p. 28, Oct 2008.

[35] F. Kärtner, *Fundamentals of Photonics : Quantum Electronics, Chapter 6*. MIT: MIT Open Courseware, spring 2006.

[36] C. Gene, *Quantum Physics of Light-Matter Interactions, Lecture Notes*. Friedrich-Alexander Universtät (FAU) Lectures, Max Plank Institute for the Science of Light (MPL), Summer 2019.

[37] C. P. Williams, *Quantum Universality, Computability, & Complexity.* In: Explorations in Quantum Computing. Texts in Computer Science., London: Springer, 2011.

[38] M. Verschuren, *Coherent States in Quantum Mechanics.* Bachelor Thesis at Radboud University Nijmegen, Published online by thesis supervisor Professor W.D. Suijlekom, July 2008.

[39] A. C. Vutha, E. A. Bohr, A. Ransford, W. C. Campbell, and P. Hamilton, "Displacement operators: the classical face of their quantum phase," *European Journal of Physics*, vol. 39, p. 025405, Jan 2018.

[40] A. Sørensen and K. Mølmer, "Entanglement and quantum computation with ions in thermal motion," *Physical Review A*, vol. 62, Jul 2000.

[41] J. I. Cirac and P. Zoller, "Quantum computations with cold trapped ions," *Phys. Rev. Lett.*, vol. 74, pp. 4091–4094, May 1995.

[42] A. Ranfagni, P. Vezio, M. Calamai, A. Chowdhury, F. Marino, and F. Marin, "Vectorial polaritons in the quantum motion of a levitated nanosphere," *Nature Physics*, Aug 2021.

[43] J. Thompson, B. Zwickl, A. Jayich, F. Marquardt, S. Girvin, and J. G. Harris, "Strong dispersive coupling of a high-finesse cavity to a micromechanical membrane," *Nature*, vol. 452, pp. 72–75, 2008.

[44] Y. Ma, F. Armata, K. Khosla, and M. Kim, "Optical squeezing for an optomechanical system without quantizing the mechanical motion," *Physical Review Research*, vol. 2, 05 2020.

[45] S. Blanes, F. Casas, J. Oteo, and J. Ros, "The magnus expansion and some of its applications," *Physics Reports*, vol. 470, p. 151–238, Jan 2009.

[46] D. Prato and P. W. Lamberti, "A note on magnus formula," *The Journal of Chemical Physics*, vol. 106, no. 11, pp. 4640–4643, 1997.

[47] H.-P. Breuer and F. Petruccione, *The Theory of Open Quantum Systems.* Oxford: Oxford University Press, 2007.

[48] R. R. Puri, *Mathematical Methods of Quantum Optics.* Optical Sciences, Springer.

[49] W. H. Louisell, *Quantum statistical properties of radiation.* Pure and Applied Optics, Wiley, 1973.

[50] S. Bose, K. Jacobs, and P. L. Knight, "Preparation of nonclassical states in cavities with a moving mirror," *Physical Review A*, vol. 56, p. 4175–4186, Nov 1997.

[51] D. F. Walls, M. J. Collet, and G. J. Milburn, "Analysis of a quantum measurement," *Phys. Rev. D*, vol. 32, pp. 3208–3215, Dec 1985.

[52] D. F. Walls and G. J. Milburn, "Effect of dissipation on quantum coherence," *Phys. Rev. A*, vol. 31, pp. 2403–2408, Apr 1985.

[53] M. Srinivas and E. Davies, "Photon counting probabilities in quantum optics," *Optica Acta: International Journal of Optics*, vol. 28, no. 7, pp. 981–996, 1981.